

DETECTING BURIED REMAINS IN FLORIDA USING
GROUND-PENETRATING RADAR

By

JOHN JOSEPH SCHULTZ

A DISSERTATION PRESENTED TO THE GRADUATE SCHOOL
OF THE UNIVERSITY OF FLORIDA IN PARTIAL FULFILLMENT
OF THE REQUIREMENTS FOR THE DEGREE OF
DOCTOR OF PHILOSOPHY

UNIVERSITY OF FLORIDA

2003

Copyright 2003

by

John Joseph Schultz

This work is dedicated to my parents, Kenneth and Frances, for their boundless support and encouragement.

ACKNOWLEDGMENTS

This research could not have been completed without continued support from many individuals. Foremost, I am grateful for all of the input and support I received from my committee. Dr. Anthony Falsetti, my chairman, provided valuable guidance and funding that allowed me to pursue this research project and work at the C.A. Pound Human Identification Laboratory. Dr. Mary Collins provided access to the GPR, stimulated my interests in soil science, and was a constant source of guidance for my research. Dr. Michael Warren provided valuable guidance for my research and training in forensic anthropology. Finally, Drs. Stephen Nawrocki and David Daegling provided valuable comments while writing this dissertation.

I want to express my appreciation to Drs. Kathleen Deagan and Kenneth Sassaman for providing opportunities to further develop my GPR skills at their archaeological sites. This work could not have been completed without the numerous volunteers who continually provided their assistance in the field. Although there were many more individuals, I would like to recognize those undergraduate and graduate students who assisted me on numerous occasions: Nicolette Par, Carol Preyes, Dave Maltese, David Hines, Dora McDonald, Michael Tischler, Arden Monroe, Joseph Hefner, and Shanna Williams. I would like to thank Keith Holleran and Natalie Rodriguez at the Environmental Pedology and Land Use Laboratory at the University of Florida for valuable assistance with my soil analyses. Appreciation is due to Heather Thew for providing her protocol for scoring decomposition of buried bodies. In addition, Michael

Tischler, Rex Ellis and Joseph Hefner provided assistance with figures; and TJ Drew provided assistance with the soil analyses.

Appreciation is due to the staff in the Anthropology Department for all of their assistance while I was a graduate student at the University of Florida: Karen, Pat, and Salena. I would also like to recognize a number of friends who provided support, either directly or indirectly, to this dissertation: Bill Logallo, Pete Sinelli, Heather Walsh-Haney, Tosha Dupras, Jim Barham, and Beth Byron. Finally, I would like to thank my family for their continued support and encouragement throughout graduate school and the dissertation process.

I am thankful for the cooperation of the IFAS Animal Science Research and Education Center at the University of Florida for the use of a research field site. This study was funded through the generosity of numerous sources: the 1999 *Connective Tissue* Research Award; a 2000-2001 Forensic Sciences Lucas Research Grant; a 2002 William R. Maples Memorial Scholarship for Graduate Research in Forensic Anthropology, Department of Anthropology, University of Florida; a 2003 John Goggin Dissertation Award, Department of Anthropology, University of Florida; and a 2003 College of Liberal Arts and Sciences, Threadgill Dissertation Fellowship for the summer term, University of Florida. Finally, I would also like to thank Steven Koppenjan, of Bechtel Nevada, Special Technologies Laboratory, for the support received for another GPR project using the GPR-X.

TABLE OF CONTENTS

	<u>page</u>
ACKNOWLEDGMENTS	iv
ABSTRACT	viii
CHAPTER	
1 INTRODUCTION	1
Controlled Forensic GPR Research	2
Decomposition Studies of Burials	6
Research Objectives.....	8
2 GEOPHYSICAL METHODS	9
Magnetics	11
Electromagnetics.....	13
Resistivity	14
Applying GPR to Grave Detection	15
Ground-Penetrating Radar	21
3 HUAMAN TAPHONOMY	33
The Decomposition Process.....	34
Bone Degradation	39
4 MATERIALS AND METHODS.....	45
Research Site.....	45
Pig Cadavers	51
Ground-Penetrating Radar Methods	59
Soil Analyses	64
Analyzing Decomposition	66
Summary	71
5 DECOMPOSITON RESULTS	72
Gross Decomposition Changes	74

General Patterns of Decomposition	83
Independent Variables	86
Summary	95
6 SOIL ANALYSES	97
Florida's Soils	97
GPR Efficacy of Florida's Soil Orders	103
Classification of Soils at Research Site	105
Soil Analyses of Control Graves	109
Soil Chemistry Changes Caused by Decomposition	116
Summary	123
7 GPR RESULTS FOR LARGE PIG CADAVERS	124
The 500-MHz Antenna	124
The 900-MHz Antenna	141
Summary	156
8 GPR RESULTS FOR SMALL PIG CADAVERS	158
The 500-MHz Antenna	158
The 900-MHz Antenna	177
Summary	191
9 DISCUSSION	193
Decomposition	194
Ground-Penetrating Radar Comparisons	199
Detecting Buried Remains using GPR	213
Performing a Forensic GPR Survey	225
10 CONCLUSIONS	237
APPENDIX	
A SOIL DESCRIPTIONS	243
B SOIL ANALYSES	248
LITERATURE CITED	261
BIOGRAPHICAL SKETCH	271

Abstract of Dissertation Presented to the Graduate School
of the University of Florida in Partial Fulfillment of the
Requirements for the Degree of Doctor of Philosophy

DETECTING BURIED REMAINS IN FLORIDA USING
GROUND-PENETRATING RADAR

By

John Joseph Schultz

August 2003

Chair: Anthony B. Falsetti
Major Department: Anthropology

This research tested the applicability of using ground-penetrating radar (GPR) in Florida to detect buried bodies; and assessed the effect of body size, depth, antenna type, time, and soil type on grave detection. Furthermore, because of the emphasis on decomposition, it was possible to address the role of depth, body size, time, and soil type on decomposition. The site was located in an open pasture, where 20 pig (*Sus scrofa*) cadavers of two average weights (29.7 and 63.8 kg) were buried at two depths (50 to 60 or 100 to 110 cm). The cadavers were monitored monthly for durations up to 21 months with GPR using 900- and 500-MHz antennae. Two different soil types were used: one composed solely of sand horizons and one composed of sand with clay horizons at approximately 1.00 m. The graves were excavated at the termination of each monitoring period to collect soil samples and score decomposition.

Overall, depth was the most significant factor controlling decomposition, followed by time. Body size and soil type were not major factors. Ground-penetrating

radar can be a very effective tool for grave detection in Florida. Salient anomalies were produced for the duration of this study due to a strong enough contrast between the skeleton, or decomposing body, and the surrounding soil with that of the undisturbed soil. While cadaver size and time were not major factors in grave detection, soil type and antenna choice were. Although it was possible to detect a decomposing body and a skeleton in both shallow and deep sand graves, it was difficult to image large pig cadavers retaining extensive soft tissue buried in proximity to the clay horizon in as little as six months. The clay masked the contrast of the cadavers by reducing their relative dielectric permittivity. Pig cadaver size was not a major factor in grave detection.

The imagery of the 500-MHz antenna was preferred over the higher resolution of the 900-MHz, because the increased detail may result in difficulty differentiating the cadaver anomalies from general background noise. Postprocessing of the profile was not needed unless excessive horizontal banding was noted.

CHAPTER 1 INTRODUCTION

Ground-penetrating radar (GPR) became a popular and important remote sensing technology in the mid-1980s. Recent technological advances in GPR have made it much easier to obtain, operate, and interpret the results of this equipment. As a result, GPR is now routinely used in numerous disciplines for practical applications and controlled research. Some of the more common disciplines include archaeology, forensics, engineering, environmental science, geology, military science, mining, and soil science.

GPR has become a valuable search tool for graves from different time periods and soil types. The value of GPR in grave detection was first successfully demonstrated with historic and/or cemetery graves from various regions (Bevan 1991, King et al. 1993, Vaughn 1986). Furthermore, because of the success of locating historic period graves with GPR, there has been increasing interest in this technology for forensic applications. The number of reported forensic burials that have been successfully located with GPR has been increasing in recent years (Calkin et al. 1995, Davenport 2001a, Nobes 1999, Reynolds 1997).

The success of GPR in actual forensic situations has also led to numerous controlled GPR studies, simulating a forensic context. One aspect of GPR research that is now of prime importance is correlating state of decomposition of buried bodies to GPR imagery characteristics, in an attempt to understand whether buried bodies can be detected in various stages of decomposition and skeletonization. To do this, control

graves must be properly excavated and decomposition patterns must be recorded.

Therefore, if controlled GPR studies are constructed to include a decomposition component, variables that affect decomposition of buried bodies can be addressed at the same time.

Controlled Forensic GPR Research

Studies that test the efficacy and applicability of GPR under controlled conditions in the detection of buried bodies are becoming more popular. Most of these studies use large mammals as surrogates for human bodies. Using a 500-MHz antenna, Strongman (1992) successfully located two goats and a bear that were buried at a wooded research site in Burnaby, British Columbia five years earlier. This technology has also been used across a controlled/simulated homicide site near Rolla, Missouri that contained compact rich alluvium, during the spring, summer, and fall of 1997 (Roark et al. 1998). Although the sample size was limited to two deer carcasses buried at depths of 53 and 58 cm, the authors made several interesting conclusions regarding the GPR signatures. In particular, they determined that the radar signature was mostly a function of the fundamental differences (dielectric constant, velocity, and homogeneity) between the undisturbed soil and the backfill. Over time, there were subtle changes in the GPR signatures due to the decomposition of the deer carcasses and the compaction of the backfill.

Personnel who have been associated with NecroSearch, a Colorado based forensic organization, have conducted by far the most comprehensive controlled geophysical studies. Geoscientists and law enforcement personnel have buried pig cadavers (154 pounds on average) to concentrate on multidisciplinary methods used to detect buried remains (Davenport et al. 1990, France et al. 1992, France et al. 1997). Their 1997 article

noted that they had studied 18 gravesites including two without any pigs. One aspect of this research involved extensive surveying using three different noninvasive, geophysical methods to develop guidelines for detecting hidden graves: magnetics (MAG), electromagnetics (EM), and GPR. Without providing any specific technical information on the research design and results, they concluded that the GPR was the most important tool used to delineate graves (France et al. 1997).

More recently, the U.S. Department of Energy's Special Technologies Laboratory, operated by Bechtel Nevada, in support of the FBI Evidence Response Team, formed a collaborative forensic-GPR research project with the University of California-Santa Barbara, the University of Florida, and the University of Tennessee. The main goal of the research was to monitor graves with a stepped frequency GPR unit (GPR-X) that was developed by Bechtel Nevada (Koppenjan et al. 1998, Koppenjan et al. 2000). It is a multifrequency synthetic-aperture system that operates over the range of 200- to 700-MHz.

Preliminary results using the GPR-X and a commercial impulse GPR at our research site were first described by Schultz et al. (2002) and then in a more detailed analysis using only the GPR-X by Koppenjan et al. (2003). The forensic GPR research conducted at the University of Florida using only the commercial impulse GPR is discussed in this dissertation. At the University of Tennessee, results from GPR studies with an impulse GPR and the GPR-X have also been reported (Freeland et al. 2002, Miller et al. 2002). The research at the University of Tennessee is unique because human cadavers, and not pig cadavers, were used in graves constructed at the Anthropological Research Facility that were then covered with concrete slabs. The soils at the site are

well drained and clay is a major factor. Freeland et al. (2002) monitored one burial buried at 2 feet for eight months using the GPR-X and a GSSI pulse GPR with 400- and 900-MHz antennae. Overall, it was possible to detect the burial for the duration of the study using the GPR-X and the GSSI unit with the 400-MHz antenna. Results were less conclusive for the 900-MHz antenna because the radar wave did not penetrate deep enough to detect the floor of the grave. The lack of penetration with the 900-MHz antenna is primarily due to soil properties, but it may have also been due to a shallow range setting of only 15 nanoseconds. Using only the GPR-X, Miller et al. (2002) had success detecting one cadaver that was interred adjacent to buried debris for a monitoring period of five months.

Limitations of Previous GPR Research

It is clear from the published research of cemetery studies, controlled forensic studies, and actual forensic cases that GPR has been the most successful geophysical tool used to locate graves from a variety of soils and environments. Although the studies performed by NecroSearch have been extensive, their publications are essentially summary articles that only discuss their conclusions. They have not presented their research design, results, or methodology in detail. As a result, numerous research topics have not been addressed in the published literature. For example, no studies have reported monitoring forensic graves for durations greater than a year. The longest that controlled forensic graves have been monitored in the literature has been eight months (Freeland et al. 2002) and three seasons (Roark et al. 1998). Unfortunately, both studies only monitored shallow graves that were less than 60 cm. Furthermore, NecroSearch (France et al. 1997) did not report the length of time that graves were continuously

monitored. Monitoring of gravesites for longer than a year is important for understanding how anomalous response from the graves change due to soil compaction, decomposition of soft tissue, diagenesis of the skeleton, and mixing of soil horizons.

No research has reported whether body size is a factor in producing an anomalous response. Although NecroSearch reported using pig carcasses that represented adults, their most recent article mentioned that they had begun including smaller cadavers to represent bodies of different sizes and ages (France et al. 1997). However, no results were reported. Additionally, there is no research comparing the anomalous responses of shallow versus deep burials. Although NecroSearch experimented with a variety of antennae, they have not elucidated if high frequency antennas such as a 900-MHz antenna are of use for forensic applications (France et al. 1997). At the same time, there has been no direct comparison in the literature of unprocessed GPR imagery with GPR imagery that has been processed to remove background noise from ringing of the antenna. Antenna noise appears on all GPR profiles and may obscure detection of small subsurface features. This issue is directly related to forensic applications, because in many instances GPR assessments are conducted in the field without processing the data to remove noise.

There are conflicting views concerning whether the grave response is produced by the disturbed soil, the skeleton, or a combination of both. Furthermore, there has not been sufficient research that has tried to correlate decomposition state with specific anomaly characteristics. In order to understand if the GPR anomalies are a function of not only the backfill, but also the skeletal remains, control burials without any bones must also be constructed and monitored with the pig burials. Only NecroSearch reported

using two control burials, but did not elucidate if they were of any importance to their research. The only way to correlate decomposition state with grave anomalies is to incorporate grave excavations in the research. In addition, there have been no soil analyses to understand how the physical and chemical properties of the soil change due to the mixing of stratigraphic horizons and decomposition products of buried bodies. Soil analyses can be useful in determining what constituents of the burial produce an anomalous response. Finally, previous research has not been undertaken in a subtropical environment or in the type of sandy soils that are common in Florida.

Decomposition Studies of Burials

Background information dealing with decomposition studies of buried bodies is reviewed because of the importance of correlating the overall decomposition state of bodies with characteristics of the GPR imagery. Research in the area of human decomposition has generally focused on different factors contributing to decomposition or determining time since death. Most of the published controlled research on decomposition focuses on assessing time since death of animal cadavers on the ground surface by looking into the sequence of insect invasion. Many of the published studies have used pig cadavers as surrogates for human bodies (Payne 1965, Payne and King 1970, Payne and King 1972, Payne et al. 1968a, Payne et al. 1968b).

The only published decomposition research undertaken using human cadavers to answer time since death questions on the ground surface has been at the University of Tennessee in the areas of insect invasion (Rodriguez and Bass 1983), and volatile fatty acids and soft tissue chemistry from soft tissue decomposition (Vass et al. 1992, Vass et al. 2002). There are also studies addressing time since death by studying decay rates

from actual forensic cases in which bodies were deposited on the ground surface. For example, the data for these studies are derived from casework of medical examiner and anthropological records in the southwest U.S. (Rhine et al. 1998, Galloway et al. 1989, Galloway et al. 1997), northern New England region (Sorg et al. 1997), Edmonton, Canada (Komar 1998), and the Midwest (Megesy 2002).

Limitations of Previous Decomposition Studies of Burials

Unfortunately, there is very little controlled forensic research of buried bodies. Recently, Thew (2000) studied a large sample of buried pig cadavers to determine the effect of lime on decomposition. In all, 22 pig cadavers weighing 60 to 70 pounds were analyzed. Ten cadavers were interred for 30 months at a depth of 50 to 60 cm, six were interred for six months at a depth of 50 to 60 cm, and the remaining six were interred for six months at a depth of 10 to 20 cm.

There is only one controlled study concerning buried human bodies that was conducted at the University of Tennessee (Rodriguez and Bass 1985). Six unembalmed cadavers were buried at different depths and lengths of time. Four cadavers were buried at a shallow depth of 1 foot. One of the cadavers was exhumed at one month and the other three at two and a half months. One deep burial was at 4 feet and excavated at one year, and the last was buried at 2 feet and excavated at six months.

A number of decomposition topics have not been undertaken. For example, the relationship between cadaver size and burial depth with that of decomposition is not known. None of the previous studies examined deep graves (minimum of 1 meter in depth) that were interred for more than a year. Furthermore, there has been no research

performed in subtropical environments in the southeast dealing with decomposition of buried bodies, and no research examining the effect of body size on decomposition.

Research Objectives

The purpose of this dissertation is to enhance the ability of forensic investigators to locate clandestine burials with GPR and to better understand the taphonomic history of buried bodies. Research objectives of this study were:

- Document changes in GPR imagery characteristics of buried bodies resulting from decomposition and subsequent compaction of the backfill for periods of time longer than tested in previous studies (i.e. approximately one year);
- Assess if processing of the GPR profiles to remove antenna noise (i.e. horizontal banding) is required for grave detection;
- Determine if soil type, body size, and length of burial are factors in producing a distinctive anomalous response;
- To correlate GPR imagery characteristics with the state of decomposing of buried bodies;
- Determine if a high-resolution, 900-MHz GPR antenna is useful for locating forensic bodies;
- Document any changes in soil chemistry resulting from mixing of stratigraphic horizons and decomposition products from the bodies;
- Determine the relationship of body size, burial depth, and length of burial to the rate of decomposition.

CHAPTER 2 GEOPHYSICAL METHODS

Although “geophysics” may be defined differently depending on the particular area of inquiry, definitions that have been used to describe environmental and engineering geophysics are applicable to forensic and archaeological applications. Therefore, geophysics will be defined as “the subsurface site characterization of the geology, geological structure, groundwater, contamination, and human artifacts beneath the earth's surface, based on the lateral and vertical mapping of physical property variations that are remotely sensed using noninvasive technologies” (Sheriff 1991). The one common component that almost all geophysical technologies (except for borehole geophysical methods) share is they represent a class of subsurface investigations that are non-destructive. Hence, the main advantage of using a geophysical technology is preservation of the subsurface or site.

The purpose of a geophysical survey is to detect an anomaly that is recognized as an area of contrasting properties, either physical or chemical, in the medium that is being examined. In forensic situations where geophysical methods are employed to evaluate small, near surface anomalies, the equipment must collect high quality data at concise intervals across a survey area. Factors that can limit the quality of data in forensic scenarios include resolution, signal/noise ratio, contrast, and size/depth ratio (Davenport 2001a).

The ability to differentiate objects that are close together is referred to as resolution, and it can be related to either the proximity of objects or their similarity in physical properties. Noise can be a major limiting factor in forensic target identification. Target identification is only possible when the signal being measured is more than the strength of the randomly generated background signals (noise). Noise can be classified as natural or cultural. Natural noise is due to naturally occurring events and conditions such as wind, rainfall, lightening, etc. Cultural noise is the result of human-made objects such as traffic, metal fences, overhead power lines, underground utilities, etc. The stronger contrast between the properties of forensic targets and the host medium, the stronger the returning signal and chance of detection. Furthermore, the size/depth relationship is important because the larger the target, the deeper it can be detected. However, there is an inverse relationship between signal depth and resolution; the deeper the signal penetrates, the less resolution of forensic targets.

Geophysical prospecting methods respond to the physical properties of the subsurface (rocks, soil, water, voids, etc.) and can be classified into two basic types: passive and active (Reynolds 1997). Both methods involve the measurement of signals that are either natural or induced. Variations within the natural fields of the earth such as gravitational and magnetic fields are measured by passive methods. Active methods use induced human-made signals that are transmitted into the ground and followed by the measurement of signals returning from the ground by a receiver.

The four most common geophysical methods that have been utilized for grave detection include magnetics (MAG), electromagnetics (EM), resistivity, and ground penetrating radar (GPR). MAG is a passive tool and EM, resistivity, and GPR are active

tools. The general use of MAG, EM, and resistivity for forensic applications will be described briefly before the application of GPR for grave detection and GPR methods are described in detail. Table 2-1 summarizes advantages and disadvantages of these geophysical technologies for forensic applications.

Magnetics

Magnetic surveys are generally used to detect ferrous material. Variations in the earth's magnetic field are detected with MAG surveys by a magnetometer and measured in nanotesla (nT). Detection of anomalies is a function of the differences in contrast due to the magnetic properties, size, shape, orientation, and distance between a ferrous object and point of measurement (Davenport 2001b). MAG surveys generally do not detect graves but will detect ferrous materials such as weapons. The main advantage of using this equipment is that it can detect ferrous objects at deeper depths than a metal detector. In addition, this method has shown promise in a few arson investigations where it has been used to determine the source point and spread pattern of a fire (Bruchlinsky et al. 1997). In addition, MAGs can be conducted over uneven terrain; and this equipment is unaffected by ground water.

It is easier to detect forensic targets that are closer to the surface (Killam 1990). However, it may be difficult to detect weapons because they may result in a relatively small magnetic contrast in the subsurface (Davenport 2001b). Another disadvantage is that this equipment is sensitive to interference (noise) from nearby metal or electric currents, bridges, road culverts, automobiles, fences, railroad tracks, buildings, and geologic conditions (Killam 1990). Measurements are recorded along a grid and then

Table 2-1. Advantages and disadvantages of geophysical technologies that are used for forensic applications

Geophysical Method	Advantages	Disadvantages
Magnetics	Nonintrusive Equipment easily obtained Rapid coverage of large area Works over snow, fresh/salt water	Only for ferrous materials Target could be missed if grid is too large Data must be plotted and should be contoured (not real time) Magnetic interferences (natural and man made) confuse readings
	Nonintrusive Equipment relatively easily obtained Rapid coverage of large area For ferrous/nonferrous materials Records conductivity Works over/ through snow Does not have to contact the ground	Subject to cultural interferences (fences etc.) Target could be missed if grid is too large Data must be plotted and should be contoured (not real time) Difficult in rough terrain
Electromagnetics	Minimal surface and subsurface damage Relatively inexpensive equipment Some field results available Can determine lateral position and depth Easy to supervise	
Resistivity		Slow coverage speed Flat or gentle terrain Grave may show insufficient contrast from matrix Requires trained operator Requires data processing (not real time) Requires expert interpretation Interference from metal or electrical sources Must be in contact with the ground
GPR	Nonintrusive Medium coverage speed Real time display Can penetrate concrete and pavement Works over/ through snow, fresh water	Equipment relatively difficult to obtain Most units require moderately smooth and level terrain Clear ground cover required Little penetration of salt water or clay
Adapted from		

France DL, Griffin TJ, Swanburg JG, Lindemann JW, Davenport GC, Trammell V, Travis CT, Kondratieff, Nelson A, Castellano K, Hopkins D, Adair T. 1997. NecroSearch revisited: further multidisciplinary approaches to the detection of clandestine graves. In: Haglund WD, Sorg MH, editors. Forensic taphonomy: the postmortem fate of human remains. Boca Raton: CRC Press. p. 500-501, Table 1.

Killam EW. 1990. The detection of human remains. Springfield, IL: Charles C. Thomas, p. 226-230.

data processing is required to evaluate the field data. Anomalies can be recognized on a contour magnetic intensity map by contrasts between the target and matrix.

Electromagnetics

Conductivity is defined as the ability of a material to transmit electricity.

Differences in the ground's electrical conductivity are measured during EM surveys by an active electromagnetic instrument referred to as a conductivity meter.

Electromagnetic waves from a primary field are projected into the ground by the transmitter in the unit and the receiver measures an induced secondary field, in siemens per meter (S/m) that is created from conductors in the subsurface. A major advantage of EM, unlike resistivity (discussed in the next section), is that the unit does not have to be in contact with the ground surface because the EM signal is inductively coupled (Davenport 2001b, Reynolds 1997). In addition, an advantage of EM surveys for forensic scenarios is that metal objects can be detected and conductivity differences between the backfill of a grave and the undisturbed soil may be detected.

Electromagnetic instruments can be used in wooded areas and over concrete. However, cultural (fences, pipes, power lines, etc.) and geologic features in the vicinity can result in interference or noise.

A disadvantage of EM concerns noise created by metallic objects in the vicinity. As such, the operator must remove all metal items worn (car keys, belt buckles, and steel toe boots) before conducting an EM survey (Davenport 2001b). Preliminary results may be obtained in the field. Measurements are recorded at set intervals along a grid; and then data are processed to detect electromagnetic anomalies that are plotted on a

conductivity map. An isoconductivity contour map is a popular method of displaying electromagnetic anomalies beneath the surface.

Resistivity

Resistivity is the opposition of a given material to the passage of electricity; and is the reciprocal of conductivity (Killam 1990). The potential of a given area of the earth to conduct electricity is measured during resistivity surveys in ohms. This surveying method is based on the predictable electrical behavior exhibited in a solid medium of uniform density (Killam 1990). Induced electrical current flows horizontally and vertically into the ground. Any measured deviations from the predicted flow of current are due to variations in the conduction medium. Soil moisture influences resistivity which is also a factor with GPR (Killam 1990). It works best in low conductivity soils. It is possible to estimate the location of the variations, or anomalies, because this surveying method requires the placement of electrodes in the ground at known distances. An experienced operator can predict the objects producing anomalies and can estimate depth.

There are a number of disadvantages using resistivity for forensic applications (Killam 1990). Resistivity works best on flat ground and is influenced by soil moisture. Anomalies of interest may have a low contrast with the surrounding soil and may not be detected. There is a high noise factor compared to target signal with resistivity surveys. Furthermore, the method must have some type of ground contact that results in a minimal amount of surface destruction. Measurements can be taken along a grid and anomalies can be electromagnetic anomalies can be plotted on a resistivity map.

Applying GPR to Grave Detection

GPR has a long history of development throughout the 20th century. According to Reynolds (1997), the first use of pulsed radar to investigate the nature of buried features was as early as 1926, while the earliest use of electromagnetic (EM) signals to locate remote buried objects was early as 1904. As there were continued advances in GPR equipment in the 20th century, important developments that would lead to commercially available technology came during the Vietnam War. The U.S. Army further developed GPR during this period to locate labyrinths of tunnels excavated and used by the Viet Cong and National Vietnamese Army (Reynolds 1997). Geophysical Survey Systems Inc. (GSSI) identified the potential of GPR for the private sector by becoming the first company to develop impulse GPR for civilian applications. GSSI was founded in 1972 and they are still recognized as the largest international ground radar manufacturer.

GPR became enormously popular for archaeological applications in the 1980s. It is still a very important survey tool that is routinely used in archeology to locate sites, delineate the boundaries of occupation, map the locations of subsurface features, and delineate stratigraphic sequences that are the result of distinct periods of human occupation (Arnold et al. 1997, Basile et al. 2000, Conyers 1995, De Vore 1990, Fisher et al. 1980, Goodman and Nishimura 1993, Imai et al. 1987, Sassaman et al. 2003, Sternberg and McGill 1995). Preexcavation geophysical testing provides archaeologists an undisturbed view of subsurface features so target areas can be excavated. By targeting specific areas, the overall degree of destruction at archaeological sites is significantly reduced.

Cemetery Applications of GPR

Geophysical exploration with GPR has also become a valuable tool for finding unmarked archaeological graves in various geographical regions and types of soil conditions. For example, using a 325-MHz antenna, Vaughn (1986) was somewhat successful in locating anomalies that he attributed to unmarked graves at a 16th century Basque whaling station in Canada. The U.S. Army's forensic recovery team has reported using a GPR with a 500-MHz antenna in Southeast Asia to search for isolated burials, buried ordinance, and artifacts from aircraft disasters (Miller 1996). A GPR survey was used to assist in the exhumation of seven marked graves that were interred 80 years ago by discerning their exact location in a cemetery in Longyearbyen, Svalbard, Norway (Davis et al. 1998, Davis et al. 2000). A 225-MHz antenna was used because higher frequency antennas could not penetrate through the soil, which consisted of till overlying bedrock with permafrost below one meter.

Recently, a combination of electromagnetics, magnetics, and GPR methods were used to delineate probable locations of unmarked graves at an indigenous cemetery site of the Oaro urupa in New Zealand (Nobes, 1999). The site has been in use since the middle of the 19th century and possible earlier. GPR surveys were performed separately using two different antennae: 200-MHz and 450-MHz. GPR prospecting was difficult due to clay dominating the near-surface physical properties of the soil. Although archaeological confirmation was not permitted to correlate GPR anomalies with the locations of burials, the author felt the locations of the interpreted graves were consistent with elements of the oral history of the site. It was concluded that even though one technique may not reveal an anomalous response across a known grave, a combination of techniques can be helpful

in differentiating the signature of known graves that can then be used to locate unmarked graves.

There are also a number of studies conducted in the United States that have met with varying degrees of success when used to locate unmarked graves at historic period cemeteries using geophysical technologies. Regardless of which area of the country the cemetery surveys were conducted, it has been concluded that GPR is the most successful geophysical tool for locating cemetery graves. For example, in the classic study by Bevan (1991), he experimented at nine different sites with GPR and a conductivity meter. The GPR was used solely at six sites: three in Maryland (Annapolis and Rockville), one in Rhode Island (Newport), and one in Minnesota (Ely). The GPR and conductivity meter were both used at a site in Williamsburg, Virginia. Only the conductivity meter was used at the other two sites: Kettering, Ohio and Lamington, New Jersey. Sites were scanned with either a 180-MHz or 315-MHz antenna. While Bevan (1991) stated that the GPR was the most successful geophysical tool at locating burials, he concluded that the surveys provided no evidence of success. The surveys suggested that there were graves where there were none, and known graves had also been invisible to the surveys.

King et al. (1993) compared GPR and proton magnetometer surveys from an historic cemetery in St. Mary's County, Maryland. Two antennae were used to profile alternate lines: 180-MHz and 500-MHz. At the time of this study the authors felt it was the only one of its kind because they were able to confirm radar profiles by conducting an archaeological excavation of the cemetery. Overall, it was concluded that the radar was more effective than the proton magnetometer. Initially the radar detected one-third of the unmarked graves. Following the reassessment of the radar profiles in conjunction with

the results from the excavation, the radar potentially detected two-thirds of the total grave shafts. It was concluded that although the radar is not 100% effective in locating all of the grave shafts, it could be a very useful tool to identify the intrasite structure so an archaeological excavation can be more efficiently directed.

Forensic Applications of GPR

The success of GPR in locating historic graves has led to the use of this technology in the search for forensic clandestine graves, weapons, and bullion. Since the late 1980s, the frequency in which law enforcement agencies have sought a GPR survey is significantly increasing as they are educated about the potential of geophysical technologies. A forensic survey is important to not only locate clandestine bodies, but it is as equally important to clear suspected areas so law enforcement can direct investigations elsewhere. Conducting a GPR survey can eliminate or reduce destruction of evidence and the scene that is normally involved with traditional invasive search methods routinely employed by law enforcement. Furthermore, the use of GPR in actual forensic situations has also led to an increasing number of controlled forensic studies evaluating the utility of GPR and other geophysical methods to locate graves in different contexts.

Published Forensic GPR Cases

Ground-penetrating radar is proving to be a valuable search tool used to locate clandestine bodies that have been interred for various postmortem intervals and environments. For example, Mellett (1992) had success with GPR using a 500-MHz antenna at a large state park in Denton, Maryland locating a clandestine grave that was approximately eight years old. Using GPR with a 500-MHz antenna, Calkin et al. (1995)

located a body interred for 13 months in a compacted dirt basement of a residential home in Maine. Davenport (2001a) briefly described a case involving a body interred for 28 years that was located beneath a concrete pool deck with GPR in Phoenix, Arizona.

Using a combination of EM and GPR (200-MHz antenna) surveys, Nobes (1999) had success locating a 12 year old clandestine burial in a plantation forest north of Auckland, New Zealand. Reynolds (1997) explained that GPR was pivotal in locating the remains of 12 bodies concealed at three locations in and near Gloucester, UK in 1994. Ten bodies had been hidden within the thick concrete inside two homes, and two additional bodies were located in a nearby field. Finally, GPR has also been successful in locating buried banknotes. For example, without providing any specific details, Hunter (1996) briefly mentions that GPR was successfully used in the UK in 1992 to locate banknotes that were buried in a Lincolnshire field.

Geophysical Detection of Graves

The act of digging a grave and filling it with backfill results in many changes to the soil and stratigraphy caused by mixing of the horizons. These changes between the surrounding soil and disturbed soil may be present as differences in chemistry, color, texture, compactness, moisture retention, volume, organic content, and pH level (Wolf 1986). In some instances, it may be possible to locate clandestine graves visually if unnatural surface changes are present such as differing soil color, vegetation patterns, soil compactness, mounding of soil, and depressions. If surface changes are present, geophysical prospecting is not needed to locate the grave in question. However, geophysical technologies may still be used to confirm the presence of a burial instead

of using a more invasive tools such as probes or shovels that can damage or destroy evidence.

When a geophysical technology detects a clandestine or cemetery grave, many researchers have asserted that the changes to the soil contribute to the detection of human remains. According to Bevan (1991), the most distinctive feature of a grave is the disturbed excavated soil that is replaced. The earth that fills the grave shaft will have different electrical and magnetic stratification than the surrounding undisturbed earth. Bevan (1991) suggests that these differences could last indefinitely. The increased amount of air in the disturbed soil lowers the average electrical permittivity of the disturbed ground. In forensic contexts, Nobes (2000) also agrees with this assessment by asserting that an anomaly produced from a buried body may be caused by the displacement of the soil by the body, the clothing, and the soil disturbance from the grave itself. In addition, the greatest influence on electrical properties is a result of changes in local moisture content (Nobes 2000).

Both Unterberger (1992) and Mellet (1992) determined that in clay rich soils, the clay blocks the penetration of the radar waves down to the grave, and collapsed coffins and bones are almost impossible to detect in these types of soils (Davis et al. 2000). Instead, the radar locates the disturbed earth over the grave and not the burial (Mellet 1992, Unterberger 1992). The grave itself can be detected when the radar is able to penetrate sandy soil and produce a strong echo of the radar pulse. Metallic properties of the coffin may also produce an echo. If the wooden coffin has not decayed, or if there is a vault of brick or stone with an air cavity, the radar may detect the void (Bevan 1991, Davis et al. 2000, King et al. 1993). However, it has been suggested that a collapsed

coffin that is filled with soil may not be detectable by GPR, because there will be little contrast in the electrical properties of materials (Davis et al. 2000).

Davis et al. (2000) assert that it is difficult for GPR to detect bones due to their small size and because they have similar electrical properties to dry soil. King et al. (1993) also suggest that bones may be too small to detect, but conclude that the decay of the body or coffin may produce an echo by chemically altering the surrounding soil. Conversely, preliminary results by Schultz et al. (2002) suggest that it may be possible for GPR to detect a skeleton. Mellett (1992) believes that bone leaches calcium salt into the surrounding soil and the calcium salts make the bone and immediate area visible to the radar. In addition, Mellett (1992) also asserts that the shape of bones may also contribute to their detection.

Overall, it was determined that at historic cemeteries the best sites have characteristics where the radar detects few underground objects and where there was either weak or no planar stratification (Bevan 1991). In other words, the most salient radar reflections occur at the interface of subsurface features with greatly varying properties. The worst conditions were at sites with conductive, clay soils and complex stratigraphy. Radar reflections can be confirmed as a burial by the depth and the orientation of the reflection that is elongated in one direction relative to the perpendicular direction (Bevan 1991).

Ground-Penetrating Radar

The most common GPR units available from commercial manufacturers employ pulsed radar energy of one center frequency. Conversely, less common GPR units employ a stepped technology that focuses a narrower radar beam of varying frequencies

into the ground. While GPR imagery is available immediately in real-time with pulse technology, processing of GPR data from stepped technologies may be required (Koppenjan et al. 1998, Koppenjan et al. 2000). The following GPR description will focus solely on pulse technology.

Pulse GPR Equipment and Theory

Standard GPR systems consist of four main elements: the control unit, the transmitting unit (Tx), receiving unit (Rx), and the display unit (Conyers and Goodman 1997). A high-voltage electrical pulse that is produced by the control unit is sent to the transmitter via cable. The transmitter then amplifies the voltage and shapes the pulse that is emitted by the antenna. The receiving portion of the antenna records the returning signal and sends it back to the control unit along a different line located within the cable. The control unit amplifies and formats the raw reflected signal for display on a video monitor or paper print out. GPR files can also be downloaded to an external computer to be stored for processing to increase resolution of imagery using a variety of commercially available programs. It is important to note that newer commercially available GPR units contain postprocessing software loaded on the control unit. Therefore, depending on the equipment, it may be possible to perform postprocessing in the field without downloading the GPR files.

GPR antenna frequencies range in bandwidth from about 10- to 1500-MHz. The antennas come in standard frequencies that are designated by the frequency corresponding to the peak power of the radiated spectrum, or the center frequency. However, it produces radar energy that ranges around the center by two octaves (one half to two times the center frequency). For example, a center frequency antenna of 500-MHz

generates radar energy with wavelengths ranging between 200- to 800-MHz. As the frequency of the antennae decrease, the size of the antenna increases. Lower frequency antennae (e.g., 150-MHz) are wheel mounted and can be towed by an operator or pulled behind a vehicle.

GPR antennae are configured in either a monostatic or bistatic mode. In monostatic mode, the transmitter and receiver are contained within the same antenna housing. Antennas in monostatic mode can generally zero-offset, meaning that the point of transmission is also the point of reception because the transmitting and receiving antenna are located in the same position. Conversely, a bistatic configuration consists of separate receiving and transmitting antennae that are held apart at a constant distance by a rigid frame. Since the transmitting and receiving antennae are independent of each other, they can be separated at known offset distances that allow the user to configure the antennae in a variety of arrays. In addition, most antennae have an option for a trigger switch that is built into the handle of the smaller sized antennae that are hand pulled. When the switch is pushed, a reference mark is added to the top of the GPR profile. The process of adding reference marks allows the operator to accurately reference the survey grid with the GPR transects.

While the stepped GPR utilizes a coiled antenna (Noon et al. 1994), the standard transmitting antennas for a pulse GPR are referred to as a dipole or bow tie antenna. It consists of a thin copper plate in the shape of a bow tie that radiates the radar pulse into the ground (Kraus 1950). The power (measured in volts) is applied to the center of the bowtie. From the center, the applied electric current travels to the edges of the copper plate and back again to the middle. This repeated process creates an electromagnetic

field that is radiated from the center of the antenna downward, where it becomes coupled with the ground. Ground coupling is the ability of the electromagnetic field to move from transmission in the air into the ground (Conyers and Goodman 1997).

The dipole antenna radiates radar energy into the ground in the shape of an elliptical cone with the apex of the cone at the center of the transmitting antenna (Figure 2-1) (Davis and Annan 1989, Annan and Cosway 1994). Sometimes shields may be added in the antenna housing to reduce upward radiation. When a dipole antenna is located in air, or supported within a housing, the orientation of the radiation pattern is focused approximately perpendicular to the long axis of the antenna (Conyers and Goodman 1997). Although when there is ground contact with the antenna a major change in the radiation occurs due to ground coupling (Engheta et al. 1982), most of the wave is still channeled downward in a cone from the antenna.

In air, the angular width of the elliptical radiation pattern for a dipole antenna is roughly 90° from front to back and roughly 60° from side to side (Figure 2-2). The long axis of the ellipse is parallel to the direction of antenna travel, and the radiation pattern on a horizontal plane is not only directed directly below the antenna, but also in front, behind, and to the sides as it travels across the ground surface (Conyers and Goodman 1997).



Figure 2-1. The dipole antenna radiates radar energy into the ground in the shape of an elliptical cone with the apex of the cone at the center of the transmitting antenna.

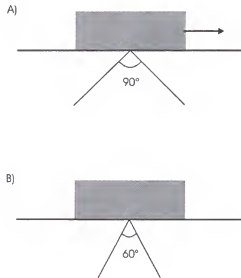


Figure 2-2. The angular width of the radiation pattern for a dipole antenna is roughly 90° from front to back (A), the direction the antenna is pulled, and roughly 60° from side to side (B).

Recording Data and GPR Imagery

The GPR dipole-transmitting antenna is placed on, or near, the ground surface and is moved over the area being surveyed. As the antenna is pulled, continuous electromagnetic pulses of short duration propagate from the transmitting unit in the antenna downward into the ground through different materials. As the signal penetrates into the subsurface, it will be reflected, refracted, and scattered as it encounters materials of contrasting electrical properties (Figure 2-3). The unscattered portion will continue downward and will once again be partially reflected as it encounters contrasting properties. The scattered portion of the wave will be lost to the environment, and a portion of the reflected wave will be received by the antenna.

During field data acquisition the radar transmission process is repeated many times a second. Reflected data from continuously moving antennae are recorded by the receiving unit in the antenna as a series of discrete waves, called traces. Each trace consists of the summation of many reflections. A cross sectional view of the subsurface is generated from the composite of the reflected wave traces along a transect creating a two dimensional profile. A series of reflections that are plotted together in a profile that create a horizontal or sub-horizontal line is usually referred to as a “reflection” (Conyers and Goodman 1997). Reflections can be produced from subsurface features that may be described as either a “point source” or planar surface (Conyers and Goodman 1997). Planar features can be due to interfaces of stratigraphic horizons, water tables, or large archaeological features, such as living floors and foundations (Figure 7-1). Conversely, point sources are more commonly referred to as anomalies and are due to smaller features such as tunnels, voids, pipes, graves, and small archaeological features (Figure 7-2).

A point source reflection is generated from one single subsurface feature and can be difficult to identify and map due to minimal surface area to reflect radar energy. Depending on the soil matrix, it may not be possible to distinguish these features. When point sources are detected they are sometimes visible as a small reflection hyperbola. This particular reflection is produced due to the wide angle of the transmitted radar beam (Conyers and Goodman 1997). As the antenna is dragged over a subsurface object, it will detect it prior to arriving directly over it, it will detect it when it is directly over it, and the antenna will continue to detect the subsurface after passing it (Figure 2-4). When the point source is detected prior to and after the antenna has passed, it is recorded as if the point source is directly beneath the antenna, but the travel time to the object is increased. The correct travel time to the object is only when the antenna is directly over the object. The hyperbolic characteristic, or tails, of the anomaly is due to the increased travel time of the radar signal before and after the disturbance.

In addition, it is also important to note that horizontal banding, or antenna noise, appears in most GPR profiles due to “ringing” of some antennas (Shih and Doolittle 1984, Sternberg and McGill 1995). The banding may obscure reflection data if it is not removed. It can be removed by most processing programs in an arithmetic process that sums all the amplitudes of reflections reordered at the same time along a profile and then divides by the number of traces summed (Conyers and Goodman 1997). The resulting composite digital wave that is an average of all the background noise is then subtracted from the data set. The final postprocessed file consists of only nonhorizontal reflections, or those horizontal reflections that are short in length.

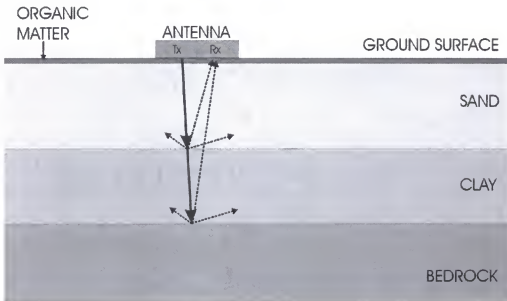


Figure 2-3. Generalized soil profile with transmitted radar waves that have been reflected and scattered as they encounter horizon interfaces of differing electrical properties.

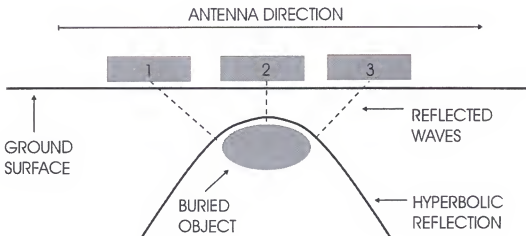


Figure 2-4. A "point source" reflection is generated from one single subsurface feature due to the wide angle of the transmitted radar beam. Adapted from Conyers L.B, Goodman D. 1997. Ground-penetrating radar: an introduction for archaeologists. Walnut Creek, CA: AltaMira Press, p. 30, Figure 3.

Physical Parameters Affecting Radar Transmission

The depth of penetration of the radar wave is a function of the antenna frequency and the dielectric properties of the material through which the radar wave is passing. Depending on chemistry of the soil and the antenna frequency, penetration of radar waves has been observed to depths of 5 to 30 m in sandy soils, 1 to 5 m in loamy soils, and less than 0.5 m in clayey soils (Doolittle and Collins 1998).

Antenna frequency

The frequency of the antenna controls both the wavelength of the propagating wave and the amount of weakening, or attenuation of the waves in the ground. Low frequency antennae (10- to 120-MHz) produce long-wavelength radar energy that can penetrate up to fifty meters in ideal conditions, but are only capable of resolving very large subsurface features (Conyers and Goodman 1997). Conversely, a high frequency antennae such as a 900-MHz produces a short-wavelength radar energy that may only penetrate a meter or less in most soils, but may be able to resolve features down to a few centimeters. Therefore, antenna choice is a compromise between depth of penetration and subsurface resolution.

Higher frequency antennae (e.g., 900-MHz) produce better resolution and are used for shallow subsurface targets. Lower frequency antennae (e.g., 300-MHz) are used for much deeper surveys, but have a lower resolution of shallow subsurface targets. In some instances, a higher resolution antenna may yield so much detail or clutter (small discontinuities that reflect energy but are not the target of the survey) that the target may not be readily identified (Nobes 1999). Antenna frequencies of either 400-MHz or 500-MHz are appropriate for most forensic and archeological applications because they

provide an excellent compromise between depth of penetration and resolution of subsurface features.

Soil or ground properties

The speed of the electromagnetic pulse is directly proportional to the characteristics of the material it passes through. Material such as soils, sediment, or rocks that are “dielectric” allow electromagnetic energy to pass through it without dissipating. Relative dielectric permittivity (RDP), also called the dielectric constant, is defined as the capacity of a material to store, and then allow the passage of electromagnetic energy when a field is imposed upon it (Von Hippel 1954). Or, it is the ability of a material within an electromagnetic field to become polarized, and to respond to propagated waves (Olhoeft 1981). RDP is calculated as the ratio of a material’s electrical permittivity to the electrical permittivity of a vacuum, which is 1 (Conyers and Goodman 1997). The RDP is a complex quantity with real and imaginary parts (Olhoeft 1998). The real part describes the ability to store energy. The imaginary part of the dielectric permittivity refers to the energy that is lost while charges are moving into the new force equilibrium that stores energy. Dielectric constant, rather than RDP, will be used for the remainder of this dissertation. The values for the dielectric constants range from 1 to 81, air and sea water, and depend upon the dielectric properties of subsurface materials (Geophysical Survey Systems, Inc. 1999).

Materials that are less dielectric, such as air, are less electrically conductive and only exhibit negligible electromagnetic polarization. As such, GPR is most successful in areas of sandy materials, weathered soils and areas underlain by crystalline rocks where the dielectric constant is low (Doolittle and Collins 1998). The depth of penetration

decreases as electrical conductivity of soil increases due to increases in cation exchange capacity (CEC), the amount of dissolved salts such as calcium carbonate and sodium chloride, the moisture content, and the amount and type of clay (Doolittle and Collins 1995, Doolittle and Collins 1998). For example, in clay rich soils that are moist with a dielectric constant of 27 (Geophysical Survey Systems, Inc. 1999), there is limited penetration of the radar wave, and there is no penetration of the radar wave in salt water with a dielectric constant of 81. Therefore, when the subsurface consists of highly conductive materials, or a higher dielectric constant, the radar signal is dissipated or attenuated, limiting penetration.

The degree to which radar reflections can be “seen” on profiles is related to the amplitude of the reflected waves (Conyers and Goodman 1997). Significant reflections occur when the change in dielectric constants between two materials must occur over a short distance. Furthermore, the greater contrast between the dielectric constants of buried features will result in higher amplitudes of the reflected signal and an increase in the resolution of reflections. The strongest reflections occur at the interface of two thick layers with greatly varying electrical properties such as soil horizons. Conversely, lower-amplitude reflections usually occur when there are only small differences in electrical properties between layers, and result in decreased resolution of subsurface features.

Radar reflections are always recorded in two-way “travel time,” which is the time it takes a radar wave to travel from the antenna into the ground, be reflected off a subsurface discontinuity, and be recorded back at the surface. The travel time, referred to as the range, is a physical parameter that can be adjusted as nanoseconds (ns). As the range is increased, the depth of penetration of the radar wave is increased. However, the

range can only be increased to a certain point depending on the antenna that is used. When the range is set beyond its maximum limit, there is no longer any usable data, because the entire signal has been backscattered or lost.

A major advantage of using GPR is the mapping of subsurface features in real depth. In addition, depth can be calculated if the velocity of the radar wave's two-way travel through the ground is known by using Equation 2-1 (Collins 1990):

$$D(m) = t_p (0.15 (\epsilon_r^{1/2})^{-1}). \quad (2-1)$$

In Equation 2-1, $D(m)$ is depth in meters; t_p is two-way travel time in ns; and ϵ_r is the dielectric constant of the material that is being penetrated. Velocity propagation and the dielectric constant are only approximations because most earthen material is not uniform in physical or chemical properties. Therefore, the depth of penetration is an approximation.

For depth to be accurate, the dielectric constant of the soil must be determined. In the field, there are a number of methods that are commonly employed. A metallic object can be buried at a known depth and profiled with the radar. The dielectric constant is then adjusted until the target object appears at the correct depth on the GPR profile. Another method employs using a stratigraphic horizon that will produce a reflection such as clay. Once the depth to the horizon is determined by soil auguring, the dielectric constant can also be adjusted until the horizon appears at the correct depth on the profile.

CHAPTER 3 HUMAN TAPHONOMY

The field of “taphonomy” was originally introduced in 1940 by the paleontologist Efremov from the Greek words *taphos* (burial) and *nomos* (laws) to represent the “laws of burial” (Efremov, 1940). Although originally introduced in paleontology, other scientific disciplines such as archaeology, zooarchaeology, paleoethnobotany, paleoanthropology, and more recently forensic anthropology, have recognized the importance of taphonomy. Since its introduction, there have been modifications to the original definition as it has been applied to each specialized field of scientific inquiry. For example, Behrensmeyer and Kidwell (1985:105) introduced a definition of taphonomy for paleontology as “the study of processes of preservation and how they affect information in the fossil record.” Koch (1989:2) further refined Behrensmeyer and Kidwell’s definition so that it would be more applicable to archaeology and paleoanthropology as “the study of the processes of preservation and modification, and how they affect geological, biological, and cultural information in the geologic record.”

Although forensic anthropology shares many of the same goals as traditional taphonomic research, there has been a bias in these earlier definitions due to the treatment of skeletal material without soft tissues. Therefore, Haglund and Sorg (1997:3) recently introduced a definition of taphonomy for forensic anthropology that would encompass the immediate postmortem interval and soft tissue decomposition. They assert that forensic taphonomy is “the use of taphonomic models, approaches, and analyses in

forensic contexts to estimate the time since death, reconstruct the circumstances before and after depositions, and discriminate the products of human behavior from those created by the earth's biological, physical, chemical, and geological subsystems."

There are numerous taphonomic processes to consider while reconstructing the postdepositional history of skeletal remains. With an emphasis on burials, Nawrocki (1995) classified taphonomic processes that alter human remains from recent and ancient contexts into three major groups: environmental, individual, and cultural. Environmental factors can be the result of biotic and abiotic forces. Individual factors are the effects of the remains to the decomposition process such as stature, age, weight, etc. Cultural factors deal with unique element of human intervention such as established mortuary practices and assailing activities associated with disposing of and concealing the identity of bodies. In this synergetic model outlined by Nawrocki (1995), any given taphonomic factor can be associated with more than one broad category. Hence, the process of decomposition, particularly with burials, is a complex interaction of various factors that can influence one another.

The Decomposition Process

Autolysis and Putrefaction

Decomposition begins almost immediately after death with autolysis and putrefaction. Autolysis or self digestion is a process that results in the release of hydrolytic enzymes into the cytoplasm of the cell that are present in the cytoplasmic granules in all cells, called lysosomes. It is believed that autolysis initiates due to a decrease in intracellular pH as a result of decreased oxygen levels that occur after death (Cormack 1987). Proteins and carbohydrates are digested by hydrolytic enzymes and

fats are affected to a lesser degree. As a result of autolysis, cellular membranes are disrupted releasing digested molecules that are taken up as nutrients by the invading microorganisms. Following death of an organism, autolysis affects all cells beginning shortly after death. Autolysis generally begins earlier in cell types that contain large numbers of lysosomes (e.g., pancreas) than those with fewer lysosomes (e.g., muscle) (Clark et al. 1997). Refrigeration or cold temperatures can retard the process of autolysis.

An almost entirely anaerobic environment is created as the body's cells reach end-stage autolysis. Normal homeostatic mechanisms of the body prevent bacterial overgrowth during life. However, the anaerobic environment favors the rapid growth of the enteric bacteria in the soft tissues of the gastrointestinal tract and organisms in the soil (Micozzi 1991). With somatic death, normal homeostasis ceases and the bacteria flora of the gastrointestinal tract spread throughout the body resulting in putrefaction (DiMaio and DiMaio 2001). Purification is fueled by the breakdown of carbohydrate, protein, and fat products that are released by autolysis. Putrefaction results in catabolism of tissues into various acids, liquids, and simple molecules that are the basis of color changes, odors, and bloating.

Active Decay

Active decay, or soft tissue decomposition, follows putrefaction shortly after purging of gases (Gill-King 1997, Clark et al. 1997). Soft tissue decomposition generally proceeds until only bone and teeth are left, or skeletonization. Generally, skin, muscle and organs decompose before ligaments and cartilage. Therefore, even though there can be significant soft tissue decomposition, there may be minimal disarticulation of the skeleton if ligaments and cartilage are preserved. Rodriguez and Bass (1985) have

observed disarticulation of the body proceeding from the head downward, the separation of the mandible from the head and the head from the body, and from central to peripheral, from vertebral column to limbs. The rate of decomposition is contingent upon numerous factors acting independently or in concert with one another. Therefore, the time involved for complete skeletonization of a body varies considerably depending on the environment.

Adipocere

A description of decomposition would not be complete without discussing adipocere development. Adipocere, or the saponification of fats, is more common and significantly increased in moist conditions and aqueous environments, but may also develop without saturated conditions. Adipocere development is commonly noted in burials and may result from moist soils or soils with clay (Rodriguez 1997).

Water and mild acidity are first required for the hydrolytic cleavage of free fatty acids from glycerol (Gill-King 1997). Over time the process will create a soapy byproduct as carboxylic acids attach to sodium and/or potassium ions that are present in tissues fluids from decomposition. A neutral or slightly alkaline intercellular pH is required. Furthermore, adipocere may become hardened if Na and K ions are displaced in either aqueous environments or soil with a high mineral content (Gill-King 1997).

Factors Affecting Decomposition

The primary factors of decomposition that have been gleaned at the University of Tennessee are summarized by Mann et al. (1990). Of the many variables that have an affect on decomposition, burial depth is the most influential because burying a corpse significantly changes the decompositional environment and thus results in a significantly

reduced rate of decomposition (Mann et al. 1990). According to Rodriguez (1997), there are two main factors responsible for reduced decompositional rates below ground. The first factor is the limitation of carrion insects and animal activity. Burial depth and soil compactness are directly related to the degree of access to insects and animals, and carrion depredation is primarily restricted to burial depths of a foot (30.5 cm) or less (Rodriguez and Bass 1985).

The second major factor is the soil environment, which provides an efficient barrier to solar radiation (Rodriguez 1997). Since temperature fluctuation decreases with soil depth, so to does the rate of decomposition by cooling of the body. At depths less than 1 foot (30.5 cm), temperatures are similar to those above ground and also fluctuate daily (Rodriguez and Bass 1985). At depths greater than 2 feet (61 cm) thermal stabilization in soil occurs with no significant temperature fluctuations other than by season (Rodriguez 1997). Depths of approximately four feet (121.9 cm) or greater provide a significantly reduced rate of decomposition due to consistent cool tissues and inhibition of depredation (Rodriguez 1997). According to Rodriguez (1997), decays rates of cadavers buried in Tennessee and observations in the Northeast have shown that it takes approximately two to three years for a buried corpse at depths of at least 4 feet (121.9 cm) to reach complete skeletonization. Furthermore, for most latitudes in North America it takes less than six months to one year to reach complete skeletonization at a shallow depth of 1 foot (30.5 cm) or less (Rodriguez 1997).

Significance of Decomposition Chemistry

The breakdown of soft tissues produces biochemical indicators that can be found in decomposition fluids. Collecting soil samples from under bodies that contain

decomposition fluids may provide useful time since death estimates. For example, studying the soil solution of above ground depositions of bodies, it has been recently demonstrated that volatile fatty acids (VFAs), the primary breakdown products of both muscle and fat, and other decompositional compounds are deposited in the soil in specific ratios (Vass et al. 1992, Vass et al. 2002). Furthermore, VFAs have shown promise for estimating PMI because the reported accuracy of this method for preskeletonized remains has been reported as ± 2 days (Vass et al. 1992).

In addition, the breakdown products of decomposition may have forensic significance for pH changes of the immediate around the burials, though there appears to be some confusion in the literature concerning the initial change in pH due to the presence of VFAs during early decomposition. According to Gill-King (1997), early in the decomposition process, buried bodies create an acidic environment in the surrounding soil due to the release of products rich in organic acids, including VFAs (Gill-King 1997). Conversely, in the study by Vass et al. (1992) using one overall mean value for seven human cadavers on the ground surface, an increase in pH was reported almost immediately following decomposition. This pH increase correlates with the production of VFAs. While there may be some discrepancies concerning an initial acid environment, there appears to be a consistent increase, not decrease, in pH due to the release of decompositions products into the soil.

Most studies, including above ground (surface) depositions and burials, report an alkaline environment, or near alkaline, eventually developing in the soil surrounding decomposing bodies (Reed 1958, Rodriguez and Bass 1985, Thew 2001, Vass et al. 1992). For example, Vass et al. (1992), reported mean pH values for all seven study

cadavers greater than 9.0; initial pH values of the soil were less than 6.0. Gill-King (1997) suggests the alkaline environment may be caused from proteolysis, but does not elaborate his opinion. However, when muscle and fat are finished decomposing or the point at which VFAs are no longer produced (Vass et al. 1992), there appears to be direct correlation with the drop in alkalinity. Given enough time after decomposition and the breakdown of most soft tissue, the soil pH will eventually return to near normal values. Furthermore, Vass et al. (1992) demonstrated that after skeletonization and the decline in alkalinity, the concentrations of Ca and Mg in the soil solution were at the highest levels. They felt the increased concentrations of these minerals came directly from the bone.

This early alkaline environment can have significance locating clandestine burials. For example, higher alkaline soil readings were successfully used to locate bodies in Japan had been buried several months (Murray and Tedrow 1992). A 4 foot (115.68 cm) auger was used to collect soil samples that were tested with litmus paper for a strong alkaline reaction.

Bone Degradation

After a buried body is skeletonized, the remaining hard tissues will breakdown at a much slower rate. The destruction of bone is the result of numerous mechanical and chemical forces. Before discussing factors that contribute to bone degradation, a brief overview on the structural organization of bone will be presented. Next, the role of weathering on buried skeletal remains is briefly discussed, and a general overview of diagenesis is presented by focusing on the major factors that promote dissolution of bone. Finally, the last section discusses the dissolution of bone hydroxyapatite with an emphasis on bone chemistry.

Structural Organization of Bone

The three major components of bone are water, minerals, and organics. The mineral and organic constituents combine into an extracellular matrix making the bone strong and elastic. In addition, the density of bone varies according to the proportions of these three components with the proportions of each being governed by species, age, health status, and type of bone (i.e. compact or cancellous).

Although bone serves numerous functions, the unique properties of this structural material are due to the combination of organic and inorganic materials. According to Paterson (1983), dried bone contains approximately 25% organic and 75% inorganic material. The organic component consists mainly of collagen and the inorganic material, mainly hydroxyapatite, consists of a calcium phosphate mineral with the general composition $\text{Ca}_{10}(\text{PO}_4)_6\text{OH}$ (LeGros 1981, Lowenstein and Weiner 1989). According to Nielsen-Marsh (2000), apatite a more ambiguous term than hydroxyapatite is more suitable because it reflects the uncertainty of the structure of the mineral phase and its organization with collagen. The general configuration of the inorganic and organic composite consists of hydroxyapatite crystals supported in a collagen matrix of intertwined fibers

Weathering

According to Behrensmeyer (1978:153), weathering of bone is defined as “the process by which the original microscopic organic and inorganic components of bone are separated from each other and destroyed by physical and chemical agents operating on the bone *in situ*, either on the surface or within the soil zone.” The destruction and decomposition of bones is “part of the normal process of nutrient recycling in and on

soils" (Behrensmeyer 1978:150). The critical factor with weathering appears to be time, but the relationship between time and weathering is not straightforward (Lyman 1994). Although buried bones weather, they weather at a much slower rate than exposed bones on the surface. Furthermore, since weathering of buried bones is so minimal, Lyman (1994:430) states that weathering of bone occurs "mainly in subaerial or surface contexts."

Overview of Diagenesis

Referring to vertebrate faunal remains, Lyman (1994) recognizes diagenesis as the alteration of bone subsequent to burial. Diagenesis as a process can be considered as occurring in three environments: 1) the bone tissue; 2) the pore spaces and cavities within the bone; 3) and the sediment surrounding the bone (Martill 1990). In the bone tissue, ionic substitution of apatite crystals with other minerals is a common process. The pore spaces and cavities fill with diagenetic materials. Furthermore, the rate of diagenic change of buried vertebrate skeletal material is highly contingent on the sedimentary matrix. The sedimentary matrix affects the outer surface of bone, the nature of ground water (chemical makeup and transportability), and crushing or deformation of the remains based on the presence or absence of diagenetic cements in the sediment.

The preservation of bone is affected by chemical and physical changes after burial. The rate of bone diagenesis is affected by intrinsic factors such as the size, porosity and of the chemical structure of a specimen, and extrinsic factors such as pH, water, temperature, and microorganisms (Chaplin 1971, Henderson 1987, Von Endt and Ortner 1994, White and Hannus 1983). It is important to note that the different extrinsic factors can be somewhat related.

Intrinsic factors

Chaplin (1971) notes the porosity of a structure is an important factor in the decay and dissolution of tissue. Hence, more porous tissues will decay more rapidly than porous structures. Furthermore, in experimental studies, Von Endt and Ortner (1983) found that small bone particles do not preserve as well as large particles. The increased disintegration of smaller bone particles is most likely due to a higher surface to volume ratio.

Extrinsic factors

While preservation of bone is increased in basic sediments, it is decreased in acidic sediments. According to Lindsay (1979), bone apatite is one of the most stable calcium phosphate phases at pH levels that characterize most groundwater. Hydroxyapatite is most stable at pH 7.8 and has a low solubility in alkaline ($\text{pH} > 7.5$) to slightly acid ($\text{pH} = 6.0$) aqueous environments, while the solubility of hydroxyapatite is high in highly acidic environments ($\text{pH} < 6.0$) (White and Hannus 1983, Rottander 1976).

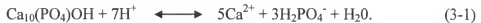
Furthermore, bone degradation can be due to biological or chemical processes. In an aerobic weathering environment, the degradation of the organic component begins with decomposition of collagen by microorganisms (White and Hannus 1983). White and Hannus (1983) further suggest that microorganisms may have a role in the initial chemical weathering of bone, independent of soil properties, through the formation of organic and carbonic acids that are formed by the microbial decomposition of collagen.

In anaerobic environments protected from enzymatic degradation of the organic phase of bone, percolating groundwater is one of the most critical factors in chemical diagenesis of the organic phase of bone. Soluble protein compounds are leached from the

bone through soil solution by breaking collagen into polypeptides (Hare 1980). The rate of leaching depends on the degree of saturation of water in sediment and the rate of movement (Hare 1980). Water also results in dissolution of the bone apatite and leaching of the mineral component of bone if the soil solution is not saturated with the minerals that make up the bone tissue (Dodd and Stanton 1981). Finally, in experimental studies Von Endt and Ortner (1984) suggest that protein in bone is lost more quickly at higher temperatures, but White and Hannus (1983) suggest that heating of bone does not accelerate chemical weathering of the inorganic phase of bone.

Bone Hydroxyapatite Dissolution

All of the calcium phosphates in the soil, including apatite, become more soluble with a reduction in pH. Nielsen-Marsh et al. (2000) discuss the role of the hydrogen ion on the solubility of hydroxyapatite by providing Equation 2-1:



As indicated in Equation 3-1, the hydroxyapatite is dissolved when the reaction is forced to the right with an increase in hydrogen ion concentration. Although hydroxyapatite is more stable at alkaline conditions, calcium will precipitate out of solution as bicarbonate in the presence of CO_2 , but will be limited by the concentration of CO_2 . The reaction can be pushed to the left when hydroxyapatite dissolves because H^+ ions are consumed reducing the acidity.

Although pH is the main factor controlling the dissolution of apatite, groundwater and porosity further promote the rate of dissolution. In more specific terms, groundwater movement plays an important role in the mineral dissolution of bone because it controls the saturation of the immediate area with respect to Ca^{2+} and PO_4^{3-} ions. Hence, the more

saturated immediate area of these ions, the less mineral dissolution. Buried bone in soil may survive for indefinite periods if water movement is limited and the concentrations of Ca^{2+} and PO_4^{3-} ions is high (Nielsen-Marsh et al. 2000). In addition, the dissolution of the mineral phase increases the porosity of bone, resulting in an increased accessibility of the organic component of bone for microbial destruction.

CHAPTER 4 MATERIALS AND METHODS

Research Site

Description

The field research site (Figure 4-1) is located on the southern boundary of the University of Florida's Beef Research Unit (BRU) in northeast Alachua County on County Road 225, immediately south of the Gainesville Raceway. The area is relatively flat and is located in an open grass pasture that is not managed (Figure 4-2). There are a number of large trees in the pasture. The graves were placed far enough away from the trees so the roots would not interfere with the GPR surveys. It is important to note that the subsoil in this field contains an abundance of old stumps and roots that are detected by the GPR as small hyperbolic anomalies. However, the small anomalies from the roots do not obscure detection of the pig cadavers.

The soils at the BRU (Figure 4-3) are dominated by Ultisols, Spodosols, and Entisols (Thomas et al. 1985), which are the three best soil orders in Florida for GPR applications (Collins et al. 1996). The site was chosen because of a number of ideal characteristics for GPR surveying: the field is open, the ground surface is flat, the topography is generally flat, there is good drainage, and the soils provide optimum conditions for GPR. In addition, the research site was far enough off the road and hidden from view preventing people from disturbing the burials.

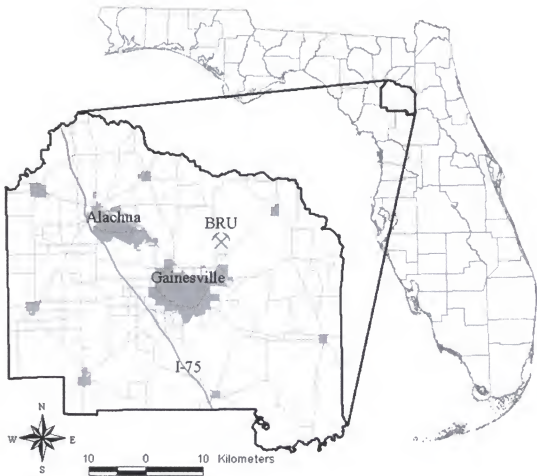


Figure 4-1. Map showing the location of the University of Florida's Beef Research Unit (BRU) in northeast Alachua County.



Figure 4-2. Aerial image showing the location of the research area at the Beef Research Unit from County Road 225. Note the location of the two grave areas in the open field.

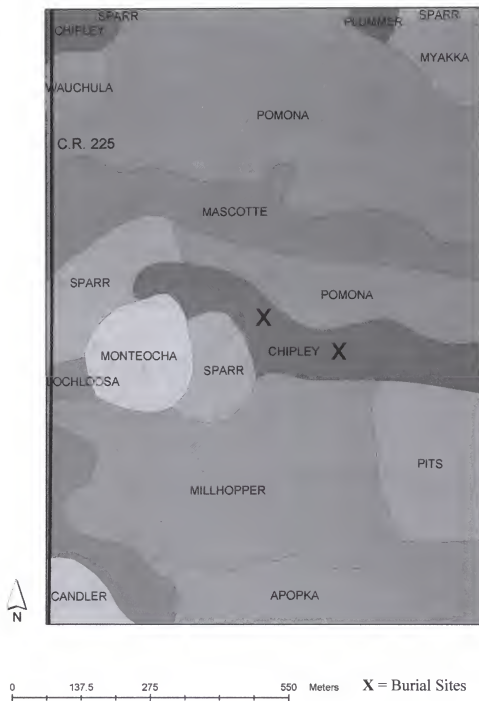


Figure 4-3. Soil survey map showing soil series at the Beef Research Unit. The map was created in ArcGIS 8.1 using data derived from the Alachua County Soil Survey (Thomas BP, et al. 1985).

Soils

Two soils were used at the BRU: the Ultisol and Entisol (Figure 4-3). The soils were described to a depth of 2 meters when possible. The soil descriptions were then compared to the previously mapped soils of the area. The large pig cadavers were buried at the western area of the research site in an Ultisol and the small pig cadavers were buried at the eastern area in an Entisol. The major difference between the two soils with regards to GPR performance is the presence of an argillic (clay) horizon at approximately 100 cm in the Ultisol (Figure 4-4). Conversely, the Entisol consists only of horizons high in sand content (>90%) at the depths studied. The response from the shallow pig graves at 50 to 60 cm in both soils will be similar because the stratigraphic horizons at this depth are comprised primarily of sand (Figure 4-5). However, the response of the deep graves at 100 to 110 cm will differ due to the argillic horizon in the Ultisol. The large pig cadavers were buried in the upper limit of the argillic horizon in the Ultisol, while the smaller pig cadavers were buried in a sand horizon (Figure 4-6).

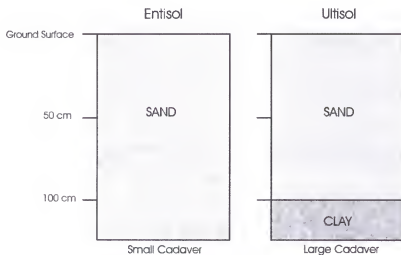


Figure 4-4. The major difference between the two soils is the presence of an argillic horizon at approximately 100 cm in the Ultisol.

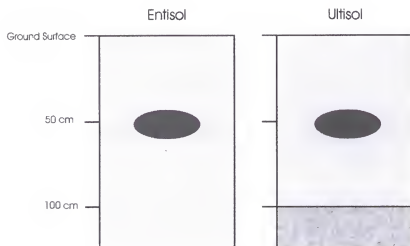


Figure 4-5. The response from the shallow pig graves at 50 to 60 cm in both soils will be similar because the stratigraphic horizons are comprised primarily of sand

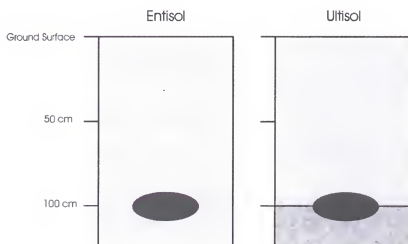


Figure 4-6. The response of the deep graves at 100 to 110 cm will differ between the soils because of the argillic horizon in the Ultisol.

Pig Cadavers

Pig (*Sus scrofa*) cadavers were used as surrogates for human bodies in this study. Because of the difficulty in acquiring human cadavers for research, pig cadavers are commonly used in taphonomy experiments that replicate humans. Also, the current ethical climate effectively prohibits the use of human cadavers for decomposition studies. Pigs are easy to obtain and out of all medium sized nonprimate mammals, they are the most biologically similar to humans. For example, they have similar integument and fat-to-muscle ratio as humans and lack excessive body hair (France et al. 1997), and pigs are currently the preferred source for xenotransplantation (transplantation, implantation, or infusion of nonhuman products into a human) (Chapman and Bloom 2001). For example, pig heart valves are routinely transplanted into humans (Schoen and Levy 1999, Bloomfield et al. 1991). In addition, further evidence of the biochemical similarity between pigs and humans has been shown by implanting neurologic cells from pigs to human patients with degenerative disorders such as Huntington's and Parkinson's disease (Deacon et al. 1997, Fink et al. 2000).

The pigs were euthanized by a veterinarian to ensure humane treatment. They were first sedated with an intramuscular injection of Telazol, Ketamine, and Xylazine, injected behind one of their ears. The dose varied from 0.5 to 0.75 ml titrated to body weight. Once sedated, euthanasia was accomplished with an intracardiac injection of Beuthanasia. The dose varied from 7 to 10 ml titrated to body weight. The pigs were euthanized in the morning and the burial process was completed in the afternoon of the same day.

A total of 20 pig cadavers of two average weights (small and large) were buried at one of two depths (shallow and deep) for one of two time frames (long and short) (Table 4-1). The cadavers were divided into two major groups by size to represent children and adults. The general layout of the large graves in the Ultisol on the western end of the research site are mapped in Figure 4-7, and the general layout of the small graves in the Entisol on the eastern end of the research site are mapped in Figure 4-8. Twelve cadavers weighing an average of 63.8 kg (140.75 pounds) were designated as the large group (Table 4-2), and eight cadavers weighing an average of 29.7 kg (65.5 pounds) were designated as the small group (Table 4-3). Ten cadavers, six large and four small, were interred between 12 and 13.25 months and are designated as the short-time frame group. The remaining ten cadavers, six large and four small, were interred between 21 and 21.5 months and are designated as the long-time frame group. At the termination of one year, 10 pig burials were excavated and decomposition was scored. At the termination of 21 months, the other ten burials were excavated and decomposition was scored. Furthermore, half of the large (six) and small (four) cadavers were interred at a depth of 50 to 60 cm and are designated as the shallow group. The remaining large (six) and small cadavers (four) were buried at a depth of 100 to 110 cm and are designated as the deep group.

Table 4-1. General summary data of pig cadaver scenarios

Time Frame		12 to 13.25 Months		21 to 21.5 Months	
Depth		50 to 60 cm	100 to 110 cm	50 to 60 cm	100 to 110 cm
Quantity (20)	Large (12)	3	3	3	3
	Small (8)	2	2	2	2

These variables were chosen for a number of reasons. The depths were chosen to represent deep and shallow burials that are generally encountered in forensic scenarios. It must be noted that the shallow burials at depths ranging from 50 to 60 cm more closely replicate actual shallow burials at their deepest limits. Two size groups were chosen to represent children and small adults. The time frames for this study were determined based on a combination of the following: reported estimates for the length of time it takes for the decomposition of a body buried at shallow and deep depths (see section entitled Factors Affecting Decomposition in Chapter 3); and a reasonable time frame to monitor graves with GPR and to correlate decomposition state with GPR imagery. Moisture and temperature were not controlled in this study. Two wells were installed in the Entisol at a depth of 144.6 cm (5 feet) to monitor grave anomaly changes caused by groundwater. Unfortunately, it was not possible to collect any daily depth data to the water table, because water never collected in the wells due to a serious drought in Florida during the majority of data collection for this study. Overall, the effect of temperature was not studied because it was not possible to bury all of the graves during the same time of year. Since seasonal temperature fluctuations in Florida are not as drastic as other areas of the country, the effect of temperature was treated as a constant.

Nine control burials were also monitored with the GPR (Table 4-4). Five control graves were in the Ultisol and four were in the Entisol. The control graves were dispersed within the rows of pig graves and were constructed of similar dimensions as the pig graves. The majority of the control burials consisted of only backfill. The hole was dug and only the backfill was returned to the empty control graves. These blank controls were designed to qualitatively estimate the proportion of the grave

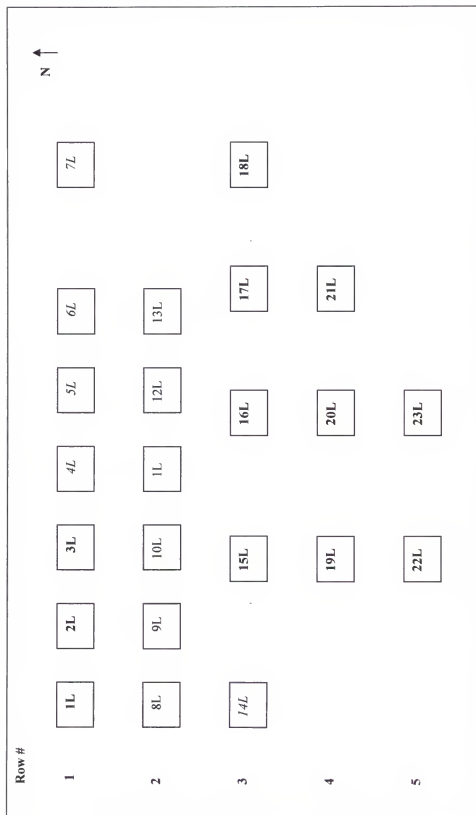


Figure 4-7. Map showing the general distribution of large graves in five rows at the western research area at the BRU. Graves are designated by their grave site number. See Tables 4-2 and 4-4 for grave designations. Row 2 did not contain any graves with pig cadavers and was not monitored. Graves with bold numbers contained a pig cadaver, graves with italics were control graves without cadavers that were monitored, and the graves that are neither bold nor italicized were control graves without cadavers that were not monitored. Map is not drawn to scale.

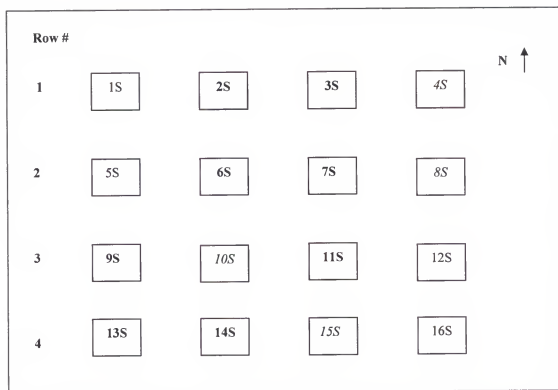


Figure 4-8. Map showing the general distribution of small graves in four rows at the eastern research area at the BRU. Graves are designated by their grave site number. See Tables 4-3 and 4-4 for grave designations. Graves with bold numbers contained a pig cadaver, graves with italics were control graves without cadavers that were monitored, and the graves that are neither bold nor italicized were control graves without cadavers that were not monitored. Map is not drawn to scale.

Table 4-4. Detailed summary data of control graves that were monitored with GPR

Control Grave Number	1	2	3	4	5	6	7	8	9
Grave Site Number	4L	5L	6L	7L	16L	4S	8S	10S	15S
Soil Order	Ultisol	Ultisol	Ultisol	Ultisol	Ultisol	Entisol	Entisol	Entisol	Entisol
Scenario	Backfill	Gravel Lens	Branches	Backfill	Backfill	Backfill	Backfill	Backfill	Backfill
Depth	Deep	Deep	Deep	Shallow	Shallow	Deep	Shallow	Deep	Shallow

Table 4-3. Detailed summary data for the small pig cadavers

Cadaver Number	13	14	15	16	17	18	19	20
Grave Site Number	2S	3S	6S	7S	9S	11S	13S	14S
Cadaver Weight (lbs)	68	70	68	70	57	71	63	57
Cadaver Size	Small	Small	Small	Small	Small	Small	Small	Small
Soil Order	Entisol Deep	Entisol Deep	Entisol Shallow	Entisol Shallow	Entisol Deep	Entisol Deep	Entisol Shallow	Entisol Shallow
Depth	21	21	21	21	13	13	13.25	13.25
Internment Length (months)	10/3/00	10/3/00	10/3/00	10/3/00	4/11/01	4/11/01	4/11/01	4/11/01
Date Interred	6/28/02	6/28/02	7/2/02	7/2/02	5/6/02	5/6/02	5/18/02	5/18/02
Date Excavated								

Table 4-2. Detailed summary data for the large pig cadavers

Cadaver Number	1	2	3	4	5	6	7	8	9	10	11	12
Grave Site Number	11L	2L	3L	16L	17L	18L	19L	20L	21L	22L	23L	24L
Cadaver Weight (lbs)	114	140	125	133	143	136	148	152	141	152	151	154
Cadaver Size	Large	Large	Large	Large	Large	Large	Large	Large	Large	Large	Large	Large
Soil Order	Ultisol	Ultisol	Ultisol	Ultisol	Ultisol	Ultisol	Ultisol	Ultisol	Ultisol	Ultisol	Ultisol	Ultisol
Depth	Deep	Deep	Deep	Shallow	Shallow	Shallow	Shallow	Deep	Deep	Deep	Deep	Deep
Interment Length (months)	21	21	21	12	21.5	21.5	21.5	13	13	13	13	13
Date Interred	12/8/99	12/8/99	12/8/99	5/10/00	5/10/00	5/10/00	5/10/00	4/18/01	4/18/01	4/18/01	4/18/01	4/18/01
Date Excavated	9/8/01	9/8/01	9/8/01	5/4/01	2/21/02	2/21/02	2/21/02	5/16/02	5/15/02	5/13/02	5/16/02	5/16/02

anomaly produced solely by the disturbed soil, and not the pig. The imagery from the blank controls was visually compared to the imagery from the pig graves to determine the component of the grave anomaly caused by the pig and disturbed soil.

Two additional control graves were constructed at the Ultisol area. A layer of gravel was placed at the bottom of one control grave at 100 cm and then the backfill was returned to the hole. In the last control grave, branches were placed at the bottom of the pit at 100 cm. These two control graves were designed to simulate false anomalies, or a false positive, that geophysical surveys commonly image. A false positive is commonly produced by buried rocks or gravel lenses, roots, and buried stumps during a GPR survey for some other subsurface object. In addition, these two control graves were placed in the Ultisol because of the difficulty in imaging graves in clay. Specifically, they were in the same row as the deep pigs that were buried for the long-time period (A-4). When there was difficulty detecting a deep pig grave in the clay, the control holes provided a reference in the clay horizon for size and depth of anomalies.

Ground-Penetrating Radar Methods

Equipment

The GPR system used in this study was the Subsurface Interface Radar (SIR) 2000, manufactured by Geophysical Survey Systems, Inc (GSSI) (Figure 4-9). This unit is a commercial pulse system consisting of a digital control with a color VGA screen, keypad, and internal hard drive. The screen is used for viewing real-time data in the field and the internal hard drive stores GPR files that can be downloaded to an external computer and viewed with RADAN for Windows NT, proprietary software of GSSI. The

unit is powered by a twelve-volt battery and can also be powered by a car battery. A 60 meter cable attaches one antenna at a time to the control unit.



Figure 4-9. SIR 2000 GPR control unit (center) with 500-MHz antenna (left) and 900-MHz antenna (right).

Two dipole antennae were used for this project, center frequencies of 500- and 900-MHz. They are both monostatic configurations; the transmitter and receiver are contained within one antenna housing. The antennas have a handle that is grasped to pull it while walking during surveying, and each antenna has a marker switch built into the handle.

GPR Data Collection

GPR surveys were conducted monthly from December 1999 to late June 2002 with both antennae. GPR data were collected for each row of graves in one long transect by pulling the antenna over the length of the graves at the midline in both directions. Transects were first conducted in a west to east direction and then from east to west.

Since the pig cadavers were oriented lengthwise in each grave, the cadavers were scanned in length when the grave was scanned in this dimension (Figure 4-10). In addition, each month the width of a representative number of graves was scanned at the midline in both directions.

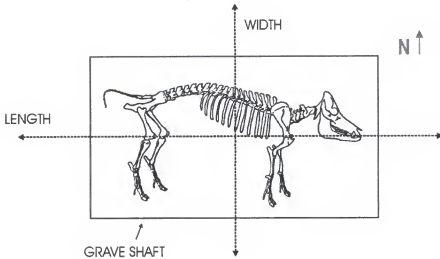


Figure 4-10. Orientation of pig cadaver within the grave and the position of the GPR transects over the grave.

GPR surveys were normally conducted with one or two volunteers. Separate individuals would operate the antenna and control unit. If a third individual was available, they would assist with the cable by preventing it from getting caught on the ground. If only two people were available, the control unit operator would occasionally assist pulling the cable. Antenna pullers were instructed to maintain a normal, continuous pace while pulling the antenna horizontally across the ground surface. If there was difficulty imaging the grave due to a walking pace that was too quick, the transect was repeated at a slower pace. Reference markers were added to each transect

by the antenna operator in order to note the beginning and end of each transect and the boundaries of each grave. Two markers were added to the beginning and end of each transect, and one marker was added at the beginning and end of each grave.

The GPR depth was calibrated in the field by scanning a metal rod that was buried in the ground at approximately 1.16 m in the Entisol. Since the metal rod was buried at a known depth, it was possible to calibrate the equipment for daily moisture changes by adjusting the dielectric constant so the depth scale was accurate. Figure (4-11) represents three profiles of the metal rod that were taken performed the same day using a different dielectric constant each time. Since the depth of the rod is at 1.16 m, the depth is adjusted by changing the dielectric constant until the apex of the anomaly is at this depth. In the first GPR profile (A), the depth of the anomaly is at 1.28 m with a dielectric constant of 3. In the third profile, (C), the depth is approximately 1.00 m with a dielectric constant of 5. Conversely, in the middle profile (B) the depth of the anomaly is almost exactly at 1.16 m at a dielectric constant of 4. During most instances of field data collection, a dielectric constant of 4 provided an accurate depth. This dielectric constant was accurate for the Entisol, but may have been slightly off for the Ultisol depending on the daily moisture conditions.

Analysis of GPR Data

The GPR files were downloaded to the computer for further analysis with RADAN for Windows NT, version 2.0.9.2, proprietary software of GSSI. The files were viewed using a Color Table of 10 and Color Xform of 11. These colors provided the optimum contrast for interpreting and detecting grave anomalies. The imagery of the grave anomalies was compared over time to qualitatively assess if the pig cadavers could

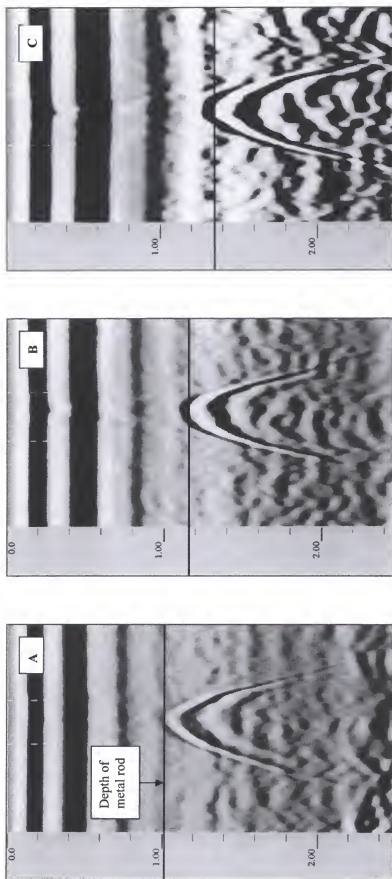


Figure 4-11. Three GPR profiles of a metal rod buried at a depth of approximately 1.16 m that were used to calibrate depth by changing the dielectric constant: A = 3, B = 4, and C = 5. The depth was accurate with a dielectric constant of 4.

be detected for the duration of the study, and how the grave anomalies changed over time from compaction of the backfill and decomposition of the pig cadaver. One objective of this study was to assess if processing of the GPR profiles to remove antenna noise (i.e. horizontal banding) was a necessity for target identification. The GPR data was processed using a boxcar filter that is a type of horizontal high pass filter. Both processed and unprocessed data were compared to assess resolution of the imagery for the cadaver anomalies and backfill increased by removing the horizontal banding. The images were then printed in gray scale.

Soil Analyses

Each cadaver was excavated to collect soil samples and assess decomposition (see the following section). Soil samples were collected on a representative number of pig burials and control burials when they were first constructed. The samples were collected every 10 cm to the bottom of the grave and two samples were collected at the bottom of the grave floor to an additional depth of 10 cm. After the pig graves and control graves were excavated, soil samples were also collected again every 10 cm for a representative number of graves. In addition, samples were also collected from the grave floor under the head, thorax, and pelvic regions after the remains were displaced to score decomposition. The soil samples collected prior to burial were compared to those collected when the cadavers were excavated to determine how soil properties changed from mixing of the backfill and products of pig decomposition and bone diagenesis.

The specific soil analyses included particle size, organic carbon, pH, extractable iron (Fe), extractable calcium (Ca), and extractable phosphorus (P). Particle-size analysis is used to determine textural classes in terms of percent clay, sand, and silt. It was used

to corroborate the physical classifications of the soils. Organic carbon content (OC) was performed to corroborate the classification of mineral soils. In mineral soils, OC must be lower than 12% and normally there is a decrease with depth (Soil Survey Staff, 1999). Both particle-size and OC were analyzed at the Environmental Pedology and Land Use Laboratory, Institute of Food and Agricultural Sciences, Soil and Water Science Department, at the University of Florida.

Extractable Ca, extractable P, extractable Fe, and pH were conducted to determine if mixing of soil horizons and products of decomposition and diagenesis changed soil chemistry. In particular, Ca and P were analyzed to determine if bone diagenesis occurred because they are the two most common minerals of bone. Extractable Ca, P, Fe, and pH were analyzed at the Analytical Research Laboratory, Institute of Food and Agricultural Sciences, Soil and Water Science Department, at the University of Florida. Statistical analyses of the soil samples were performed with *t*-tests and Pearson correlations using SPSS for Windows version 10.

Physical Analysis

Particle-size analysis was determined using the pipette method (Day, 1965). Soil samples of 50 g were treated with hydrogen peroxide and heated on hot plates to oxidize organic matter. They were then dispersed with sodium hexametaphosphate in deionized water, followed by immersion in a 20⁰ C water bath and pipetted to retrieve the clay fraction. The clay fractions were dried and weighed. Sand fractions were obtained from original sample by repeated washing to remove the remaining silt and clay. The samples were then oven-dried and weighed. The silt fraction was determined by subtraction of sand and clay weight from the original total sample weight.

Chemical Analysis

Organic carbon content was determined by a modification of the dichromate-sulfuric acid method, known as the Walkley-Black method (Soil Survey Staff, 1996). The double-acid method, more commonly known as Mehlich 1 (Mehlich, 1953), was used to determine extractable P, Ca, and Fe with a filtrate of 5 g of soil to 20 mL 0.05 M HCL + 0.0125 M H₂SO₄. pH was calculated using a 2:1 soil to water solution by glass electrode using a portable pH meter and deionized water.

Analyzing Decomposition

Each cadaver was excavated to assess decomposition and pictures taken to corroborate the written descriptions. The excavation process for each cadaver was completed in one day. After the remains were completely exposed, pictures were taken of the remains *in situ* and the orientation of the pig remains was noted in each grave. The overall gross decomposition of the body was first described and then the remains were displaced from the grave floor to accurately score the decomposition stage for each body region. The purpose of describing decomposition in this study is two fold. First, major decomposition states will be correlated with GPR imagery. Second, factors of decomposition such as cadaver size, depth, time, and soil type will also be accessed to determine their effect on decomposition of buried bodies.

Body Regions

Studying buried pig cadavers in Indiana, Thew (2000) used a scoring protocol based on five regions of the body: head, neck, thorax, abdomen and pelvis, and appendages. It was necessary to modify the regions of the body in this study based on the progression of decomposition that was observed. Decomposition was described for five

areas of the body: head, thorax, abdomen, forelimbs, and hind limbs (Table 4-5). Each of the five body regions were assigned a decomposition score based on the stage it most closely exhibited. The neck and thorax were compressed together because it was observed that they decomposed as one complex. In addition, because there is a large degree of musculature that covers the upper arm and upper thigh, the proximal ends of the femur and humerus do not undergo the same pattern of soft tissue decomposition as the rest of the appendages. Decomposition of the proximal humerus progresses more closely with the thorax, and decomposition of the proximal femur progresses more closely with the abdomen and pelvis. As a result, the proximal humerus was compressed into the thorax region and the proximal femur was compressed into the abdomen and pelvis region. Finally, each cadaver was also assigned a "Total Body" decomposition score by summing the scores from the five body regions.

Table 4-5. The anatomical regions scored for decomposition

Region of Body	Specific Skeletal Structures
Head	Cranium and mandible
Thorax	Cervical and thoracic vertebrae, rib cage, pectoral girdle, and proximal humerus
Abdomen and Pelvis	Lumbar vertebrae, pelvis, sacrum, and proximal femur
Forelimb	Upper humerus diaphysis to distal phalanges
Hindlimb	Upper femur diaphysis to distal phalanges
Total Body	Summing the scores from five body regions

Protocol for Scoring Decomposition

The scoring protocol used in this study was modified to differentiate degrees of skeletonization and not minute subjective differences in soft tissue decomposition. More recent studies using buried pig cadavers in Indiana (Thew 2000), and human bodies

deposited on the ground surface from numerous geographic areas (Megyesi 2001) have used modified versions of the scoring protocol by Galloway et al. (1989). The scoring protocol by Galloway et al. (1989) is based on surface depositions of human bodies in the southern Arizona. It consists of five major stages: fresh, early decomposition, advanced decomposition, skeletonization, and extreme decomposition. Each major stage is then further divided into numerous substages. Thew (2000) modified the scoring protocol by Galloway et al. (1989) for burials by using three main categories: early decomposition, advanced decomposition, and skeletonization. The advanced decomposition and skeletonization stages were further modified by Thew (2000) to directly correlate the decomposition progression of buried pig cadavers.

The scoring protocol used in this study was devised to directly reflect the decomposition progression of buried pig cadavers in Florida and to assess major decomposition stages and not subtle changes within each stage. It was necessary to devise a scoring system to address the goals in this study (i.e. correlate state of decomposition with GPR imagery), and to reduce the subjectivity of scoring areas of the body that could be assigned to more than one decomposition stage if a liberal scoring system was used. This study used a modified version of the scoring method outlined by Thew (2002). Although Thew (2000) incorporated three major categories, this study omitted the early decomposition category because the remains were not fresh. Furthermore, the last stage, extreme decomposition, used by Galloway et al. (1989) was omitted because the remains were not buried long enough for bone degradation. The scoring protocol incorporates two major stages: advanced decomposition and skeletonization, with scores ranging from 1 to 7 (Table 4-6).

Table 4-6. Decomposition criteria used in scoring decomposition of the body regions for the pig cadavers.

Major Categories	Description of Decomposition Stage	Score
Advanced Decomposition	Extensive preservation of internal structures with areas of preserved flesh.	1
	Mummification or moist tissue decomposition with no bone exposure; either minimal retention of internal structures or no preserved structures.	2
	Mummification or moist decomposition of outer tissues with only internal structures lost; bone exposure less than one-quarter of the area.	3
	Mummification or moist decomposition with bone exposure of one-quarter to one-half the area.	4
Skeletonization	Bone exposure of one-half to three-quarters of the area.	5
	Bone exposure of more than three-quarters of the area.	6
	Bone fully skeletonized	7

Adapted from Thew HA. 2000. Effects of lime on the decomposition of buried remains. Master's Thesis in Human Biology, University of Indianapolis, Indiana, p. 33, Table 3.

Modifications of the scoring protocol in Table 4-6 were required for the thorax and limbs. If there was minimal rib exposure of the thorax due to it caving in and not from decomposition, the minimal bone exposure was ignored and a score was assigned that was more consistent of the entire decomposition stage of this region. Also, if both of the forelimbs or hindlimbs were at different states of preservation, an average score was used to represent these body regions. For example, if the right hindlimb was assigned a score of 5 and the left hindlimb a score of 1, the average score for the hindlimbs would be 3. Finally, adipocere development was noted but not scored because it does not appear to correlate to specific degrees of decomposition (Evans 1963, Thew 2000).

Statistical Analysis

Table 4-7 summarizes the main variables that were used in this study. The dependent variable, decomposition state, was scored as a pseudocontinuous variable ranging from 1 to 7 (Table 4-6) because the progression of decomposition is a continuous process that cannot be scored very precisely. The dependent variables included the head, thorax, abdomen, forelimb, hindlimb, and the total body decomposition that was calculated by summing the five independent decomposition scores of each cadaver. The independent variables are ordinal, categorical variables and were assigned either a 1 or 2 for statistical purposes. For SIZE, 1 indicated a small cadaver and 2 a large cadaver. For TIME, 1 indicated a short-time period between 12 to 13.25 months, and 2 indicated a long-time period between 21 to 21.5 months. For DEPTH, 1 indicated a shallow depth between 50 to 60 cm, and 2 indicated a deep depth between 100 to 110 cm. Furthermore, SOIL was not analyzed statistically because it was not controlled for with the small cadavers. While only half of the large pig cadavers were buried in proximity to the clay, all of the small cadavers were buried in the Entisol without the clay.

To assess differences in decomposition, full-model analysis of variance (ANOVA) analyses were run to examine the effects of the independent variables on the expression of decomposition. ANOVA is used to analyze data sets that are comprised of multiple independent variables that simultaneously affect the dependent variable. Unlike bivariate analysis, ANOVA can analyze multiple independent variables at once to assess their interactions. The theoretical model that can best explain the relationship between the variables in this study is:

$$\text{Decomposition State} = \text{SIZE} + \text{DEPTH} + \text{TIME} + \text{SIZE*DEPTH} + \text{SIZE*TIME} + \\ \text{DEPTH*TIME} + \text{SIZE*DEPTH*TIME} + \text{Error}$$

SIZE, DEPTH, and TIME are the main effects in this model, and SIZE*DEPTH, SIZE*TIME, DEPTH*TIME, and SIZE*DEPTH*TIME are the interactions among the independent variables. The statistical program used to perform the ANOVAs was SYSTAT 5.2.1 for the Macintosh.

Table 4-7. Summary of dependent and independent variables used for the statistical analysis of decomposition.

Variable	Type	Scale	Character States
Decomposition state for five body regions	Dependent	1 to 7	See Table 4-6
Total Body decomposition score	Dependent	5 to 35	Sum scores from five body regions
SIZE	Independent	1 or 2	Small or large
TIME	Independent	1 or 2	Short or long
DEPTH	Independent	1 or 2	Shallow or deep

Summary

This study used 20 pig cadavers buried in an open field in Alachua County, Florida for up to 21.5 months at depths ranging between 0.50 to 1.10 m. Graves were monitored monthly with GPR using both 900- and 500-MHz antennae. At the termination of the GPR monitoring period, the graves were excavated to collect soil samples and score decomposition of each cadaver.

CHAPTER 5 DECOMPOSITION RESULTS

As stated in Chapter 4, the decomposition state of each pig cadaver is first described with an emphasis on degree of skeletonization, rather than minute changes in soft tissue decomposition. This is followed by comparisons of the average scores of the five body regions for the small and large groups of pig cadavers in order to assess overall patterns of decomposition. Finally, the results of the four independent variables are discussed in terms of their relationship to decomposition. Abbreviations are used for the eight pig cadaver scenarios in each of the results chapters for easier reading of the text and interpretation of the figures (Table 5-1). In addition, the raw decomposition scores are listed in Table 5-2.

Table 5-1. Abbreviations for each of the eight pig cadaver scenarios

Abbreviation	Scenario
LSLU	large, shallow, long-time period, and Ultisol
LSSU	large, shallow, short-time period, and Ultisol
LDSU	large, deep, short-time period, and Ultisol
LDLU	large, deep, long-time period, and Ultisol
SSLE	small, shallow, long-time period, and Entisol
SSSE	small, shallow, short-time period, and Entisol
SDSE	small, deep, short-time period, and Entisol
SDLE	small, deep, long-time period, and Entisol

Table 5-2. Raw decomposition scores for the 20 cadavers in this study.

Cadaver							
Number	Scenario	Head	Thorax	Abdomen	Forelimbs	Hindlimb	Total
1	LDLU	4	2	2	3	3	14
2	LDLU	4	2	2	4	4	16
3	LDLU	4	2	2	4	3	15
4	LSSU	7	7	6	7	7	34
5	LSLU	7	7	7	7	7	35
6	LSLU	7	7	7	7	7	35
7	LSLU	7	7	7	7	7	35
8	LDSU	4	1	1	3.5	3.5	13
9	LDSU	4	1	1	2.5	1	9.5
10	LDSU	5	1	1	3	3	13
11	LSSU	4	2	2	3	4	15
12	LSSU	6	4	4	7	6.5	27.5
13	SDLE	4	2	2	4	4	16
14	SDLE	4	2	2	5	4	17
15	SSLE	7	7	7	7	7	35
16	SSLE	7	7	7	7	7	35
17	SDSE	3	2	2	4	3.5	14.5
18	SDSE	4	2	2	4.5	5	17.5
19	SSSE	6	6	7	7	7	33
20	SSSE	5	2	2	5	4	18

Gross Decomposition Changes

LSSU Scenario

There was a considerable degree of variation in skeletonization of the large, shallow pig cadavers (4, 11, and 12) buried between 12 and 13 months for the LSSU scenario. Cadaver 4 was almost completely skeletonized, exhibiting a small amount of mummified tissue in the abdominal area. Wet adipocere was also noted in the head, thorax, and abdomen regions. Furthermore, an ant infestation was noted in the pig remains during the excavation.

Cadaver 12 exhibited the median degree of skeletonization within this group. While the forelimbs were completely skeletonized, one hindlimb was completely skeletonized and the other still retained a small amount of mummified tissue on the femur. An average decomposition score of 6.5 (7 and 6) was assigned to the forelimbs. The head was more than 75% skeletonized and mummified tissue was still retained on the inferior surface in contact with the grave floor. The thorax and abdomen still retained a considerable amount of mummified hide and there was less than 50% bone exposure at these regions. Mummified tissue of varying degrees and adipocere was also present in the head, thorax, and abdomen regions.

Finally, cadaver 11 exhibited the least advanced decomposition. The head was less than 50% skeletonized, with skeletonization on the face and mandible. Both the forelimbs and hindlimbs retained a fair amount of mummified tissue. The forelimbs were less than 25% skeletonized and the hindlimbs were less than 50% skeletonized, with skeletonization of the distal ends of the limbs. In stark contrast to the other two pig

cadavers in this group, there was incredible preservation of the thorax and abdomen, which were both assigned decomposition scores of 2. A number of rib ends were sticking out of the mummified hide due to collapsing of the body cavity. The bone exposure was ignored when assigning a decomposition score to the thorax because there was extensive moist decomposition products and minimal preservation of structures. The abdomen also retained extensive moist decomposition products and minimal preservation of structures. Overall, the average scores (Figure 5-1) for the head, hindlimbs, and forelimbs are fairly advanced, while the average scores for the thorax and abdomen are less advanced because of the decreased decomposition of pig 11.

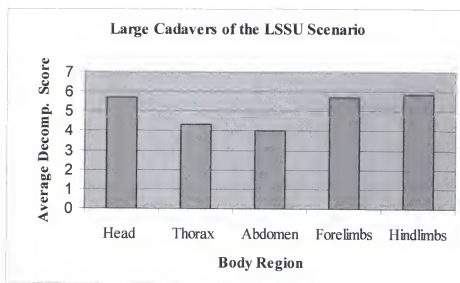


Figure 5-1. Average scores (five body regions) of the three large cadavers (4, 11, and 12) at 12 to 13 months for the LSSU scenario.

LSLU Scenario

Overall, all of the three large, shallow cadavers (5-7) at 21.5 months for the LSLU scenario were completely skeletonized and received the highest possible decomposition

score of 35 (Figure 5-2). Dry adipocere was present in all of the graves in the abdominal area. In addition, there was minimal retention of moist adipocere on the inferior surfaces of the bones comprising the shoulder and pelvic girdles that were in contact with the grave floor.

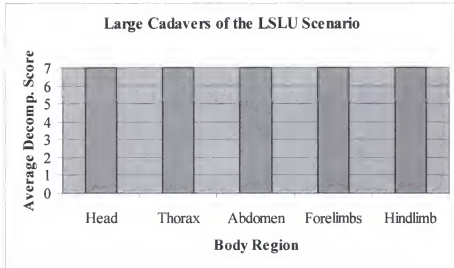


Figure 5-2. Average scores (five body regions) of the three large cadavers (5, 6, and 7) at 21.5 months for the LSLU scenario. The three cadavers were completely skeletonized, which reflects the advanced scores.

LDSU Scenario

The decomposition patterns of the three large, deep cadavers (8, 9, and 10) at 13 months for the LDSU scenario were the least decomposed of the entire study group (Figure 5-3). Overall decomposition of the abdomen and thorax regions was consistent among the three cadavers. There was no bone exposure in the thorax and abdomen and there was extensive preservation of internal structures. At the same time, the inferior surface of the hide that was in contact with the grave floor still retained relatively fresh skin. In addition, in grave 12, a large mass of adipocere was noted under the trunk.

The decomposition state of the head region was fairly consistent between the three cadavers. Each cadaver was assigned a decomposition score of 4 or 5 for the head region. Cadavers 8 and 9 still retained mummified tissue and moist decomposition products at the head region and were less than 50% skeletonized, with skeletonization of the face and mandible. The head region of cadaver 10 was between 50% and 75% skeletonized at the head and snout, while pink flesh was still retained in the oral cavity.

There was considerable variation in the degree of skeletonization of the limbs. The forelimbs of cadaver 10 exhibited differing stages of preservation. While the upper forelimb was between 50% and 75% skeletonized, the bottom forelimb still retained areas of fresh skin and muscle. Decomposition of the limb was reduced because it was protected by the body trunk. A decomposition score of 3 was assigned by averaging the scores from both limbs (5 and 1). Decomposition of the lower limbs was also reduced with both limbs exhibited less than 25% skeletonization.

The limbs of cadaver 9 exhibited the least advanced decomposition scores of the LDSU group. The forelimbs were assigned an average score of 2.5 (4 and 1). While the upper forelimb exhibited less than 50% bone exposure, the bottom forelimb still retained areas of fresh skin and muscle. At the same time, the hindlimbs of cadaver 9 received a score of 1 because both limbs retained areas of fresh skin and muscle. Lastly, the forelimbs and hindlimbs of cadaver 8 were in similar states of decomposition and both received average decomposition scores of 3.5 (3 and 4). While the upper forelimb and hindlimb were between 25% and 50% skeletonized, the lower limbs were less than 25% skeletonized. Overall, the decomposition of the thorax and abdomen is significantly less than the other body regions, while the head is the most advanced region (Figure 5-3).

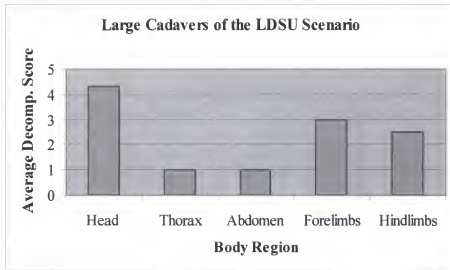


Figure 5-3. Average scores (five body regions) of the three large cadavers (8, 9, and 10) at 13 months for the LDSU scenario. The three cadavers were the least decomposed of the study group, which reflects their low scores.

LDLU Scenario

Overall, the degree of decomposition for the large cadavers (1, 2, and 3) buried in the deep graves for 21 months in the LDLU scenario was consistent among the cadavers. There was extensive mummification of the hide with limited bone exposure (Figure 5-14). The head was between 25% and 50% skeletonized with portions of the maxilla and mandible exposed. The thorax and abdomen exhibited the same degree of decomposition. There was no bone exposure, the abdomen was collapsed, the hide was mummified, there were no apparent internal structures present, but decomposition products were still retained. The major difference in decomposition was the degree of bone exposure of the limbs. Less than 25% of the hindlimbs and forelimbs were skeletonized with cadaver 1. The degree of skeletonization of the limbs was increased for the other two cadavers. Cadaver 2 exhibited between 25% and 50% skeletonization of the forelimb and hindlimbs. Cadaver 3 exhibited between 25% and 50%

skeletonization of the forelimb and less than 25% of the hindlimbs. Overall, the skeletonization of the thorax and abdomen was significantly less than the other body regions (Figure 5-4).

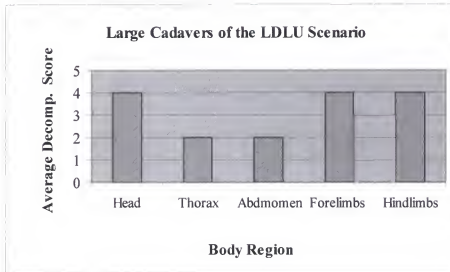


Figure 5-4. Average scores (five body regions) of the three large cadavers (1, 2 and 3) at 21 months for the LDLU scenario.

SSSE Scenario

The pattern of decomposition for the two small, shallow cadavers (19 and 20) at 13.25 months for the SSSE scenario was highly variable. Cadaver 19 exhibited completely skeletonized forelimbs, hindlimbs, and abdomen, while the head and thorax were more than 75% skeletonized. A small amount of moist tissue and decomposition products were still retained on the underside of the bones adjacent to the ground and along the thoracic vertebrae. Conversely, cadaver 20 still exhibited a fair degree of moist and mummified tissue. Both the thorax and abdomen were completely covered with mummified hide and extensive moist decomposition products were retained. A small

amount of adipocere was noted in the grave, particularly along the thoracic segment of the spinal column. The head was between 50% and 75% skeletonized, with the face and top of the skull clean. The forelimb was between 50% and 75% skeletonized and the hindlimb was less than 50% skeletonized. The extensive soft tissue that was still retained on cadaver 20 resulted in average decomposition scores that does not reflect the extensive skeletonization of cadaver 19 (Figure 5-5).

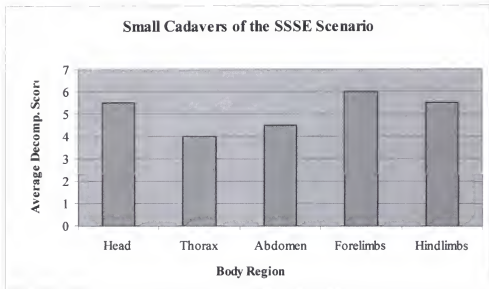


Figure 5-5. Average scores (five body regions) of the two small cadavers (19 and 20) at 13.25 months for the SSSE scenario.

SSLE Scenario

Overall, the small, shallow cadavers (15 and 16) at 21 months for the SSLE scenario were completely skeletonized and received the highest possible decomposition score of 35 (Figure 5-6). Minimal dry adipocere was present for both cadavers particularly in the thoracic region.

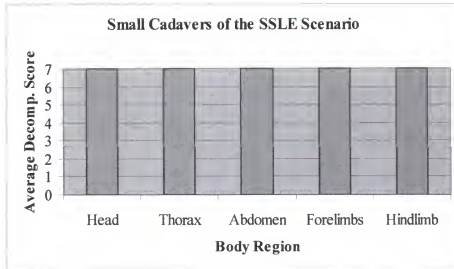


Figure 5-6. Average scores (five body regions) of the two small cadavers (15 and 16) at 21 months for the SSLE scenario. The three cadavers were completely skeletonized, which reflects the advanced scores.

SDSE Scenario

The pattern of decomposition for the two small, deep cadavers (17 and 18) at 13 months for the SDSE scenario was similar. The decomposition pattern of the thorax and abdomen were both identical. While there was no bone exposure or retention of internal structures, there was extensive preservation of decomposition products. Furthermore, there was minor variation in skeletonization of the head and limbs for both cadavers. The head region of cadaver 17 was less than 25% skeletonized. While both forelimbs were between 25% and 50 % skeletonized, the forelimbs were assigned an average score of 3.5 (3 and 4). The exposed limb on the top was between 25% and 50% skeletonized, and the lower limb was less than 25% skeletonized.

The bone exposure of the head and limbs of cadaver 17 were slightly more advanced than cadaver 18. The head was between 25% and 50% skeletonized. While both hindlimbs were between 50% and 75% skeletonized, the forelimbs were assigned an

average score of 4.5 (4 and 5). The exposed limb on the top was skeletonized between 50% and 75%, and the lower limb was less than 50% skeletonized. Overall, the skeletonization of the thorax and abdomen was significantly less than the other body regions (Figure 5-7).

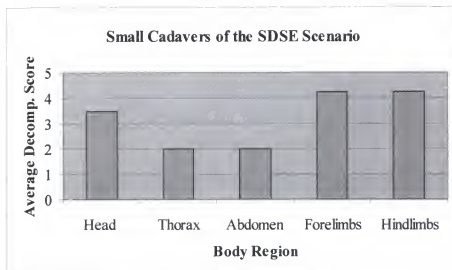


Figure 5-7. Average scores (five body regions) for the two small cadavers (17 and 18) at 13 months for the SDSE scenario.

SDLE Scenario

Interestingly, the progression of decomposition for the two small deep pig cadavers (13 and 14) at 21 months for the SDLE scenario was very similar to the decomposition pattern of the two small deep cadavers at 13 months (SDSE scenario). The decomposition extent of thorax and abdomen was identical for cadavers 13 and 14. There was no bone exposure or retention of internal structures; however, there was extensive preservation of soft tissue products. In addition, there was almost no variation in decomposition at the head and limbs between both cadavers. Both of the heads and

hindlimbs were between 25% and 50 % skeletonized. While the forelimbs of cadaver 13 were between 25% and 50% skeletonized, the forelimbs of cadaver 14 were between 50% and 75% skeletonized.

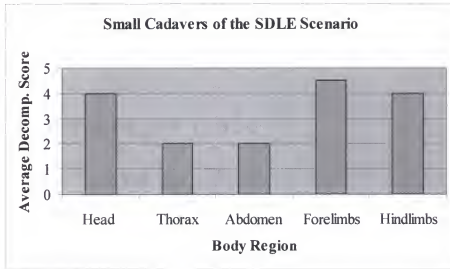


Figure 5-8. Average scores (five body regions) of the two small cadavers (13 and 14) at 21 months for the SDLE scenario.

General Patterns of Decomposition

Herein, general trends in the pattern of decomposition are described for the small and large cadaver scenarios. In Figure 5-9, the average scores for three (SDSE, SSSE, and SDLE) of the four groups of small pig cadavers is plotted to compare the decomposition patterns. The group of small pig cadavers that were buried at a shallow depth for the long-time period (SSLE) was not plotted with the other three groups because they were completely decomposed. Regardless of the scenario, the decomposition rate of the thorax and abdomen regions was always reduced in comparison to the head and limbs. The decomposition state for the limbs was slightly more advanced

then the head region for the deep cadavers regardless of the amount of time buried.

However, for the shallow cadavers, the decomposition rate of the head region was similar to the limbs, and the forelimbs were slightly more decomposed than the hindlimbs.

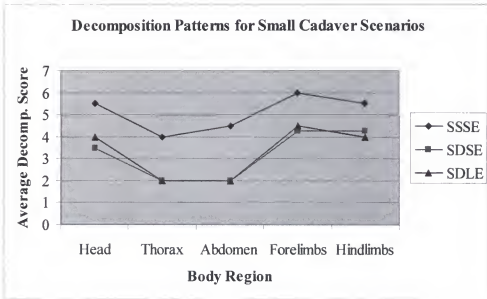


Figure 5-9. Decomposition patterns for three of the small cadaver scenarios by body region.

In Figure 5-10, the average scores for three (LDLU, LSSU, and LDSU) of the four groups of large pig cadavers is plotted to compare the decomposition patterns. The group of large pig cadavers that were buried at a shallow depth and for the long-time period (LSLU) was not plotted with the other three groups because they were completely decomposed. Regardless of the scenario, the decomposition rate of the thorax and abdomen body regions was always significantly reduced in comparison to the head and limbs.

The head region is the most advanced region for the deep pig cadavers, regardless of time buried. The decomposition rate of the head region is just as advanced as the limbs. Interestingly, while the decomposition progression was slightly more advanced for the hindlimbs in comparison with the forelimbs of the shallow graves, the opposite pattern was observed with the graves that were buried at deep depths regardless of time period. In both instances, the forelimbs were slightly more decomposed than the hindlimbs.

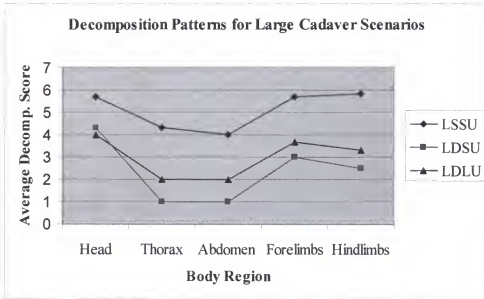


Figure 5-10. Decomposition patterns for three of the large cadaver scenarios by body region.

Overall, similar patterns of decomposition were observed for the pig cadavers regardless of size. The distal ends of the limbs and the snout were the first areas to become skeletonized. Skeletonization progression continued with the limbs and head region. The trunk was the last area to become skeletonized. Out of the five regions that

were scored, the thorax and abdomen followed similar patterns of decomposition and were always the last body regions to become skeletonized.

Independent Variables

The following section will discuss the results of decomposition on the independent variables DEPTH, TIME, SIZE and the interactions between the variables using ANOVA analysis. The ANOVA analyses are first listed in six tables corresponding to each of the dependent variables that were studied: the total body score (Table 5-3), head (Table 5-4), thorax (Table 5-5), abdomen (Table 5-6), forelimb (Table 5-7), and hindlimb (Table 5-8). Next, the results of the ANOVA analyses are discussed within each section corresponding to the independent variables DEPTH, TIME, SIZE, and the interactions between the variables. The effect of SOIL is discussed qualitatively in a separate section while only emphasizing decomposition patterns of deep burials.

Table 5-3. ANOVA results for the total body score

Dependent Variable: Total Body					
Number: 20					
Multiple R: 0.909					
Squared Multiple R: 0.826					
Source	Sum-of-Squares	DF	Mean-Square	F-Ratio	P-value
SIZE	9.633	1	9.633	0.368	0.555
DEPTH	1140.833	1	1140.833	43.576	0.000
TIME	154.133	1	154.133	5.887	0.032
SIZE*DEPTH	9.633	1	9.633	0.368	0.555
SIZE*TIME	2.133	1	2.133	0.081	0.780
DEPTH*TIME	70.533	1	70.533	2.694	0.127
SIZE*DEPTH*TIME	2.133	1	2.133	0.081	0.780
Error	314.167	12	26.181		

Table 5-4. ANOVA results of the head region

Dependent Variable: Head					
Number: 20					
Multiple R: 0.914					
Squared Multiple R: 0.836					
Source	Sum-of-Squares	DF	Mean-Square	F-Ratio	P-value
SIZE	0.300	1	0.300	0.568	0.465
DEPTH	23.133	1	26.133	49.576	0.000
TIME	2.700	1	2.700	5.116	0.043
SIZE*DEPTH	0.133	1	0.133	0.253	0.624
SIZE*TIME	0.300	1	0.300	0.568	0.465
DEPTH*TIME	2.133	1	2.133	4.042	0.067
SIZE*DEPTH*TIME	0.133	1	0.133	0.253	0.624
Error	6.333	12	0.528		

Table 5-5. ANOVA results of the abdomen region

Dependent Variable: Abdomen					
Number: 20					
Multiple R: 0.909					
Squared Multiple R: 0.827					
Source	Sum-of-Squares	DF	Mean-Square	F-Ratio	P-value
SIZE	0.675	1	0.675	0.395	0.541
DEPTH	72.075	1	72.075	42.190	0.000
TIME	12.675	1	12.675	7.420	0.018
SIZE*DEPTH	0.075	1	0.075	0.044	0.838
SIZE*TIME	0.675	1	0.675	0.395	0.541
DEPTH*TIME	0.675	1	0.675	3.556	0.084
SIZE*DEPTH*TIME	0.075	1	0.075	0.044	0.838
Error	20.500	12	1.708		

Table 5-6. ANOVA results of the thorax region

Dependent Variable: Thorax					
Number: 20					
Multiple R: 0.909					
Squared Multiple R: 0.826					
Source	Sum-of-Squares	DF	Mean-Square	F-Ratio	P-value
SIZE	0.133	1	0.133	0.077	0.786
DEPTH	70.533	1	70.533	40.955	0.000
TIME	13.333	1	13.333	7.742	0.017
SIZE*DEPTH	0.533	1	0.533	0.310	0.588
SIZE*TIME	0.133	1	0.133	0.077	0.786
DEPTH*TIME	6.533	1	6.533	3.794	0.075
SIZE*DEPTH*TIME	0.533	1	0.533	0.310	0.588
Error	20.677	12	1.722		

Table 5-7. ANOVA results of the forelimb region

Dependent Variable: Forelimb					
Number: 20					
Multiple R: 0.863					
Squared Multiple R: 0.745					
Source	Sum-of-Squares	DF	Mean-Square	F-Ratio	P-value
SIZE	1.752	1	1.752	1.454	0.251
DEPTH	31.519	1	31.519	26.160	0.000
TIME	3.169	1	3.169	2.630	0.131
SIZE*DEPTH	0.919	1	0.919	0.763	0.400
SIZE*TIME	0.169	1	0.169	0.140	0.715
DEPTH*TIME	0.602	1	0.602	0.500	0.493
SIZE*DEPTH*TIME	0.002	1	0.002	0.002	0.968
Error	14.458	12	1.205		

Table 5-8. ANOVA results of the hindlimb region

Dependent Variable: Hindlimb					
Number: 20					
Multiple R: 0.882					
Squared Multiple R: 0.778					
Source	Sum-of-Squares	DF	Mean-Square	F-Ratio	P-value
SIZE	1.302	1	1.302	1.045	0.327
DEPTH	37.969	1	37.969	30.460	0.000
TIME	3.169	1	3.169	2.542	0.137
SIZE*DEPTH	2.269	1	2.269	1.820	0.202
SIZE*TIME	0.169	1	0.169	0.135	0.719
DEPTH*TIME	1.302	1	1.302	1.045	0.327
SIZE*DEPTH*TIME	0.602	1	0.602	0.483	0.500
Error	14.958	12	1.247		

DEPTH

Overall, DEPTH was the main factor controlling decomposition. The total body score ($p < 0.001$) and each of the five body regions including the head ($p < 0.001$), thorax ($p < 0.001$), abdomen ($p < 0.001$), forelimbs ($p < 0.001$), and hindlimbs ($p < 0.001$) were all highly significant in the ANOVA analyses (see Tables 5-3 to 5-8). The relationship between depth and decomposition is inversely related; at greater depths, decomposition slows. A comparison of the average decomposition scores for the total category, clearly demonstrates this relationship when the pig cadavers are placed into deep and shallow groups. For example, in Figure 5-11, all of the shallow cadavers (LSLU, SSLE, LSSU, and SSSE) have the most advanced decomposition scores regardless of SIZE. Both large and small groups of shallow cadavers buried for the long-time period (LSLU and SSLE) were completely skeletonized and received the highest possible decomposition scores of

35. Furthermore, both large and small groups of shallow cadavers buried for the short-time period (LSSU and SSSE) have identical advanced scores of 25.5. Conversely, the average total scores, ranging from 12.67 to 16.5, for the four groups of deep cadavers (SDLE, SDSE, LDLU, and LDSU) are considerably less than the scores of the shallow cadavers (LSLU, SSLE, LSSU, and SSSE), and they all cluster together regardless of SIZE or TIME.

A comparison of decomposition patterns for the five body regions also demonstrates the correlation between decomposition and DEPTH. All five body regions were completely skeletonized for the shallow cadavers (LSLU and SSLE), regardless of SIZE, that were buried for the long-time interval (Figure 5-12). Similarly, the decomposition scores for the body regions are of near similar patterns for the shallow cadavers (LSSU and SSSE), regardless of SIZE, that were buried at the short-time interval.

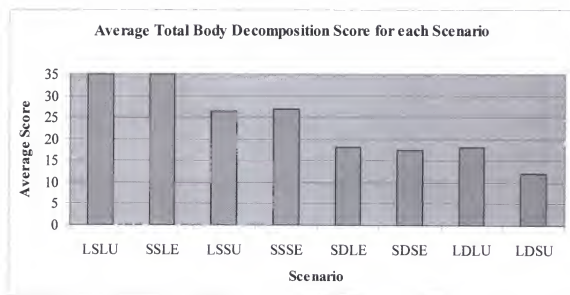


Figure 5-11. Average total body decomposition scores for each of the eight pig cadaver scenarios.

Furthermore, the role of DEPTH for each body region is also evident with the deep cadavers when analyzing the average scores for each body region (Figure 5-13). Overall, the decomposition of the pelvis and abdomen were significantly reduced in the deep groups. In three groups (SDSE, SDLE, and LDU) regardless of SIZE or TIME, the thorax and pelvis were assigned the identical scores of 2 and the fourth group (LDSU) was assigned a score of 1. Interestingly, regardless of TIME, both groups of small cadavers, SDSE and SDLE, also have almost identical scores for each of the five body regions.

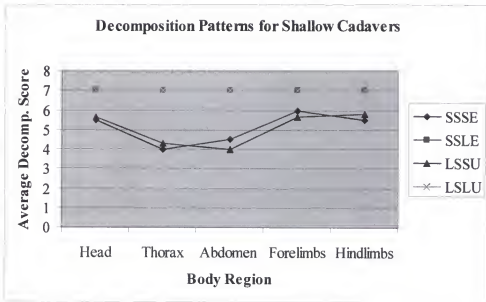


Figure 5-12. Average decompositions scores for each body region of large and small pig cadavers buried at shallow depths.

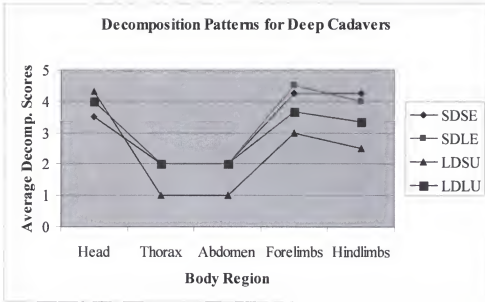


Figure 5-13. Average decomposition scores for each body region of large and small pig cadavers buried at deep depths.

TIME

Overall, TIME was also a factor controlling decomposition for the head, thorax, abdomen and total score. While the head ($p = 0.043$), thorax ($p = 0.018$), abdomen ($p = 0.017$), and total score were all significant at the $p < 0.05$ level, decomposition was not significant for the forelimbs ($p = 0.131$) and hindlimbs ($p = 0.137$). Hence, the longer the duration the more advanced the decomposition state. In a comparison of the total body decomposition scores of the cadavers in Figure 5-11, it is apparent that the shallow cadavers buried for the long-time period (LSLU and SSLE) are noticeably more decomposed than those of the short-time period (LSSU and SSSE). Conversely, decomposition was considerably reduced for the deep cadavers. While there is very little variation in decomposition between the small cadavers buried for the long-time period (SDLE) with those of the short-time period (SDSE), the large cadavers buried

for the long-time period (LDLU) were slightly more decomposed than those of the short-time period (LDSU) (Figure 5-11).

The relationship between decomposition and the body regions is discussed using Figures 5-12 and 5-13. Clearly, decomposition is increased at the thorax and abdomen with TIME for the shallow and deep cadavers. Although decomposition of the head region is variable for TIME with the deep cadavers (Figure 5-13), there is a stronger relationship with the shallow cadavers. Decomposition of the head is greater for the shallow cadavers interred for the long-time frame (LSLU and SSLE) compared to the cadavers interred for the short-time frame (LSSU and SSSE) (Table 5-12). Furthermore, the limbs regions were not significant for TIME because decomposition of the limbs was variable for the deep graves (Figure 5-13)

SIZE

Overall, SIZE was not a factor controlling decomposition for each of the body regions and the total score. Neither the head ($p = 0.465$), thorax ($p = 0.541$), abdomen ($p = 0.786$), forelimb ($p = 0.251$), hindlimb ($p = 0.327$) regions nor the total score ($p = 0.555$) were significant at the $p < 0.05$ level (see Tables 5-3 to 5-8). A comparison of the average decomposition scores for the total category further supports this conclusion. For example, in Figure 5-11, all of the shallow cadavers have the most advanced decomposition scores regardless of SIZE. Furthermore, both the large and small, shallow cadavers interred for the long-time period cluster together with identical scores, and the large and small shallow cadavers interred for the short-time period both have identical advanced scores of 25.5. At the same time, all of the average total scores for the deep graves, ranging from 12.67 to 16.5, are considerably less than the shallow scores, and they all cluster together regardless of SIZE or TIME.

Interactions among DEPTH, TIME, and SIZE

None of the interactions among the variables were significant in the ANOVA analysis. These results were surprising considering that both DEPTH and TIME were significant for the head, thorax and abdomen regions as well as the total body score. The interactions between DEPTH*TIME were not significant at the $p < 0.05$ level for the head ($p = 0.067$), thorax ($p = 0.075$), abdomen ($p = 0.084$), and total body score ($p = 0.127$). Clearly there is a strong relationship with decomposition of the shallow burials and the length of time they were buried. For example, in a comparison of the total body decomposition scores of only the shallow pig cadavers in Figure 5-11, it is apparent that the cadavers interred for the long-time period (LSLU and SSLE) are more decomposed than those of the short-time period (LSSU and SSSE). Conversely, decomposition was considerably reduced for the deep cadavers. The total decomposition scores for the four deep groups (SDLE, SDSE, LDLU, and LDSU) do not cluster by length of time buried, rather all four groups cluster together into one group (Figure 5-11). Therefore, the reduced decomposition rates of the deep cadavers decreased the significance of the DEPTH*TIME interaction.

SOIL

Since only the large deep cadavers were buried at the deep depth in the Ultisol near the clay horizon, it was not possible to statistically assess the role of SOIL because there were no small cadavers buried in proximity to this horizon. However, some general conclusions will be discussed by comparing the decomposition patterns of the deep cadavers in Figure 5-13. SIZE will be ignored because it does not appear to be a major factor with DEPTH. For the short-term groups (SDSE and LDSU), the decomposition

state of the thorax, abdomen, forelimbs was less for the LDSU group in proximity to the argillic horizon. Regardless of length of burial, the decomposition state of the forelimbs and hindlimbs for both groups of large cadavers (LDSU and LDLU) was less than that of both groups of small cadavers (SDSE and SDLE) that were in sand (Figure 5-13).

Finally, if proximity to the argillic horizon reduces decomposition, it is not a factor at the head region because the decomposition pattern observed on the four deep groups of cadavers cluster together regardless of SOIL, TIME, or SIZE (Figure 5-13). Furthermore, the large cadavers buried near the argillic horizon for the short-time period exhibited the most advanced decomposition pattern (Figure 5-13). Overall, it is possible that the reduced decomposition observed at different body regions of the large cadavers, particularly the forelimbs and hindlimbs, was caused by their proximity to the argillic horizon and not their size.

Summary

Overall, DEPTH was the most significant factor controlling decomposition for the total body score and all five body regions. TIME was also a significant factor controlling decomposition, but only for the head, thorax, abdomen, and total score. SIZE was not a factor in this study for the total body score or any of the five body regions. In addition, none of the interactions among the independent variables (SIZE, DEPTH, and TIME) were significant in the ANOVA analysis. Although DEPTH and TIME were significant when analyzed separately, the interaction between these variables was not significant because of the reduced decomposition rates of the deep cadavers. Furthermore, although the clay horizon may have slowed decomposition slightly, SOIL does not appear to be a major factor of decomposition in this study.

Regardless of geographical area or the research design of controlled decomposition studies of burials, depth and time are going to be important factors of decomposition. For example, in another study using a large sample of 22 buried pig cadavers in the Midwest, Thew (2001) also concluded that both depth and time were significant factors of decomposition even though her research design was structured differently than this study. Thew (2001) was assessing the role of lime with decomposition and analyzed pits that included multiple pig cadavers, with and without lime, and not graves containing a single cadaver. Her study also differed from this research because the cadavers were smaller, they were buried at different depths, and they were excavated at different time periods.

CHAPTER 6 SOIL ANALYSES

Florida's Soils

Before the soils that were used in this study are described, characteristics used to define the soil Orders in Florida will be briefly discussed because of the emphasis in choosing soils with optimum conditions for GPR. Unless otherwise cited, all of the technical information concerning "Soil Taxonomy" is from Soil Survey Staff (1999). The highest category in Soil Taxonomy is the soil Order. There are seven of the 12 recognized soil Orders in the state of Florida: Alfisols, Entisols, Histosols, Inceptisols, Mollisols, Spodosols, and Ultisols (Collins 1997). To classify soils to the Order level, the diagnostic horizons that are present must be known. These horizons indicate the degree and kind of soil forming processes that have occurred and include two types: a diagnostic surface horizon (epipedon) and a diagnostic subsurface horizon. In addition, soils are commonly inspected to a depth of 2 m for classification purposes; however, some soils are shallower while others have diagnostic features below this depth.

Diagnostic Surface Horizons

A diagnostic surface horizon, called an "epipedon", is at the soil surface. It includes the upper part of soil darkened by organic matter and may also include any eluvial horizon. Four epipedons exist in Florida: the histic, mollic, umbric, and ochric. Summary data of the four epipedons in Florida's soils is in listed in Table 6-1. They will be described because they are either important for soil classification at the Order level

(mollic and ochric) or may limit the potential of GPR applications (histic, mollic, and umbric).

Table 6-1. Summary data of the four epipedons used to classify Florida's soils.

Epipedon	Base Saturation	Color (moist)	Thickness	Organic Content	Horizon Type	General Description
Histic	High	Dark 10YR 2/1, 2/2	20 to 60 cm	>12%	Organic	Saturated 30 days or more in a year
Mollic	>50%	Dark 10YR 3/3 or less	>25 cm	≥0.6 to 12%	Mineral	Moist three months a year
Umbric	<50%	Dark 10YR 3/3 or less	>25 cm	≥0.6 to 12%	Mineral	Similar to Umbric but less than 50% base saturation
Ochric	0 to 100%	Light 10YR 4/4 or more	<25 cm	≤0.6%	Mineral	Fails to meet the definition of other epipedons

Histic epipedon

The histic epipedon is a dark, thick organic layer (20 to 60 cm) of peat or muck that overlies a mineral soil. It may be at the soil surface or buried and has a very high organic content (>12%) and is normally saturated for 30 or more cumulative days a year. Furthermore, it is the only epipedon in Florida that is organic in nature.

Ochric epipedon

The ochric epipedon is a mineral horizon and is the most common epipedon. It is recognized by failing to meet the definitions of other epipedons; it is too light, too thin, too dry, and contains too little organic carbon. Furthermore, the ochric epipedon may be hard and massive when dry because of its low organic matter content.

Mollic epipedon

The mollic epipedon is a mineral horizon that is noted for its dark color, dark brown to black, strong structure, and is associated with an accumulation of organic matter (≥ 0.6 to 12 % organic carbon) and thickness (generally >25 cm). It has a high base saturation (greater than 50%) and is moist at least three months a year.

Umbric epipedon

The umbric epipedon has the same general characteristics as the mollic epipedon except the base saturation is less than 50%.

Diagnostic Subsurface Horizons

A diagnostic subsurface horizon forms below the surface of the soil. Although there are many diagnostic subsurface horizons in Florida, four are important for soil classification purposes: albic, argillic, kandic, and spodic.

Albic horizon

An albic horizon is a light colored eluvial horizon that is 1.0 cm or more thick. The horizon is low in clay and oxides of Fe and Al, and the light color, ranging from white to gray, is determined by the color of the primary sand and silt particles. It generally occurs below an A horizon, and in Florida there is generally an argillic, kandic, or spodic horizon under the albic horizon (Collins 1997).

Argillic horizon

An argillic horizon is an illuvial horizon that contains significant accumulations of layer-lattice silicate clays that have moved downward from upper horizons or formed in place. The mechanism that results in illuviation of clay is due to both chemical and physical processes. However, percolating water through the soil is a major factor by

dispersing the clay. Evidence of clay translocation from the upper horizons is recognized in the argillic horizons as coatings of oriented clay on the surface of pores and peds or oriented clay as coatings or as bridges between sand grains. Furthermore, the clay films should occur on more than just the vertical sides of peds and they may differ from the interiors of the peds in color and thickness.

Although the argillic horizon forms below the soil surface, it can be later exposed at the surface by erosion. For purposes of classification in this study, if the eluvial horizon has less than 15% clay in its fine fraction, the total clay content of the argillic horizon must be 3% more. Furthermore, in soils with less than 15% clay, the illuvial horizon must be 15 cm or more thick to be an argillic horizon.

Kandic horizon

A kandic horizon has an accumulation of Fe and Al oxides and is made up of low-activity silicate clays (e.g., kaolinite), that may not contain clay skins. The low activity of these clays is evident by a CEC (cation exchange capacity) of 16 cmol(+) or less per kg of clay and an ECEC (effective cation exchange capacity) of 12 cmol(+) or less per kg of clay. The presence of a kandic horizon indicates a high degree of weathering and it may underlie an ochric, umbric, or mollic epipedon.

Spodic horizon

A spodic horizon is a dark-colored illuvial horizon resulting from the accumulation of black or reddish amorphous materials consisting mainly of organic matter, Al, and/or Fe. It is normally located below an O, A, Ap, or E horizon.

Florida's Soil Orders

The basic criteria characteristics of each of the seven soil Orders will be briefly described in the following section. Summary data of Florida's seven soil Orders is listed in Table 6-2.

Table 6-2. Summary data used to classify the seven soil Orders in Florida.

Soil Order	Diagnostic Subsurface Horizon	Epipedon	Characteristics
Alfisols	Argillic	Ochric	Medium to high base saturation (>35%)
Entisols	Albic or none; Spodic or argillic can be below 80 inches (200 cm)	Ochric	Usually very sandy (>90% sand)
Histosols	None	Can have mollic or umbric under organic soil	Organic material that is 40 cm or more in thickness
Inceptisols	None	Can have umbric, ochric, mollic, or histic	Few diagnostic features
Mollisols	May have argillic	Mollic; thin histic can overlie mollic	Base saturation >50%; dark soil
Spodosols	Spodic and usually albic; can also have an argillic or kandic	Can have thin histic	Spodic horizon within 2 m of soil surface
Ultisols	Argillic or Kandic	Ochric	Low base saturation (<35%)

Alfisols

Alfisols are characterized by the presence of an illuvial horizon of clay (argillic horizon), relatively high base saturation (>35%), and an ochric epipedon. An important characteristic of Alfisols is the formation of an argillic horizon from the translocation of silicate clays without the depletion of bases. Alfisols range from well drained to poorly drained soils.

Entisols

Entisols do not reflect any major set of major soil forming processes and therefore have little profile development. In Florida they are dominated by quartz sand and an absence of distinct pedogenic horizons except an ochric epipedon, an albic horizon, but may have and a spodic or argillic subsurface horizon that is below 2 m (Collins, 1997). In Florida, Entisols range from well to very poorly drained.

Histosols

Histosols have a very high content of organic carbon, more than half of the soil's thickness is organic material in the upper 80 cm, and in Florida, most of these soils formed from partially decomposed plant remains that accumulated in water (Collins 1997). More common names for Histosols are peats or mucks.

Inceptisols

Inceptisols are embryonic soils with few diagnostic features but generally have an umbric or ochric epipedon. Inceptisols show more profile development than Entisols and have a unique combination of properties that include water available to plants during the growing season, some unweathered minerals, a moderate to high cation exchange capacity in the clay fraction, usually textures finer than loamy sand, and one or more pedogenic horizons of alteration or concentration with little accumulation of translocated materials (Collins 1997). Inceptisols are well to poorly drained and are of minor extent in Florida (Collins 1997).

Mollisols

Mollisols have a very dark brown to black surface horizon that is rich in organic matter (mollic epipedon), a high base saturation of 50%, and many can have argillic

horizons in Florida. According to Collins (1997), the majority of Mollisols recognized in Florida are poorly to very poorly drained.

Spodosols

Spodosols are characterized by a spodic horizon and most contain an albic horizon overlying the spodic horizon. In Florida, many Spodosols are poorly to very poorly drained (Collins 1997).

Ultisols

Ultisols are similar to Alfisols in that they have an argillic horizon, however, they are more developed and leached than Alfisols. They are characterized by an argillic or kandic horizon, enough moisture for crops in most years, and a low supply of bases (<35% bases). They are deep soils and range from well-drained to poorly drained soils.

GPR Efficacy of Florida's Soil Orders

In general, Florida has excellent soils for numerous GPR applications. This is supported by a recent paper (Doolittle et al. 2002) on GPR soil suitability by the United States Department of Agriculture (USDA) - Natural Resource Conservation Service (NRCS). Out of the 48 contiguous states, a considerable area of Florida (particularly northern, central, and the panhandle) received the highest possible rating for GPR suitability (Doolittle et al. 2002). In addition, Collins et al. (1996) rated the soils in Florida at the Order level for their potential use of GPR to detect buried objects to a maximum of two meters. Soils were characterized by analyzing samples for their physical, chemical, and EM (electromagnetic) characteristics.

Ultisols, Spodosols, and Entisols were rated the best soils for using GPR in Florida with a rating of "good." Histosols, Inceptisols, and Alfisols followed with a

“fair” rating and Mollisols was the only soil Order with a “poor” rating. Mollisols are the poorest soils for GPR due to saturated conditions and a mollic epipedon. Inceptisols and Histosols had a fair rating due to saturated conditions and either the presence of a mollic, umbric, or histic epipedon. Also, Alfisols have a fair rating because the clay horizon has a high base saturation that may attenuate the radar wave.

The main reason that Florida soils provide advantageous conditions for GPR is because the three soils with the best conditions are also the three most extensive soil Orders that have been mapped in Florida. The combined coverage of Entisols, Spodosols, and Ultisols in Florida represents almost three quarters of the total hectares in the state (Collins 1997). The Entisol has advantageous conditions for GPR due to horizons dominated by sand in the first 2 m. Although Ultisols have an argillic horizon in the first 2 meters, these soils are still advantageous for GPR because the argillic horizon has a lower base saturation than argillic horizons in Alfisols. Also, Spodosols provide advantageous conditions because the spodic horizon helps to retain moisture in the soil and the increase in moisture helps to highlight soil features.

Overall, it is easier to detect buried objects that are in mineral soils with stratigraphic horizons comprised primarily of sand horizons such as Entisols or Spodosols. However, if objects in question are buried in a shallow argillic horizon that is common in Alfisols, there may be difficulty with grave detection. Since clandestine forensic burials are usually placed at a depth less than 1 meter, Entisols and Spodosols should provide the most efficacious soil conditions for locating forensic burials. In addition, there may also be favorable conditions for locating a buried body in Ultisols if the body is buried above the argillic horizon.

Classification of Soils at Research Site

The first task at the research site was to classify the soils at the BRU where the pig cadavers were buried. Figure 4-3 represents a soil survey map of the research site at the BRU that was constructed using soil data from the Alachua County Soil Survey (Thomas et al. 1985). Both areas for the pig cadavers have been mapped as Entisols in the Chipley series. The Chipley series (Table A-1), a common soil in the southeast, is somewhat poorly drained, has a very rapid or rapidly permeable soils, an ochric epipedon, and only horizons high in sand (> 90%) with little or no pedogenic alteration in the first 2 m (Thomas et al. 1985).

At the eastern area of the research site at the BRU where the small cadavers were buried, the morphological and physical analysis confirmed the Chipley series. The morphological description of the Chipley at the BRU (Table A-1) is very similar to the established series in Florida (Thomas et al. 1985). Also, particle-size distribution confirmed horizons that were dominated in all samples by the sand fraction, ranging between 95.4 to 98.0%, with low values for silt (2.0% or less) and clay (3.1% or less), and chemical analysis of organic carbon content confirmed a mineral soil with low values of organic carbon that decreased with depth (Table 6-3).

Although the soil at the western area of the research site where the large pig cadavers were buried was listed as a Chipley series in the Entisol Order (Thomas et al. 1985), both morphological (Table A-3) and physical analysis (Table 6-4) indicated an argillic horizon within 2 m that would automatically exclude this soil from the Entisol Order and include it in the Ultisol Order. Particle-size distribution also confirmed the presence of the argillic horizon. The first 90 cm were dominated in all samples by the

sand fraction, ranging between 93.0% to 95.7%, with low values for silt (3.4% or less) and clay (4.2% or less) (Table 6-4). At a depth of 90 to 100 cm, the clay content was 12.2% in comparison to the horizon directly above the argillic that was only 4.2% clay. This increase in clay satisfies one of the criteria for an argillic horizon, which only has to increase by 3% or greater (Soil Survey Staff 1999). Furthermore, chemical analysis of organic carbon content confirmed a mineral soil with low values of organic carbon that decreased with depth (Table 6-4).

The physical characteristics of the Ultisol (Table A-3) indicate that it is a Sparr series and is similar to the established series in Alachua County by the USDA-NRCS (Thomas et al. 1985). The Sparr series has already been mapped at the BRU, and coincidentally, it is immediately southwest of the large grave area (Figure 4-3). The Sparr series consists of somewhat poorly drained soils with low to moderately slow permeability, and diagnostic features include an ochric epipedon and an argillic horizon (Thomas et al. 1985).

However, one difference worth noting between the Sparr at the BRU and the established series is the depth to the argillic horizon. The argillic horizon is listed as 1.34 m for the established series in Alachua County (Table A-4). Conversely, it is shallower at the BRU at approximately 1 m (Table A-3). The depth of the argillic horizon did vary slightly the BRU. Although a survey of the depth to the argillic horizon was not undertaken across the research site, the shallowest location was noted at approximately 94 cm near row 1, and the depth increased past a meter further south near row 4 and 5 (Figure 4-7).

Table 6-3. Selected soil analyses of the Chipley series at the Beef Research Unit where the small pig cadavers were buried.

Depth (cm)	Horizon Designations	Particle-Size Distribution (%) (Composite for deep grave)			Particle Size-Distribution (%) (Shallow grave)			Organic Carbon Content (g kg ⁻¹)	
		Sand	Silt	Clay	Sand	Silt	Clay	Sample 1	Sample 2
0-10	Ap	96.0	1.0	3.0	95.4	1.5	3.1	0.90	0.92
10-20	Ap/C	96.6	0.9	2.5	95.8	2.0	2.2	0.74	0.75
20-30	C	96.9	0.5	2.6	96.4	1.4	2.2	0.32	0.39
30-40	C	97.2	1.1	1.7	97.0	0.9	2.1	0.23	0.16
40-50	C	97.0	1.0	2.0	97.0	0.8	2.2		
50-60	C/Cg1	97.4	0.8	1.8	97.2	1.1	1.7		
60-70	Cg1	97.6	0.6	1.8	97.4	0.6	2.0		
70-80	Cg1	97.8	0.4	1.8					
80-90	Cg1/Cg2	97.8	0.4	1.8					
90-100	Cg2	97.8	0.4	1.8					
100-120	Cg2	98.0	0.2	1.8					
100-120	Cg2	97.8	0.5	1.7					

Table 6-4. Selected soil analyses of the Sparr series at the Beef Research Unit where the small pig cadavers were buried.

Depth (cm)	Horizon Designations	Particle-Size Distribution (%) (Composite for deep grave)			Particle-Size Distribution (%) (Shallow grave)			Organic Carbon Content (g kg ⁻¹)	
		Sand	Silt	Clay	Sand	Silt	Clay	Sample 1	Sample 2
0-10	Ap	93.2	3.2	3.4	93.0	3.4	3.6	0.67	0.77
10-20	Ap/Bw1	93.8	2.0	4.2	93.2	2.0	3.4	0.50	0.47
20-30	Bw1/Bw2	94.4	2.5	3.1	94.6	2.0	3.4	0.22	0.27
30-40	Bw2	95.2	1.2	3.6	94.2	2.8	3.0	0.27	0.27
40-50	Bw2	95.4	1.3	3.3	94.8	1.8	3.4		
50-60	Bw2/Bw3	95.2	1.4	3.4	94.8	1.5	3.7		
60-70	Bw3	95.2	1.2	3.6	95.7	0.6	3.7		
70-80	Bw3/E	95.6	1.0	3.4					
80-90	E	94.3	1.6	4.2					
90-100	E/Bt	86.3	1.5	12.2					
100-110	Bt/Bt _g	88.7	1.5	9.8					

Physical Comparison between Soils

The only major difference between the two soils in terms of GPR performance and their effect on the decomposition of buried bodies is caused by the argillic horizon in the Ultisol. When the percentage of clay is compared with depth, clay increased in the Ultisol started at 90 to 110 cm where the argillic horizon is located (Figure 6-1). Conversely, the Entisol exhibits fairly consistent low values for clay content (3.1% or less) because of the high sand fraction that is greater than 95% in the soil horizons where the cadavers are buried.

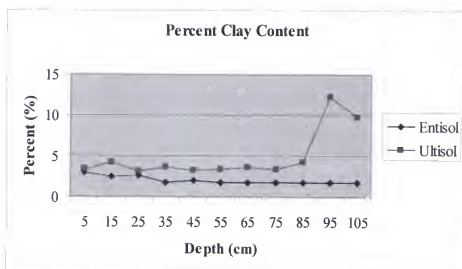


Figure 6-1. Comparison of total clay content of the Entisol and Ultisol at the BRU

Soil Analyses of Control Graves

In order to determine how the soil chemistry changed due to decomposition, it is important to first determine how the soil analyses (P, Ca, Fe, and pH) were affected by mixing of soil horizons. The means of the preburial samples were compared to those of

those of the postburial samples by calculating *t*-tests, and comparisons of the soil data between the two soil groups were further described.

Preburial and Postburial Samples of the Entisol

The preburial sample in the Entisol was collected from control grave 6 when the grave was originally dug, and the postburial sample was collected from control grave 8 after the burials were excavated. Mixing of soil horizons did not significantly change the concentrations of P ($t = 1.735$, $p = 0.111$) and Fe ($t = -0.977$, $p = 0.349$), and interestingly the mean values for both decreased with depth in the postburial samples (Table 6-5). It is important to note that the mean preburial and postburial values for P (17.71 and 11.82 mg/kg) and Fe (6.60 and 10.94 mg/kg) are low values that also decrease with depth in both samples (Figures 6-2 and 6-3).

Conversely, mixing of the soil horizons did significantly change the values of Ca ($t = -3.370$, $p = 0.006$). However, it is important to note that although the values significantly increased in the postburial group, the means only changed from 6.60 to 10.9 mg/kg caused by an increase of Ca in the shallower horizons such as the Ap. The values decreased in depth in both samples (Figures 6-2 and 6-3). In addition, at the deeper depths where the pig cadavers were buried, the values were still very low at 10 mg/kg in the postburial group. Therefore, when larger increases, or the highest values, of Ca are sampled at the deepest depths in the graves with only skeletons, the increased levels will be caused by diagenesis of the skeleton and not mixing of the soil horizons. Furthermore, while pH was not significant ($t = -1.670$, $p = 0.123$) due to mixing of horizons (Table 6-5), all the values in the postburial soil samples were lower than the original pH values (Figure 6-4).

Table 6-5. Results of *t*-tests for preburial and postburial samples in the Entisol that were calculated using data derived from Table B-1. *The significance of pH was calculated using hydrogen-ion activity values.

Phosphorus (mg/kg)	Postburial	Preburial
Mean	11.828	17.718
Std. Deviation	2.868	13.14
Observations	12	11
Df	11	
t Stat	1.735	
P(T<=t) two-tail	0.111	
Calcium (mg/kg)	Postburial	Preburial
Mean	10.937	6.60
Std. Deviation	6.229	5.097
Observations	12	12
Df	11	
t Stat	-3.370	
P(T<=t) two-tail	0.006	
Iron (mg/kg)	Postburial	Preburial
Mean	6.478	5.702
Std. Deviation	2.887	4.777
Observations	12	12
Df	11	
t Stat	-0.977	
P(T<=t) two-tail	0.349	
pH	Postburial*	Preburial*
Mean	0.000048	0.000023
Std. Deviation	0.000095	0.000022
Observations	12	12
Df	11	
t Stat	-1.670	
P(T<=t) two-tail	0.123	

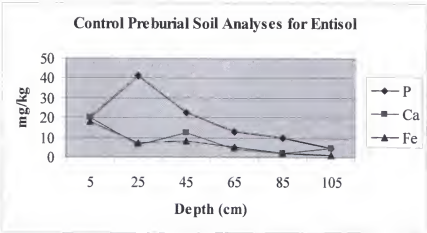


Figure 6-2. P, Ca, and Fe values of the preburial sample in the Entisol plotted to show the general decrease in concentrations with depth. Data were derived from Table B-1.

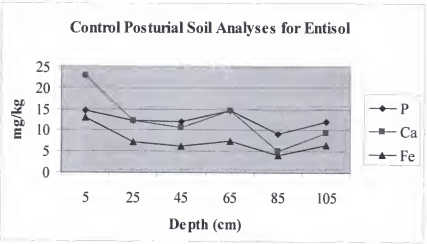


Figure 6-3. P, Ca, and Fe values of the postburial sample in the Entisol plotted to show the general decrease in concentrations with depth. Data were derived from Table B-1.

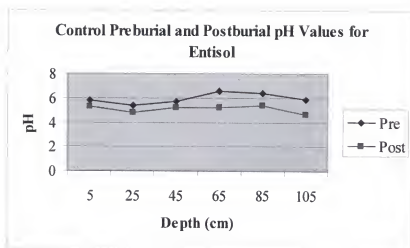


Figure 6-5. pH values of the preburial and postburial samples in the Entisol plotted to show the decreased values of the postburial group. Data were derived from Table B-1.

Preburial and Postburial Samples of the Ultisol

The preburial sample in the Ultisol was collected from grave 1L when it was originally dug for cadaver 1, and the postburial sample was collected from control grave 3 after all of the graves were excavated. Mixing of soil horizons did not significantly change the concentrations of P ($t = -1.517$, $p = 0.155$), Ca ($t = 1.866$, $p = 0.076$), and Fe ($t = -0.482$, $p = 0.636$) (Table 6-7). The mean preburial and postburial values barely changed for P (4.90 and 4.96 mg/kg) and decreased for Fe (10.75 and 7.46 mg/kg). Furthermore, the values for both P and Fe are low throughout the soil in both groups (Figures 6-5 and 6-6).

Mixing of the soil horizons did significantly change the concentrations of Ca ($t = -2.146$, $p = 0.057$) (Table 6-6). Although the mean values increased from 7.46 mg/kg in the preburial group to 13.55 mg/kg in the postburial group, the values are low and decrease with depth in both samples (Figures 6-5 and 6-6). Furthermore, the pH concentration significantly changed ($t = 7.1472$, $p = 0.000$) caused by mixing of soil

horizons (Table 6-6). However, it is important to note that the values are less than pH 5.0 and are consistent throughout the depth of the soil in the postburial group (Figure 6-7).

Table 6-6. Results of *t*-tests for preburial and postburial samples in the Ultisol that were calculated using data derived from Table B-6. *The significance of pH was calculated using hydrogen-ion activity values.

Phosphorus (mg/kg)	Postburial	Preburial
Mean	4.958	4.901
Std. Deviation	0.81	1.858
Observations	11	11
Df	10	
t Stat	-0.119	
P(T<=t) two-tail	0.908	
Calcium (mg/kg)	Postburial	Preburial
Mean	13.547	7.457
Variance	7.115	7.20
Observations	11	11
df	10	
t Stat	-2.146	
P(T<=t) two-tail	0.057	
Iron (mg/kg)	Postburial	Preburial
Mean	7.457	10.749
Std. Deviation	2.414	5.911
Observations	11	11
df	10	
t Stat	1.030	
P(T<=t) two-tail	0.327	
pH	Postburial*	Preburial*
Mean	0.000021	0.000049
Std. Deviation	0.0000083	0.000011
Observations	11	11
df	10	
t Stat	7.142	
P(T<=t) two-tail	0.000	

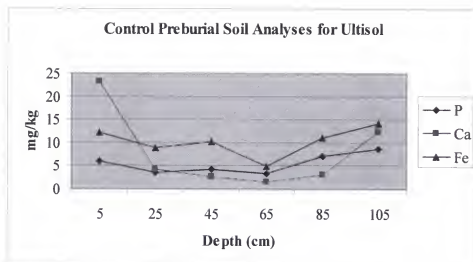


Figure 6-5. P, Ca, and Fe values of the preburial sample in the Ultisol plotted to show the general decrease in concentrations with depth. Data were derived from Table B-6.

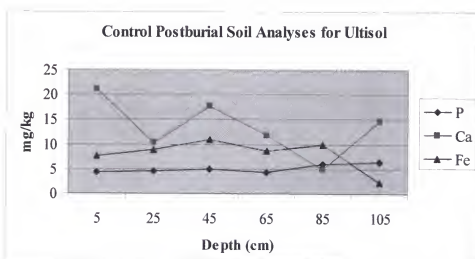


Figure 6-6. P, Ca, and Fe values of the postburial sample in the Ultisol plotted to show the general decrease in concentrations with depth. Data were derived from Table B-6.

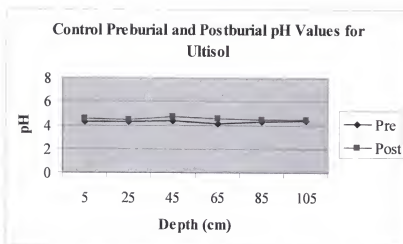


Figure 6-7. pH values of the preburial and postburial samples in the Ultisol plotted to show the low values for both groups. Data were derived from Table B-6.

Soil Chemistry Changes Caused by Decomposition

Overall, the chemical changes in the soils caused by only mixing of the soil horizons were minimal for both the Entisol and Ultisol. The important trend noted for the P, Ca, and Fe samples included low values that decreased with depth. Although the mean Ca value for the soils increased for both postburial groups and was significant for the Entisol, the values were still low and decreased with depth. Therefore, if large increases in the concentrations of P, Ca, and Fe are sampled only in the area surrounding the pig remains, it can be inferred that the increased concentrations are caused by the buried remains and not mixing of soil horizons.

When P, Ca, and Fe are plotted with depth, the concentrations of these elements in the soil surrounding the pig remains differ based on the decomposition patterns of the cadavers. The following examples were calculated by averaging the soil values from the group of graves for each scenario, which was two or three. The last two deep values for

each figure were taken under the head and pelvis, and if one of these samples was not available, the value under the thorax was substituted.

As a generalization, increases of P, C, and Fe concentrations caused by decomposition were only sampled in the soil surrounding the remains within a 20 to 30 cm depth, regardless of cadaver scenario. Figure 6-8 is an example of a shallow grave in the Entisol using averaged values from the two cadavers of the SSLE scenario. For this scenario, a large increase in P and Ca is first noted at a depth between 40 to 50 cm and the highest concentrations of these elements were sampled below the pig remains at 60 to 70 cm. The same trend is also observed for the deep graves in the Entisol. For example, Figure 6-9 is an example of a deep grave in the Entisol using averaged values from the two cadavers of the SDSE scenario. In this example, the highest increases are with P directly below the cadaver.

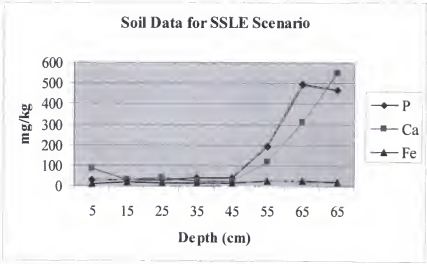


Figure 6-8. The average values for the SSLE scenario were calculated using the soil samples from the graves of cadavers 15 and 16. Data were derived from Table B-2.

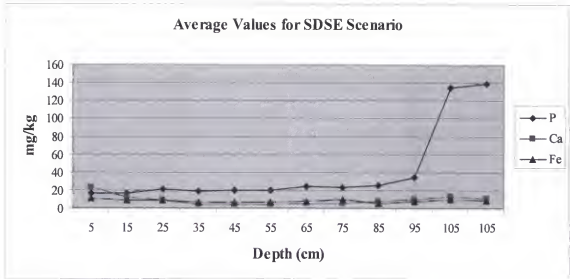


Figure 6-9. The average values for the SDSE scenario were calculated using the soil samples from the graves of cadaver 17 and 18. Data were derived from Table B-4.

The same trend with the soil data is also noted for the shallow and deep burials in the Ultisol. For example, Figure 6-10 is an example of a shallow grave in the Ultisol using averaged values from two cadavers of this LSSU scenario. In this example, the increases in P, Ca, and Fe begin above the decomposing cadavers between 30 -40 cm and the highest increases of the three elements are directly below the cadavers. Furthermore, Figure 6-11 is an example of a deep grave in the Ultisol using averaged values from two cadavers of this scenario. Increases in P, Ca, and Fe are noted between 80 and 90 cm and the highest increases of the three elements are located directly below the cadavers.

Correlation of Soil Analyses with Decomposition

It is apparent from the soil examples that were just provided that there is a limited area surrounding the pig remains, between 20 and 30 cm that is affected by decomposition and diagenesis. Only the soil directly around the pig cadavers is affected, and the highest differences of P, Ca, and Fe were in samples collected directly under each

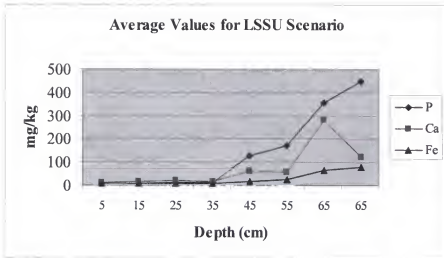


Figure 6-10. The average values for the LSSU scenario were calculated using the soil samples from the graves of cadavers 11 and 12. Data were derived form Table B-10.

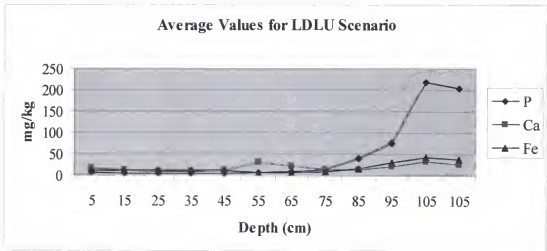


Figure 6-11. The average values for the LDLU scenario were calculated using the soil samples from the graves of cadavers 2 and 3. Data were derived from Table B-7.

cadaver. Therefore, in order to understand how the soil properties are changing from decomposition and diagenesis of the cadavers, the soil samples collected directly under each pig cadaver will be further compared.

The most informative way to present the relationship between decomposition and soil chemistry is to combine the small and large cadavers into one group for comparison because identical relationships were observed. Each cadaver received an average value for P, Ca, Fe, and pH that were calculated using two samples collected directly under each cadaver. The samples were used from under each cadaver because the highest increases of P, C, Fe, and pH were observed at this location. The values were generally calculated using the samples collected under the head and pelvis. If one of these samples was not available, then the sample collected under the thorax was used.

A ratio of P and Ca was constructed for each pig cadaver by dividing P by Ca and then graphing it with pH and the total decomposition score (Figures 6-12 and 6-13). It is obvious from the two figures that a relationship exists between P/Ca, pH, and the total decomposition that is further supported by correlations. For example, there is a highly significant, inverse relationship between P/Ca and total decomposition score ($r = -0.752$, $p < 0.000$), and a positive relationships exist between P/Ca and pH ($r = 0.689$, $p < 0.000$), and between the total decomposition and pH ($r = 0.689$, $p < 0.000$). Hence, the lower the decomposition score, the higher levels of P and pH, while there are lower levels of Ca. Conversely, when the P/Ca ratio is low, there are high P levels, high decomposition scores, high Ca levels, and low pH levels. For example, the highest ratios of P/Ca and pH values were sampled for the LDSU scenario (cadavers 8, 9, and 10), which had the lowest total decomposition scores (Figure 6-12). The lowest ratios of P/Ca were sampled

for the LSSU scenario (cadavers 5, 6, and 7), which had the highest total decomposition scores (Figure 6-12).

Interestingly, the relationship between these variables is also expressed for each cadaver within a scenario when there are different patterns of decomposition between cadavers. For example, in Figure 6-13, cadavers 11 and 12 of the LSSU scenario expressed different patterns of decomposition. Cadaver 12 had a high total decomposition score, and a low pH, and a low ratio of P/Ca due to the increased Ca in the soil. While cadaver 11 had a lower total decomposition score than cadaver 12, the P/Ca ratio and pH of 11 were higher than 12. In addition, this relationship is also expressed in the SSSE scenario with cadavers 19 and 20 (Figure 6-13). While cadaver 19 had a very high decomposition score, there was a low P/Ca ratio and low pH due to the increased Ca in the soil. Conversely, cadaver 20 had a lower total decomposition score than cadaver 19, but a higher P/Ca ratio due to less Ca in the soil.

Surprisingly, there were also increased levels of Fe. Since Fe is not a major mineral in the body, it was not deposited in the soil through decomposition and diagenesis. While no significant relationship exists between Fe and Ca ($r = -0.108$, $p = 0.669$), Fe and pH ($r = 0.310$, $p = 0.210$), and Fe and the total decomposition score ($r = 0.337$, $p = 0.172$), a significant relationship exists between Fe and P concentrations ($r = 0.571$, $p = 0.013$). In other words, the higher the concentration of P, the higher the levels of Fe (Figure 6-14). Since the increased Fe is not coming from decomposition and diagenesis of the pig remains, it is coming directly from the soil solution by bonding with the increased P in the soil surrounding the cadaver to form iron phosphates.

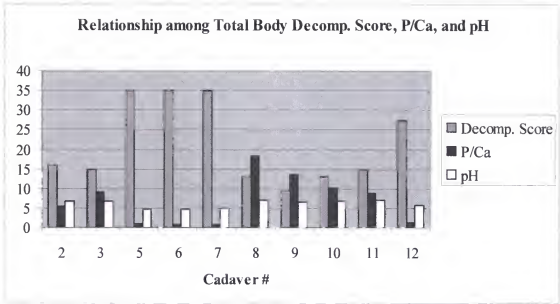


Figure 6-12. Relationship among the total body decomposition score, the P/Ca ratio, and pH for the large pig cadavers. The P/Ca ratio is unit less. Data were derived from Table B-11.

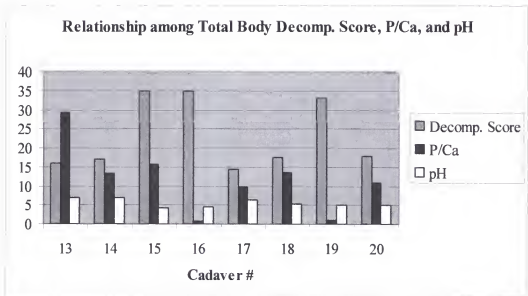


Figure 6-13. Relationship among the total body decomposition score, the P/Ca ratio, and pH for the small pig cadavers. The P/Ca ratio is unit less. Data were derived from Table B-12.

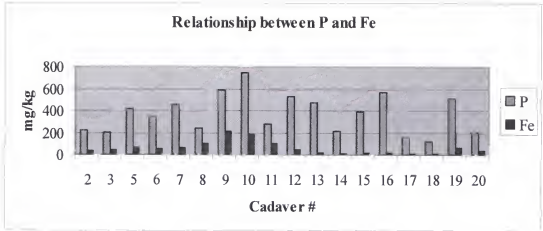


Figure 6-14. Relationship between P and Fe in the soil collected under the pig cadavers. Data were derived from Tables B-11 and B-12.

Summary

The only major difference between the two soils that were used in this study in terms of GPR performance and their effect on the decomposition of buried bodies is the argillic horizon in the Ultisol. Overall, there are high correlations between P, Ca, and pH levels, calculated from soil samples collected under each cadaver, with that of the total decomposition score for each cadaver. For example, the highest values of P/Ca (high P and low Ca) and pH were sampled for cadavers with low decomposition scores or those that retained extensive soft tissue. Conversely, the lowest values of P/Ca (high P and Ca) and pH were sampled for cadavers with advanced decomposition scores or those that were completely skeletonized. Furthermore, high increases of Fe were also sampled under the remains of a number of cadavers. Fe was correlated with the increased P from the decomposition of the bodies. The increase in Fe came directly from the soil solution by binding with the increased P as iron phosphates.

CHAPTER 7 GPR RESULTS FOR LARGE PIG CADAVERS

The 500-MHz Antenna

GPR-Soil Profile

The GPR profile of the Ultisol using the 500-MHz antenna exhibits a distinctive reflection from the argillic horizon (Figure 7-1). This profile was performed immediately north of row 1 (Figure 4-7). In this soil profile, the depth to the argillic horizon is between 1.0 to 1.2 m. The argillic horizon appears as series of horizontal layering, and the depth to this horizon varied slightly across the research area where the pig cadavers were buried. While the shallowest depth of the argillic horizon was recorded at approximately 1.0 m in the area of row 1, the horizon was deeper further south near rows 4 and 5. No other stratigraphic horizons, including the water table, were detected with the GPR using the 500-Mz antenna.

The prominent horizontal banding across the profile starting at 0.0 m and continuing to 1.0 m, being most concentrated from 0.0 m to 0.6 m, is due to antenna noise and does not represent any stratigraphic horizons (Figure 7-1a). The intensity and depth of the horizontal banding changed minimally during the study. Processing the GPR file to remove the antenna noise eliminates the horizontal banding (Figure 7-1b).

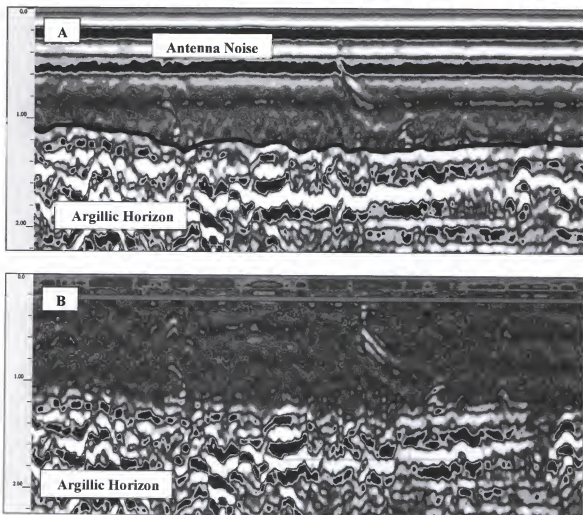


Figure 7-1. Ground-penetrating radar profile of the Ultisol using the 500-MHz antenna. A) Note the prominent antenna noise, horizontal banding from 0 to 0.60 m, and the depth to the argillic horizon that ranges between 1.00 to 1.20 m in the unprocessed profile. B) The horizontal banding at the top of the profile is removed with processing. The profile is approximately 2.20 m deep and 23 m long.

Shallow Cadavers (LSSU and LSLU Scenarios)

Distinctive grave anomalies were produced for the large pig cadavers that were buried at shallow depths. At 2 weeks, two hyperbolic anomalies from the LSSU scenario (cadavers 11 and 12) (Figure 7-2a) begin at approximately 0.45 m and continue inferiorly to the argillic horizon. Each anomaly consists of a vertical series of hyperbolic or bell

shaped curves. The cadaver is located at the apex of each anomaly. Although backfill above the cadavers is not detected, a stratigraphic break of the argillic horizon is located directly below the second anomaly. This is the result of radar attenuation by the cadaver that blocks the electromagnetic wave from reaching the argillic horizon. Although there is extensive antenna noise noted from 0.0 to 0.6 m on the GPR profile, the noise does not mask or obstruct the grave anomalies.

With the removal of the antenna noise (Figure 7-2b), there is only a slight increase in the resolution of the anomalies. Of interest, is the increase in resolution of the tails that contribute to the hyperbolic shape of the anomalies. In addition, a significant change in the profile is the detection of the backfill above both cadavers from 0.0 m to 0.25 m. The backfill is only detected when the antenna noise is removed. The resolution of the argillic horizon has not changed, and the break in the argillic horizon below the second anomaly is still visible. Overall, there is no need to process the profile to detect these cadavers at 19 days.

The large cadavers buried at the shallow depths were detected for the duration of this study for both scenarios (LSSU and LSLU). While the cadavers from the LSSU group were detected for the duration of the monitoring period at 13 months while expressing variable degrees of skeletonization (see Chapter 5), excessive antenna noise reduced the contrast of the returns. For example, Figure 7-3a is the last profile of cadavers 11 and 12 from the LSSU scenario that was collected at 12 months and 23 days, just prior to excavation at 13 months. Although there is thick horizontal banding extending from 0.0 to 0.90 m that reduces the contrast of both cadavers, two hyperbolic anomalies begin at approximately 0.45 m and continue inferiorly to the argillic horizon.

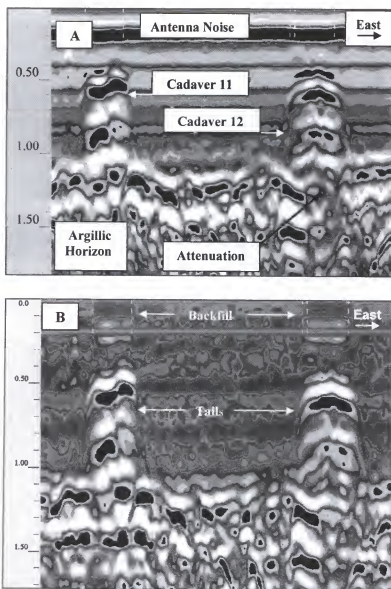


Figure 7-2. Ground-penetrating radar profile using the 500-MHz antenna of two cadavers from the LSSU scenario (11 and 12) at 12 months and 23 days. A) The cadavers are easily detected with the prominent banding in the unprocessed profile. B) The backfill above both cadavers is detected and the resolution of the hyperbolic tails is increased in the processed profile. The profile is approximately 1.70 m deep and 12 m long.

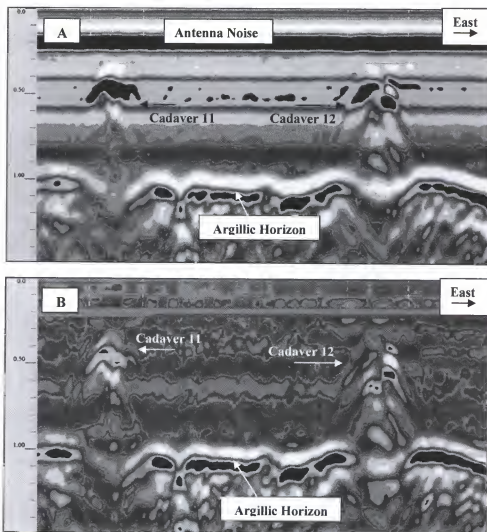


Figure 7-3. Ground-penetrating radar profile using the 500-MHz antenna of two shallow cadavers from the LSSU scenario (11 and 12) at 13 months. A) The returns from both cadavers are masked by the excessive antenna noise in the unprocessed profile. B) The contrast of both anomalies has significantly increased by removing the antenna noise. The profile is approximately 1.70 m deep and 14 m long.

The attenuation of the argillic horizon below each cadaver helps to highlight their locations. However, in an actual forensic situation, it may be difficult to locate a buried body exhibiting the same general anomaly characteristics as cadaver 11 if there is extensive antenna noise that obscures the anomaly. However, the anomalies of both

cadavers are easily discernable as hyperbolic shapes with prominent tail when the antenna noise is removed (Figure 7-3b), and attenuation of the argillic horizon is still discernable below both cadavers.

Discernable grave anomalies were produced for cadavers (5, 6, and 7) of the LSLU scenario during the entire monitoring period. Figure 7-4a is the last GPR profile collected from this group of cadavers and control grave 5 before they were excavated at 21.5 months, which confirmed complete skeletonization for each cadaver (see Chapter 5). The only major change to the anomalies over time was a decreased return that is represented by a smaller, yet distinctive, grave anomaly. Three large cadavers represented by hyperbolic anomalies with discernable tails that descend to the argillic horizon are easily detected without removing the antenna noise. Although the GPR profile is only deep enough to detect the top portion of the argillic horizon, it is possible to discern attenuation of the radar wave below each cadaver as disruptions of the argillic horizon. Of interest are the two small hyperbolic anomalies between cadavers 5 and 6 caused by a stump and an old soil auger hole. In addition, the control grave with only backfill barely exhibits a discernable response. It is clear from the comparison of the control hole with the pig graves, that the grave anomaly is the result of the pig skeleton and not the disturbed soil. Overall, there was no problem detecting these pig cadavers when they were completely skeletonized.

Processing the profile did not increase the resolution of the three cadaver anomalies (Figure 7-4b), but resolution of the backfill above each cadaver increased slightly. In addition, the resolution of the soil auger hole on the eastern border of the anomaly from cadaver 5 increased and is now visible as a narrow series of vertical hyperbolic

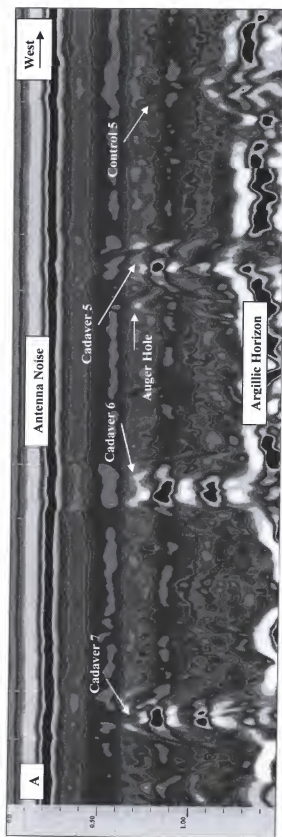


Figure 7-4. Ground-penetrating radar profile of three shallow cadavers (7, 6, and 5 from left to right) from the LSLU scenario using the 500-MHz antenna. A) The cadavers are easily detected in the unprocessed profile with the prominent banding caused by the antenna noise. B) Note the increased contrast of the backfill and auger hole in the processed profile. The profile is approximately 1.40 m deep and 27 m long.

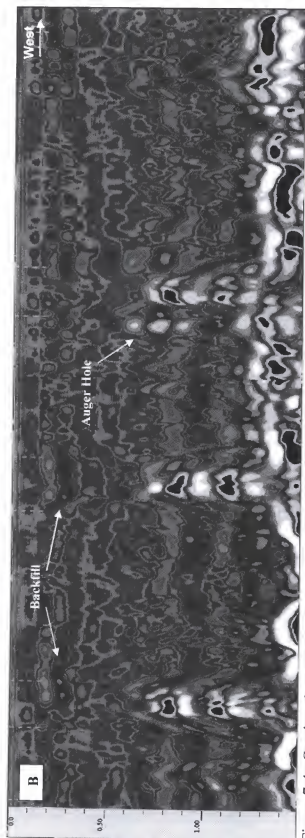


Figure 7-4. Continued

anomalies, or a spike, that terminates at the argillic horizon.

Deep Cadavers (LDSU and LDLU Scenarios)

Overall, in comparison to the shallow graves in the Ultisol, there was a decreased response from the large cadavers for both scenarios (LDSU and LDLU) that were buried at a deep depth in the Ultisol due to the argillic horizon. These cadavers are either buried into the top segment of the argillic horizon or they are directly above the horizon. Figure 7-5a represents a GPR profile of three large cadavers (8, 9, and 10) from the LDSU scenario collected at four months. All three cadavers exhibit clear hyperbolic anomalies, and minimal soil disturbances are retained above each cadaver. The anomalies from cadavers 8 and 9 begin at approximately 0.85 to 0.90 m, and they extend into the argillic horizon resulting in disruptions of the horizon that are easily detected. In addition, the small anomaly to the west of cadaver 9 at 0.70 m is caused by a stump. Although there is no disruption of the argillic horizon by cadaver 10, the hyperbolic anomaly has the strongest return of the three graves. Processing the data to eliminate antenna noise did not increase the resolution of the grave anomalies and only slightly increased the resolution of the backfill.

Over the first year the response from the graves decreased considerably. In particular, the return from cadaver 9 decreased significantly at five and a half months. Overall, they were still detected as hyperbolic images and disruptions within the argillic horizon. For example, at 13 months (Figure 7-6a) there are major changes to the grave anomalies even though the pig cadavers had undergone very little decomposition and still retained extensive soft tissue structures (see Chapter 5). The return from the first two cadavers decreased significantly. Cadaver 8 is represented by a small hyperbolic

reflection at 0.90 m. Immediately below the reflection is a major break within the argillic horizon that travels completely through the argillic horizon. It is as wide as the pig grave and is the result of attenuation. The return from cadaver 9 is very similar to 8 with respect to depth, anomaly shape and attenuation through the clay layer.

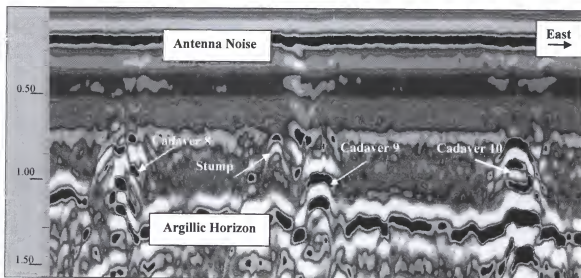


Figure 7-5. Unprocessed GPR profile of three deep pig cadavers (8, 9, and 10) from the LDSU scenario at four months using the 500-MHz antenna. The arrows show the location of the grave anomalies. The profile is approximately 1.60 m deep and 21 m long.

The return from cadaver 10 is the most distinctive of the three cadavers. It is represented by a number of prominent hyperbolas around 0.70 m that terminate at the superior surface of the argillic horizon at a depth of 1.05 m. There is also a small disruption through the argillic horizon due to attenuation that is directly inferior to the apex of the grave anomaly. It is fairly apparent that there would be no problem detecting cadaver 10 in an actual forensic situation. However, there would obviously be difficulty detecting cadavers 8 and 9 using the unprocessed profile. An experienced operator may

discern the location of the two graves based on the faint hyperbolic response and the attenuation of the argillic horizon.

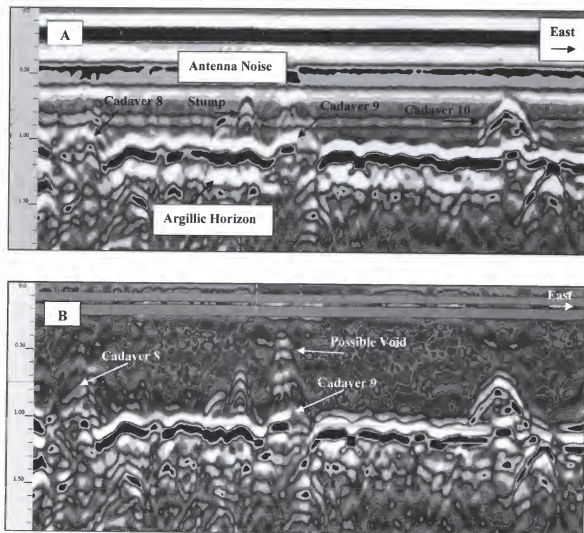


Figure 7-6. Ground-penetrating radar profile (500-MHz) of three deep cadavers (8, 9, and 10) of the LDSU scenario at 13 months. A) Note the decreased response of cadavers 8 and 9 in the unprocessed profile. B) However, when the antenna noise is removed, there is a slight increase in the resolution of the anomalies from cadavers 8 and 9. The profile is approximately 1.80 m deep and 21 m long.

It is important to note that the horizontal banding due to the antenna noise in Figure 7-6a is more prominent than usual. The banding extends from 0.0 to 0.90 m and is very dense from 0.0 to 0.70 m. It is not a surprise that removing the antenna noise increased the resolution of anomalies for cadavers 8 and 9, and did not change the response of cadaver 10 (Figure 7-6b). A weak, but increased hyperbolic response is present for cadaver 8 at 0.75 m that extends inferiorly to the argillic horizon. Immediately below the reflection there is also a major break within the argillic horizon caused by attenuation. The response for cadaver 9 is also easily discernable. A weak hyperbolic reflection above the cadaver anomaly starts at 0.4 m and continues inferiorly to the argillic horizon. The shallow response above the cadaver is due to the backfill and is more than likely a void that developed during settling of the backfill. The return from cadaver 9 has increased slightly, and is still recognizable at 0.9 m as a hyperbolic anomaly within the argillic horizon. There is more differentiation of the anomaly within the argillic horizon without the antenna noise.

The deep cadavers (1, 2, and 3) from the LDLU scenario that were interred in the Ultisol for 21 months are further examples of the difficulty in differentiating a recognizable grave response after a year when the pig cadavers were buried in close proximity to the argillic horizon. There were also significantly reduced returns from these cadavers as early as 6 months. Figure 7-7a is a GPR profile at 15.5 months of this group of pig cadavers and three control graves that were buried at a depth of 1.0 m to show the decreased returns after a year. The control graves consist of one with backfill (control 1), one with gravel (control 2), and one with branches (control 3). The control graves with the gravel and branches produce distinctive grave anomalies that are easily

discernable above the clay. The return from the gravel lens is a very distinctive hyperbolic anomaly that starts at 1.0 m and extends inferiorly almost a meter through the clay. The distinctive layering of the hyperbolas that make up the anomaly is consistent with a dense subsurface object. The hyperbolic anomaly for the control hole with the branches is also distinctive within the clay, beginning around 0.8 m and continuing inferiorly for over a meter. The blank control hole lacks a distinctive grave anomaly and is essentially represented as a soil disturbance within the clay layer. The control graves with the gravel and branches provided a much needed reference for size and depth of the grave anomalies in the argillic horizon, while the blank control grave is a clear indication that the anomalies are the result of the objects in the graves and not just the disturbed soil.

The return from the three cadavers is extremely weak and differentiation within the argillic horizon is difficult even though a considerable degree of soft tissue still remains (see chapter 5). It is important to note that cadavers 1, 2, and 3 are buried closer in proximity to one another than cadavers 8, 9, and 10. Their proximity may also contribute to the difficulty in recognizing them along the GPR transect, because there is not enough contrast between the anomalies from the pig graves and the undisturbed argillic horizon. This observation is partly true for the area between cadavers 1 and 2 which is somewhat obscured by the hyperbolic tails that are produced from both of these cadavers.

Cadaver 1 is represented by a small hyperbolic reflection at 0.75 m. Although the reflection does not continue through the clay horizon as a series of hyperbolas, the right tail of the hyperbolic anomaly is present through the clay layer to a depth of 2 m. In addition, a disruption through the clay horizon is located directly below the apex of the

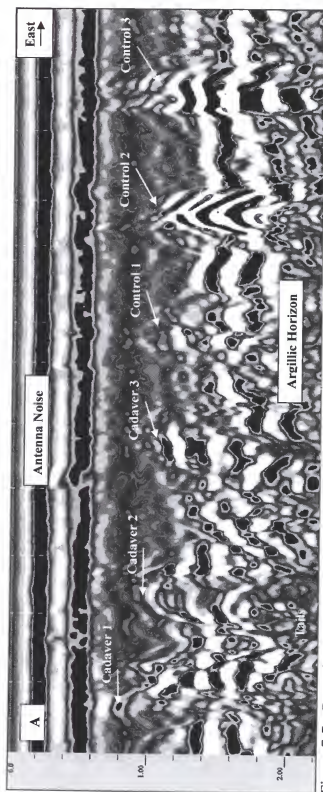


Figure 7-7. Ground-penetrating radar profile (500-MHz) of three deep pig cadavers (1, 2, and 3) of the LDLU scenario and three control graves (1, 2, and 3) in the Ultisol at 15.5 months. The first control grave is a blank, the second is a gravel lens, and the third contains branches. A) Note the poor differentiation of the pig anomalies within the argillie horizon in the unprocessed profile. B) There is a slight increase in the resolution of the cadaver anomalies in the processed profile. The profile is approximately 2.0 m deep and 25 m long.

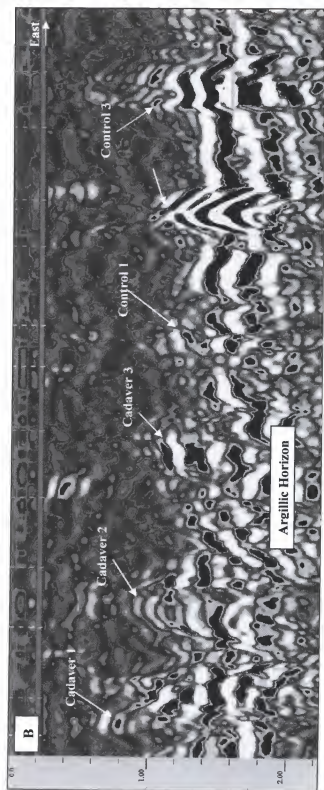


Figure 7-7. Continued

hyperbolic anomaly. The return of cadaver 2 is the most distinctive of the three cadavers. It is represented by disturbance around 0.8 m and a number of prominent hyperbolas around 1.0 m that continue weakly through the clay horizon. The left tail is present through the argillic horizon to a depth of 2 m, and a disruption through the clay horizon is visible below the hyperbolas. The return of cadaver 3 is the weakest of the three. It is visible at a depth of 1.0 m as a vertical density, without a defined hyperbolic shape. There may be two weak tails on either side of the anomaly, and a soil disruption is also present through the argillic horizon. Removing the antenna noise did not increase the resolution of the densest anomalies from cadavers 1, 2, and 3 at 15.5 months (Figure 7-7b), because the antenna noise is only concentrated on the upper part of the profile above the buried cadavers.

Figure 7-8 is the last profile of cadavers 1, 2, and 3 at 20.33 months before they were excavated at 21 months. A profile was not collected of the graves prior to excavating them at 21 months because the equipment broke in the field while collecting the data. Figure 7-8 exhibits a much weaker return from the cadavers and control graves in comparison to Figure 7-7a. Although the returns from the control graves with the gravel lens (control 1) and branches (control 2) are considerably reduced, the control graves still provide a reference for size and depth of the grave anomalies in the argillic horizon. Overall, the weak returns from the three cadavers (1, 2, and 3) are very similar in appearance. However, in comparison to Figure 7-7a, the returns are significantly reduced for cadavers 1 and 2 and increased for cadaver 3. The cadaver anomalies for this group appear as hyperbolic shapes at approximately 0.80 m with associated tails that continue inferiorly to the bottom of the profile. In addition, in Figure 7-8, the lack of a

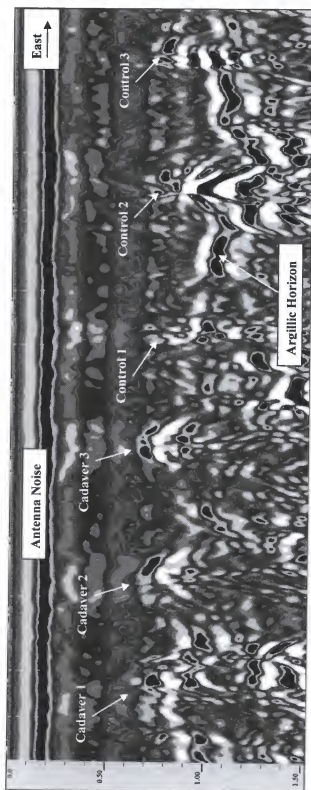


Figure 7-8. An unprocessed GPR profile (500-MHz) of three pig cadavers (1, 2, and 3) from the LDLU scenario and three control graves (1, 2, and 3) at 20.33 months. The first control grave is a blank, the second is a gravel lens, and the third contains branches. The profile is approximately 1.5 m deep and 2.5 m long.

recognizable return from the blank control grave (control 1) is still a clear indication that the anomalies are caused by the objects in the graves and not just the disturbed soil. Removing the antenna noise did not increase the resolution of the anomalies from cadavers 1, 2, and 3 at 20.33 months (Figure 7-8), because the densest antenna noise is only concentrated on the upper part of profile above the buried cadavers.

The 900-MHz Antenna

GPR-Soil Profile

The GPR profile of the Ultisol using the 900-MHz antenna also exhibits a distinctive reflection from the argillic horizon (Figure 7-9a). This profile was taken between rows three and four (Figure 4-7). There are three major differences between the profiles from the two antennas. Horizontal banding from antenna noise is also present on the profile from the 900-MHz, however, it is not as distinctive across the profile. Antenna noise is still present between 0.0 to 1.0 m, but the densest banding across the top of the profile extends only to a depth of 0.15 m. Processing of the GPR profiles with the 900-MHz is generally not required for grave detection because the obtrusive banding is too shallow to mask the diagnostic features (Figure 7-9b). The second major difference with the 900-MHz antenna is an increase in the resolution of noise caused by stumps and roots that are generally not detected by the 500-MHz antenna. This general noise is visible as small hyperbolas throughout the profile.

The third difference concerns the resolution of the argillic horizon. Although it is a continuous horizon, the presence and density of the horizon is highly variable on the GPR profiles. It may be present as either a dense, homogenous horizon or a highly variable horizon in density such as Figure 7-9a. In addition, in some instances the argillic

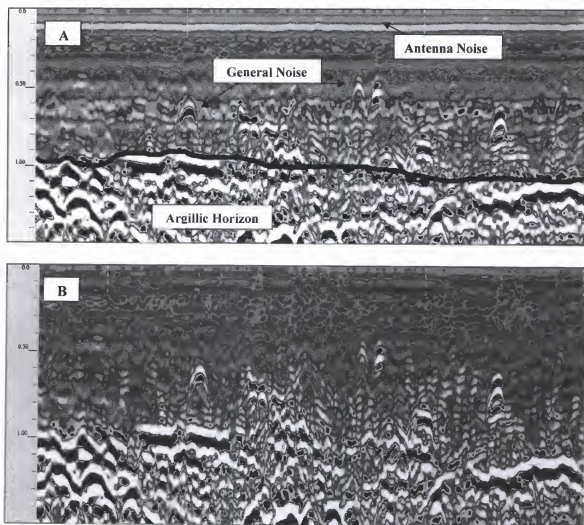


Figure 7-9. Ground-penetrating radar profile of the Ultisol using the 900-MHz antenna. A) Note the shallow horizontal banding from 0 to 0.15 m, the noise due to roots and stumps, and the depth to the argillic horizon that ranges from 1.00 to 1.15 m. B) The only major change in the processed profile is the removal of the antenna noise on the superior aspect of the profile. The GPR profile is approximately 1.50 m deep and 23 m long.

horizon is completely absent using the 900-MHz antenna, even though it is present using the 500-MHz antenna. For example, Figure 7-10a is a profile of the Ultisol using the 900-MHz antenna that was collected on the same day and from the identical location as the profile with the 500-MHz (Figure 7-1a). However, while the argillic horizon is

clearly detected using the 500-MHz antenna, it is not using the 900-MHz antenna. In addition, there is no change detecting the argillic horizon when the antenna noise is removed (Figure 7-10b).

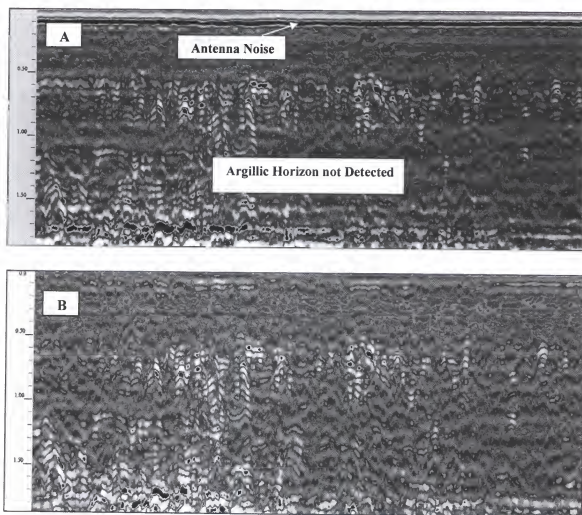


Figure 7-10. Ground-penetrating radar profile of the Ultisol using the 900-MHz antenna. A) Note that the argillic horizon is not detected in the unprocessed profile. B) The argillic horizon is still not detected when the profile is processed. The profile is approximately 1.80 m deep and 23 m long.

Shallow Cadavers (LSSU and LSLU Scenarios)

Distinctive grave anomalies were produced for the small pig cadavers (11 and 12) of the LSSE scenario that were buried at shallow depths. At 14 days, two hyperbolic anomalies (Figure 7-11a) begin at approximately 0.4 m and continue inferiorly to 0.75 m. Each anomaly consists of a vertical series of hyperbolic or bell shaped curves. The cadaver is located at the apex of each anomaly. Interestingly, the second grave anomaly appears to be a composite of two vertical hyperbolas. The western half of the return from the cadaver is shallower than the hyperbola from the eastern half of the cadaver. When the grave was excavated it was noted that the shallower part of the anomaly corresponds to the head end of the pig, which was shallower than the tail end of the body. When the pig was originally placed in the grave, the head was leaning against the grave wall.

There are a number of apparent differences in the details that are exhibited between the profiles of the 900- and 500-MHz antennae. Comparisons will be made between Figure 7-11a and Figure 7-2a, which are profiles using the 900- and 500-MHz antennae on the same day with the same cadavers (11 and 12). First, although the shape of the anomalies is similar between antennae, the 900-MHz detects the shallower, anterior end of cadaver 12, while the anomaly from the 500-MHz antenna does not discern a difference in the height of the cadaver. Only one uniform anomaly for cadaver 12 is exhibited using the 500-MHz antenna. Second, although both grave anomalies appear at the same depth, the anomaly from the 500-MHz antenna extends to the argillic horizon at a depth of 1.0 m, while the grave anomalies from the 900-MHz only continue inferiorly for a shorter distance at 0.75 m. In addition, the tails from the 900-MHz

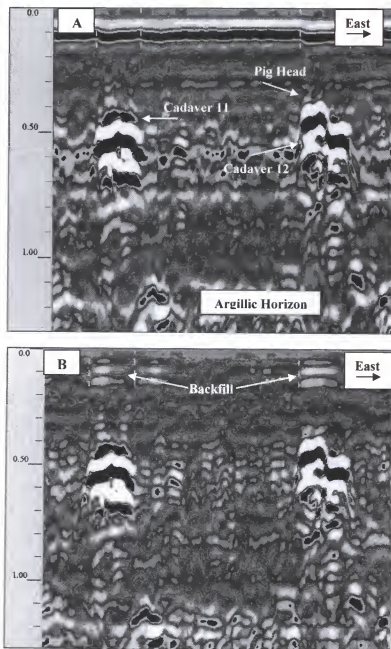


Figure 7-11. Ground-penetrating radar profile (900-MHz) of two shallow buried pig cadavers (11 and 12) from the LSSU scenario at 2 weeks. A) Note the poorly defined argillic horizon, and the double anomaly of cadaver 12 caused by the shallower head end. B) Backfill is detected above both cadaver anomalies when the banding is removed in the processed profile. The profile is approximately 1.30 m deep and 12 m long.

anomalies are generally oriented more vertically (there can be exceptions), while the tails from the 500-MHz are oriented further away from the body at a greater angle. As a result the 500-MHz anomalies usually appear broader than the 900-MHz anomalies.

The last major difference between the two profiles concerns the resolution of the argillic horizon. Although the argillic horizon is clearly demarcated in Figure 7-2b using the 500-MHz antenna, it is not defined in Figure 7-11a with the 900-MHz antenna. Prominent, horizontal bandings characteristic of a clay horizon are not present in the known area of the argillic horizon. The argillic horizon was still absent in the profile with the antenna noise removed (Figure 7-11b). Overall, removing the antenna noise has no effect on the resolution of the grave anomalies because the most prominent banding is near the surface (Figure 7-11b). However, disturbed backfill above both cadavers is detected in the processed profile from 0.0 m to 0.25 m. It was masked by the antenna noise in the unprocessed profile Figure (7-11a).

Overall, the large shallow pig cadavers in the Ultisol from both scenarios (LSSU and LSLU) were detected for the duration of this study at 13 and 21.5 months respectively using the 900-MHz antenna. For example, Figure 7-12a is a GPR profile of control grave 5 and cadavers 5, 6, and 7 at 19 months from the LSLU scenario. The inferior portion of the profile exhibits a strong reflection from the upper argillic horizon. Pronounced hyperbolic anomalies are present for each cadaver at 0.5 m and continue inferiorly to 0.80 m. Each anomaly exhibits well developed tails, and although the GPR profile is only deep enough to detect the top portion of the argillic horizon, it is possible to discern attenuation of the radar wave below each cadaver as disruptions of the argillic horizon. For a number of cadavers, it is possible to still discern the interface between

backfill and grave wall as a vertical straight line on the profile. In addition, the control grave with only backfill barely exhibits a discernable hyperbolic response. It is clear from the comparison of the control hole with the graves, that the grave anomaly is a result of the pig skeleton and not the disturbed soil.

A number of smaller anomalies are visible on the profile caused by buried stumps. Of particular interest is the increased resolution of the old auger hole on the eastern boundary of the anomaly from cadaver 5. Using the 500-MHz antenna, the auger hole is narrow and slightly prominent with the antenna noise removed (Figure 7-3b). Conversely, at times the anomaly from the auger hole is extremely prominent and is comparable in size and intensity to the cadaver anomalies using the 900-MHz antenna. Furthermore, the only change major change with the processed profile was an increase in the backfill above the cadavers (Figure 7-12b). The backfill is detected from the top of the profile and continues to the superior surface of the cadaver anomaly.

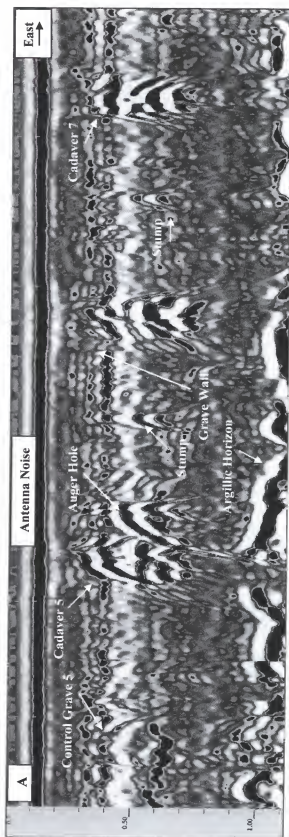


Figure 7-12. Ground-penetrating radar profile (900-MHz) of three shallow buried pig cadavers of the LSLU scenario and a blank control grave at 19 months. A) Note the demarcated argillic horizon, the grave wall, and the large anomaly from the old auger hole. B) Note the increase in the resolution of the backfill above the cadaver anomalies when the antenna noise is removed. The profile is approximately 1.20 m deep and 27 m long.

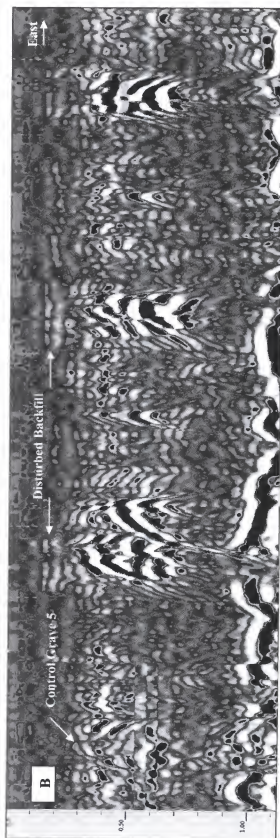


Figure 7-12. Continued

Deep Cadavers (LDSU and LDLU Scenarios)

The anomaly of the deep buried pig graves may be initially comprised of three components using the 900-MHz antenna: the disturbed soil, the outline of the grave feature, and the body. These three features of the graves are present in Figure 7-13a, a GPR profile of three large pig cadavers (8, 9, and 10) from the LDSU scenario at 2.3 months in the Ultisol. Within the grave shaft, the imagery of the disturbed soil is markedly different than the surrounding undisturbed soil because it is less compact. Although the percent of disturbed soil that is detected differs between the three graves, a vertical shaft of equal width generally extends from the ground surface to the apex of the cadaver anomaly. As the ground compacts over time, the disturbed soil is less discernable and disorganized on the profiles. The distinctive outline of the grave wall, particularly with cadaver 8, is due to the interface of the disturbed and undisturbed soil. The body is recognized at the bottom of the profile as a distinctive hyperbolic shape in the upper limit of the argillic horizon. The apex of the anomalies is visible at depths ranging from 0.90 to 1.00 m. Overall, removing the antenna noise has no effect on the resolution of the grave anomalies because the most prominent banding is near the surface (Figure 7-13b). However, backfill near the ground surface of cadaver 8 and 9 that was originally masked by the antenna noise is now visible on the processed profile. The remaining GPR profiles that are provided in this section will only include the unprocessed imagery, because the only increase in resolution of the profiles with the 900-MHz antenna is a slight detection of the backfill near the ground surface of cadaver 8 and 9 that was originally masked by the antenna noise. Overall, there is no need to process these profiles to detect the buried cadavers.

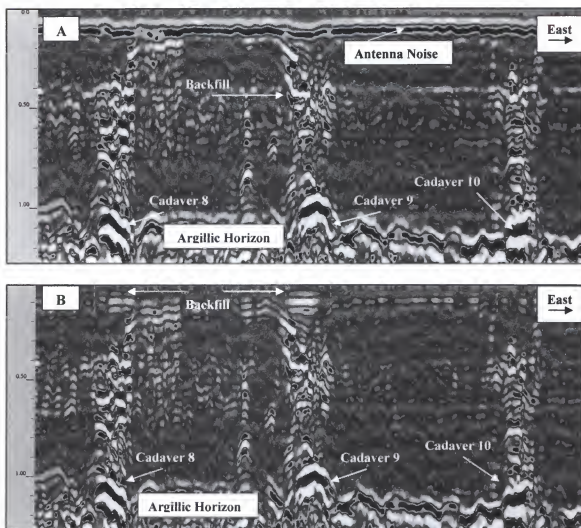


Figure 7-13. Ground-penetrating radar profile (900-MHz) of three deep cadavers (8, 9, and 10) from the LDSU scenario at 2.3 months. A) Note the response from the cadaver, the backfill, and the grave wall in the unprocessed profile. B) Backfill on the top of the profile is also detected above both cadaver anomalies when the antenna noise is removed. The profile is approximately 1.30 m deep and 21 m long.

As the backfill consolidated over time, the resolution of the pig anomalies increased. The anomalies were overall larger and the cadavers were detected at a shallower depth. Interestingly, this also occurred with the 500-MHz antenna and the same group of pig cadavers (see Figure 7-5a at 4 months). Figure 7-14 is a GPR profile

at 5.5 months exhibiting distinctive grave anomalies for cadavers 8, 9, and 10 of the LDSU scenario. The GPR profile is only deep enough to image the superior surface of the argillic horizon. All three graves exhibit clear hyperbolic anomalies and minimal soil disturbances are still retained above each cadaver. Cadaver 10 exhibits the most prominent, hyperbolic anomaly at 0.80 m that extends to the argillic horizon. The anomaly of cadaver 10 is discernable at 0.75 m and the anomaly of cadaver 9 at 0.85 m. Both descend to the argillic horizon, and backfill is detected above both cadavers. In particular, a hyperbolic anomaly is detected in the backfill above cadaver 9 at 0.40 m. It is most likely due to a void in the backfill. Removing the noise did not change the resolution of the anomalies because the banding is only at the top 0.15 m of the profile. However, backfill near the ground surface of cadaver 8 and 9 that was originally masked by the antenna noise is now visible on the processed profile.

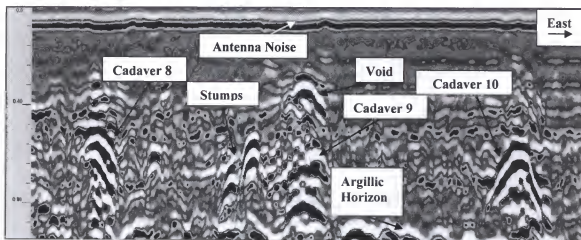


Figure 7-14. An unprocessed GPR profile (900-MHz) of three cadavers from the LDSU scenario (8, 9, and 10) in the Ultisol at 5.5 months. Note the increased response of the cadavers and the possible void above cadaver 9. The profile is approximately 1.30 m deep and 21 m long.

After 7 months it was noted that there was a decrease in the returns from the same cadavers of the LDSU scenario. In particular, while the returns of cadavers 8 and 10 decreased slightly, there was a noticeable change in resolution of cadaver 9 at 7.5 months, even though the pig cadavers have undergone very little decomposition and still retained extensive soft tissue structures (see chapter 5). Figure 7-15 is a profile of cadavers 8, 9, and 10 at 11 months. While there are no major changes with cadavers 8 and 10, the return of cadaver 9 is significantly reduced. A small hyperbolic anomaly is present from 1.00 to 1.15 m with hyperbolic tails extending into the argillic horizon. Directly below the anomaly is a break in the argillic horizon due to attenuation by the body. At the same time, the shallow anomaly in the backfill that may represent a void is also significantly reduced.

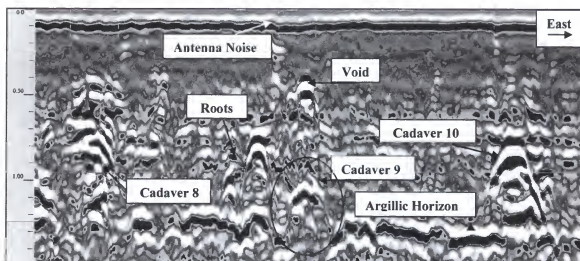


Figure 7-15. An unprocessed GPR profile (900-MHz) of three cadavers from the LDSU scenario (8, 9, and 10) in the Ultisol at 11 months. Note the decreased return of cadaver 9. The profile is approximately 1.30 m in depth and 21 m long.

The deep cadavers (1, 2, and 3) of the LDLU that were buried in the Ultisol for 21 months are further examples of the difficulty in differentiating a recognizable grave response when the pig cadaver is buried in close proximity to an argillic horizon, even with the higher resolution of the 900-MHz antenna. There were also significantly reduced returns from these cadavers as early as 6 months. Figure 7-16 is a GPR profile at 15.5 months of this group of pig cadavers and three control graves that were buried at a depth of 1.0 m to show the decreased returns after a year. This profile was also performed the same day as Figure 7-7a over the same pig cadavers and control holes with the 500-MHz antenna. The control holes consist of one with backfill (control 1), one with gravel (control 2), and one with branches (control 3). Interestingly, while the clay horizon is demarcated in Figure 7-7a between 1.00 and 1.20 m using the 500-MHz antenna, it is nonexistent in Figure 7-16 with the 900-MHz that was collected on the same day.

The control grave with gravel provides a distinctive hyperbolic anomaly that serves as a much needed reference for size and depth of the grave anomalies in Figure 7-16. In Figure 7-7a it was possible to discern hyperbolic responses from the three cadavers with the 500-MHz, however, there was poor contrast of the anomalies with the argillic horizon. Conversely, the responses are even less discernable using the 900-MHz antenna in Figure 7-16. The arrows in Figure 7-16 represent the location of the anomalies that are observed in Figure 7-7a. The return from the three cadavers is extremely weak, even though a considerable degree of soft tissue still remains (see chapter 5). Cadaver 1 has the shallowest anomaly of the three graves and is represented by a small hyperbolic reflection at 0.75 m that is adjacent to a possible buried stump.

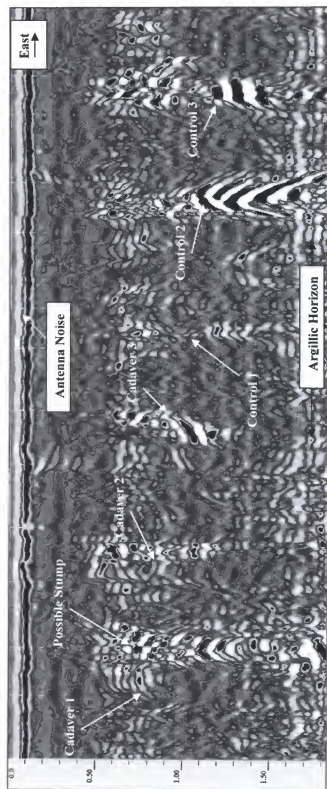


Figure 7-16. An unprocessed GPR profile (900-MHz) of three deep pig cadavers (1, 2, and 3) from the LDLU scenario and three deep control graves (1, 2, and 3) at 15.5 months. The first control grave is a blank, the second is a gravel lens, and the third contains branches. Note the poor reflections from the cadavers even though a considerable degree of soft tissue is still retained by the cadavers. The profile is approximately 2.0 m deep and 25 meters long.

The returns from cadavers 2 and 3 are represented by weak hyperbolic reflections at around 0.80 m and a number of prominent hyperbolas around 1.0 m that continue weakly through the argillic horizon. Overall, the anomalies are so poorly developed that it is difficult to discern their response even though the location of the graves is known.

Summary

Overall, the shallow graves (LSSU and LSLU) were detected for the duration of this study while there were decreased returns for the deep graves (LDSU and LDLU) caused by their proximity to the argillic horizon. Postprocessing of the data is not required for grave detection because it generally does not mask the anomaly. However, if excessive horizontal banding is noted on the profile, the data should be processed if the forensic target in question is not located because it may be obscured. Furthermore, the imagery from the 500-MHz antenna is preferred over the 900-MHz. Table 7-1 summarizes the GPR results for each large cadaver buried in the Ultisol using both antennae.

Table 7-1. Summary table of GPR results for each large cadaver buried in the Ultisol using both antennae.

Cadaver #	Scenario	500-MHz		900-MHz	
		500-MHz	900-MHz	500-MHz	900-MHz
1	LDLU	Significantly reduced return before six months; over the duration there was a weak hyperbolic anomaly that that may or may not have been discernable	Significantly reduced return before six months; over the duration there was a weak hyperbolic anomaly that that may or may not have been discernable	Significantly reduced return before six months; over the duration there was a weak hyperbolic anomaly that that may or may not have been discernable	Significantly reduced return before six months; over the duration there was a weak hyperbolic anomaly that that may or may not have been discernable
2	LDLU	Significantly reduced return before six months; over the duration there was a weak hyperbolic anomaly that that may or may not have been discernable	Significantly reduced return before six months; over the duration there was a weak hyperbolic anomaly that that may or may not have been discernable	Significantly reduced return before six months; over the duration there was a weak hyperbolic anomaly that that may or may not have been discernable	Significantly reduced return before six months; over the duration there was a weak hyperbolic anomaly that that may or may not have been discernable
3	LDLU	Significantly reduced return before six months; over the duration there was a weak hyperbolic anomaly that that may or may not have been discernable	Significantly reduced return before six months; over the duration there was a weak hyperbolic anomaly that that may or may not have been discernable	Significantly reduced return before six months; over the duration there was a weak hyperbolic anomaly that that may or may not have been discernable	Significantly reduced return before six months; over the duration there was a weak hyperbolic anomaly that that may or may not have been discernable
4	LSSU	Excellent detection for duration	Excellent detection for duration	Excellent detection for duration	Excellent detection for duration
5	LSLU	Excellent detection for duration	Excellent detection for duration	Excellent detection for duration	Excellent detection for duration
6	LSLU	Excellent detection for duration	Excellent detection for duration	Excellent detection for duration	Excellent detection for duration
7	LSLU	Excellent detection for duration	Excellent detection for duration	Excellent detection for duration	Excellent detection for duration
8	LDSU	Significantly reduced return after one year; difficult to detect	Significantly reduced return after one year; difficult to detect	Significantly reduced return after one year; difficult to detect	Significantly reduced return after one year; difficult to detect
9	LDSU	Significantly reduced return after one year; difficult to detect	Significantly reduced return after one year; difficult to detect	Significantly reduced return after one year; difficult to detect	Significantly reduced return after one year; difficult to detect
10	LDSU	Excellent detection for duration	Excellent detection for duration	Excellent detection for duration	Excellent detection for duration
11	LSLU	Decreased return at 13 months caused by increased antenna noise, but still discernable; excellent resolution of anomaly with processing	Decreased return at 13 months caused by increased antenna noise, but still discernable; excellent resolution of anomaly with processing	Decreased return at 13 months caused by increased antenna noise, but still discernable; excellent resolution of anomaly with processing	Decreased return at 13 months caused by increased antenna noise, but still discernable; excellent resolution of anomaly with processing
12	LSSU	Decreased return at 13 months caused by increased antenna noise, but still discernable; Excellent resolution of anomaly with processing	Decreased return at 13 months caused by increased antenna noise, but still discernable; Excellent resolution of anomaly with processing	Decreased return at 13 months caused by increased antenna noise, but still discernable; Excellent resolution of anomaly with processing	Decreased return at 13 months caused by increased antenna noise, but still discernable; Excellent resolution of anomaly with processing

CHAPTER 8 GPR RESULTS FOR SMALL PIG CADAVERS

The 500-MHz Antenna

GPR-Soil Profile

Unlike the Ultisol, the GPR profile of the Entisol does not exhibit a distinctive reflection from the subsurface horizons that comprise this soil. The Entisol is comprised of sandy horizons that are not easily detected by the GPR and the water table was deeper than the depth of viewing. Figure 8-1 is a GPR profile that was collected immediately north of row 1 with the 500-MHz antenna (Figure 4-8). The most distinctive feature in Figure 8-1a is the thick, horizontal banding across the top of the profile due to antenna noise that begins at 0.0 m and extends to a depth of 0.60 m. Processing the GPR profile to remove the antenna noise eliminated this thick horizontal banding (Figure 8-1b).

Shallow Cadavers (SSSE and SSLE Scenarios)

Distinctive grave anomalies were produced for the small pig cadavers buried at shallow depths with the 500-MHz antenna. At one month, two hyperbolic anomalies from cadavers 15 and 16 (SSLE scenario) begin at approximately 0.50 m and continue inferiorly to 1.70 m (Figure 8-2a). Each anomaly consists of a vertical series of hyperbolic curves with distinctive tails, and the cadaver is located at the apex of each anomaly. Backfill above the cadavers is not detected because it is masked by the antenna noise. In addition, control grave 7 that contains only backfill, barely exhibits a

discernable response. It is clear from the comparison of the control grave with the pig graves that the anomalies are due to the pig remains and not the backfill.

When the antenna noise is removed (Figure 8-2b), there is only a slight increase in the resolution of the anomalies. Of interest is the increase in resolution of the tails that contribute to the hyperbolic shape of the anomalies. The backfill directly above each cadaver is now detected when the antenna noise is removed. Overall, the profile does not need to be processed for grave detection at one month.

The small cadavers buried at the shallow depth were easily detected over the first year in the Entisol. Figure 8-3a is the last GPR profile of cadavers 19 and 20 of the SSSE scenario that was collected at 12.5 months before they were excavated. Both cadavers produce distinctive returns even though there is extensive antenna noise that extends to a depth of approximately 0.70 m. Cadaver 19 exhibits a hyperbolic anomaly at 0.55 m with prominent tails that continue to approximately 1.00 m. Cadaver 20 exhibits an overall larger hyperbolic anomaly, in length and breadth, at 0.40 m that extends to the bottom of the profile at 1.20 m. Excavations at 12.5 months indicated highly variable skeletonization between the two cadavers (see Chapter 5). Although cadaver 19 was completely skeletonized, cadaver 20 still retained a significant amount of tissue. While there were no problems detecting cadavers expressing variable degrees of skeletonization, the larger anomaly of cadaver 20 is most likely due the retention of extensive soft tissue. Of interest, on the western border of the control grave 9 is a prominent hyperbolic anomaly due to a buried stump that should not be mistaken for the response of the disturbed soil. Furthermore, it is clear from the comparisons between the graves that the grave anomaly is a result of the pig remains and not the disturbed soil.

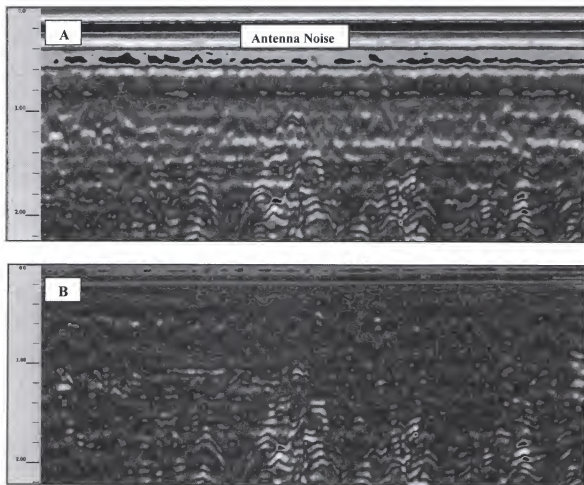


Figure 8-1. Ground-penetrating radar profile of the Entisol using the 500-MHz antenna. A) Note the prominent antenna noise, horizontal banding from 0 to 0.60 m, and the absence of any distinctive horizons. B) The horizontal banding at the top of the profile is removed with processing. The profile is approximately 2.20 m deep and 23 m long.

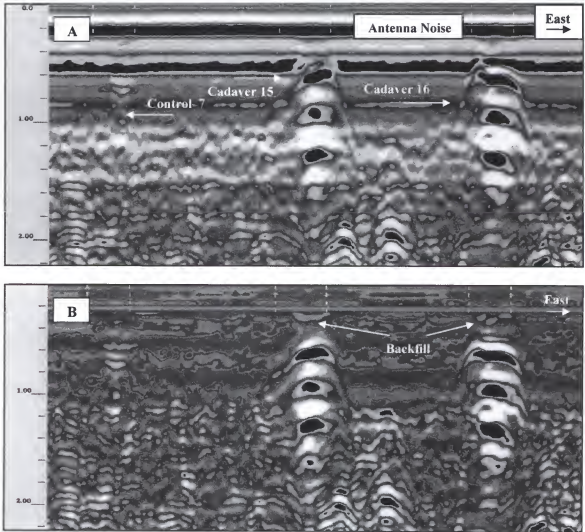


Figure 8-2. Ground-penetrating radar profile of two cadavers from the SSSE scenario (15 and 16) and control grave 7 at one month using the 500-MHz antenna. A) Note the extensive banding due to antenna noise at upper portion of the unprocessed profile. B) The backfill is now visible above both cadaver anomalies when the banding is removed in the processed profile. The profile is approximately 2.20 m in deep and 17 m long.

Removing the antenna noise significantly increased the resolution of cadavers 19 and 20 (Figure 8-3b). Although the size of the grave anomalies did not change, the vertical layering of hyperbolic curves and tails are more distinct because the antenna noise was partially masking the returns from cadavers 19 and 20. The resolution of control grave 9 also increased slightly, but the response from only the disturbed soil was significantly less than that of the pig remains.

After a year and a half, the return from the shallow pig remains was reduced, but the anomalies were still easily discernable. Figure 8-4 is a GPR profile exhibiting hyperbolic returns from cadavers 13 and 14 (SSLE scenario) at 18.5 months. The returns from the remains of the cadavers appear below the horizontal banding on the profile that begins at the ground surface and continues to 0.60 m. Although the anomaly for cadaver 15 is still slightly larger, they both appear as hyperbolic anomalies at approximately 0.60 m with prominent tails that extend to the bottom of the profile at 1.30 m. Backfill is also noted directly above each anomaly.

Furthermore, control grave 7 with only backfill barely exhibits a discernable response. It is clear from the comparisons between the graves that the prominent grave anomalies are due to the pig remains and not the disturbed soil. Removing the antenna noise barely increased the resolution of the cadavers. The size of the anomalies did not change, but the backfill that was partially masked by the horizontal banding is now visible directly above the apex of each anomaly. Overall, there is no need to process the profile to detect these cadavers at 18.5 months.

The return from the small cadavers buried at a shallow depth decreased significantly over the last two months prior to excavation. It is important to note that the

cadavers 15 and 16 (SSLE scenario) were completely skeletonized when they were excavated at 21 months (see chapter 5). For example, Figure 8-5a is a profile at 19 months and 20 days of cadavers 15 and 16. The horizontal banding on this profile begins at the ground surface and continues to the bottom of the profile at 1.30 m, with the most prominent banding at the top of the profile between 0.0 to 0.70 m. Overall, the extensive antenna noise significantly reduces the contrast of the anomalies from the pig remains.

Although cadaver 15 still exhibits a slightly a stronger return, both cadavers exhibit weak, but narrowly focused hyperbolic anomalies, and backfill is detected directly above both anomalies. Furthermore, control grave 7 barely exhibits a discernable response, and it is clear from the comparisons between the graves that the grave anomalies are still the result of the pig remains and not the disturbed soil. The resolution of the two grave anomalies increased significantly when the antenna noise is removed (Figure 8-5b). The anomalies from cadaver 15 and 16 begin at 0.55 m and continue to the bottom of the profile at 1.30 m. The return of cadaver 15 is still more prominent, and backfill is now noted above both anomalies. Although control grave 7 exhibits an increased response at approximately 0.55 m, it is still barely discernable in comparison to the returns from the pig remains.

Figure 8-6a is the last profile of control grave 7 and cadavers 15 and 16 (SSLE scenario) that was collected at 20 months and nine days before they were excavated at 21 months. Excavations at 21 months revealed that both cadavers were completely skeletonized (see Chapter 5). Once again, there is extensive antenna noise on the profile that significantly reducing the contrast of the returns from the pig remains. The horizontal banding begins at the ground surface and continues to the bottom of the profile

at 1.25 m, with the thickest banding extending from the top of the profile at 0.0 m to a depth of 0.60 m.

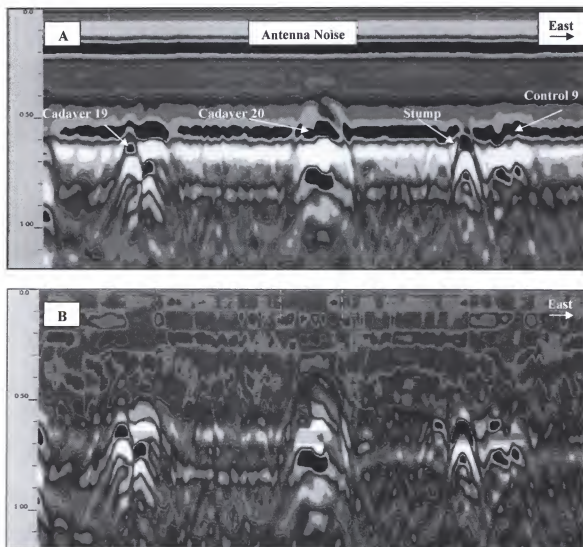


Figure 8-3. Ground-penetrating radar profile of two cadavers from the SSSE scenario (19 and 20) and control grave 9 at 12.5 months using the 500-MHz antenna. A) Even with the extensive horizontal banding, the cadaver anomalies are still distinctive in the unprocessed profile. B) The resolution of the cadaver anomalies increased in the processed profile when the horizontal banding was removed. The profile is approximately 1.20 m deep and 17 m long.

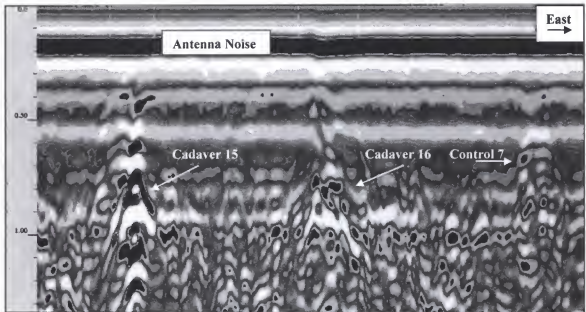


Figure 8-4. An unprocessed GPR profile of two cadavers from the SSLE scenario (15 and 16) and control grave 7 at 18.5 months using the 500-MHz antenna. The profile is approximately 1.20 m deep and 17 m long.

The stark contrast between the returns from the remains of cadavers 15 and 16 is apparent on the unprocessed profile. The remains of cadaver 15 are visible as a hyperbolic anomaly at 0.60 m with hyperbolic tails that continue to the bottom of the profile, and a soil disturbance is detected directly above the apex of the anomaly. Interestingly, there is barely a response from the remains of cadaver 16. A faint hyperbolic return is present at 0.70m with a tail that extends to 1.20 m. However, it is difficult to differentiate the poor return of cadaver 16 from the noise throughout the profile. If this grave was not marked, it may not be possible to detect this grave because there insufficient contrast with the background noise on the profile. Finally, there is no recognizable return from control grave 7. Therefore, it can be inferred that the remains of

cadaver 15, which is completely skeletonized, is the source of the anomaly and not the backfill.

The resolution of the two grave anomalies increased somewhat with the removal of the antenna noise, and there was still no distinguishable return from control grave 7 (Figure 8-6b). The anomaly from cadaver 15 is still very prominent. Of particular interest is an increase in the resolution of cadaver 16. The remains of cadaver 16 are visible as a hyperbolic anomaly at 0.50 m with hyperbolic tails that continue to the bottom of the profile, and a soil disturbance is detected directly above the apex of the anomaly. The combination of a hyperbolic response and detected backfill increases the contrast of this buried body so it can be differentiated from the general noise on the GPR profile. If the location of the grave for cadaver 16 was not known, it would be difficult to locate this grave because of the limited contrast of the anomaly with the general background noise.

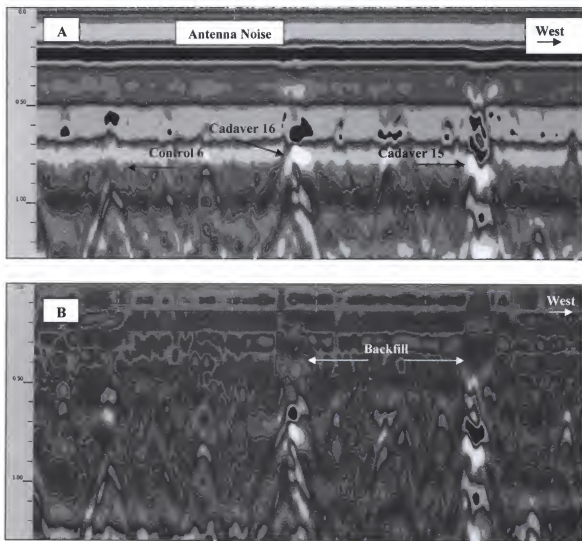


Figure 8-5. Ground-penetrating radar profile of two cadavers from the SSLE scenario (15 and 16) and control grave 7 at 19 months and 20 days using the 500-MHz antenna. A) There is poor resolution of the cadaver anomalies with the extensive horizontal banding in the unprocessed profile. B) Note the increased resolution of the pig remains and the control grave in the processed profile. The profile is approximately 1.30 m deep and 17 m long.

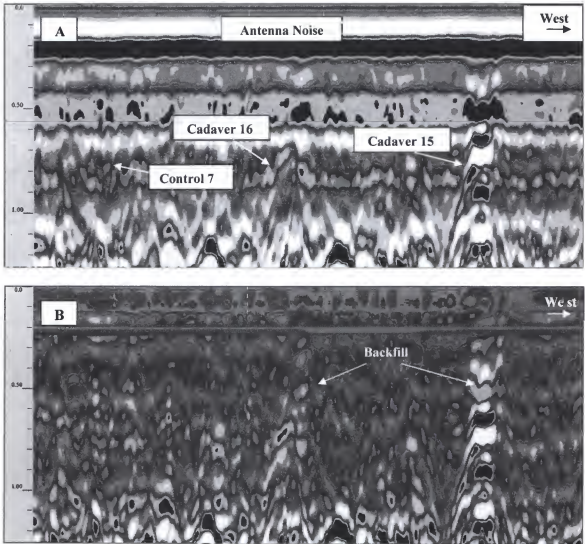


Figure 8-6. Ground-penetrating radar profile of two cadavers from the SSLE scenario (15 and 16) and control grave 7 at 20 months and nine days using the 500-MHz antenna. A) The resolution of the cadaver anomalies decreased with the extensive horizontal banding in the unprocessed profile. B) Note the increased contrast of cadaver 16 in the processed profile. The profile is approximately 1.25 m deep and 17 m long.

Deep Cadavers (SDSE and SDLE Scenarios)

Distinctive grave anomalies were produced for the large pig cadavers that were buried at deep depths using the 500-MHz antenna. At one month, two hyperbolic anomalies from cadavers 13 and 14 of the SDLE scenario (Figure 8-7) begin at approximately 0.95 m and continue inferiorly to 1.60 m. Prominent horizontal banding caused by the antenna noise extends from the top of the profile at 0.0 m to a depth of 0.60 m and is therefore not deep enough to mask the grave anomalies. Furthermore, control grave 6 with only backfill barely exhibits a discernable response, and it is clear from the comparisons between the graves that the grave anomaly is a result of the pig remains and not the disturbed soil. When the antenna noise is removed, there is only a slight increase in the resolution of the anomalies from control grave 6 and cadavers 13 and 14, and the backfill is detected from the ground surface down to the apex of the grave anomaly. Overall, there is no need to process the file to remove the antenna noise for grave detection.

Over the first year the returns from the deep graves decreased minimally with the 500-MHz antenna. There was still a strong enough contrast between the anomalies and the soil to detect the pig remains without processing the data. For example, Figure 8-8 is a profile at 9.5 months of cadavers 13 and 14 (SDLE scenario) and control grave 6. Two distinctive hyperbolic anomalies begin at 0.80 m and their tales continue to the bottom of the profile at 1.60 m. Minimal soil disturbances are barely detected above each cadaver anomaly. The most interesting characteristic of this profile is the anomaly from control grave 6; it is near identical in shape and size to the return produced from the remains of cadaver 14. The increased return of control grave 6 is most likely due to the increased

retention of moisture from rain in the backfill. The distinctiveness of the anomaly from control grave 6 decrease in subsequent profiles. However, it would not be possible to visually determine which grave out of the three did not contain a pig on this particular profile. Overall, there were no changes worth noting when the antenna noise was removed because the banding is only on the upper portion of profile from 0.0 to 0.70 m above the grave anomalies.

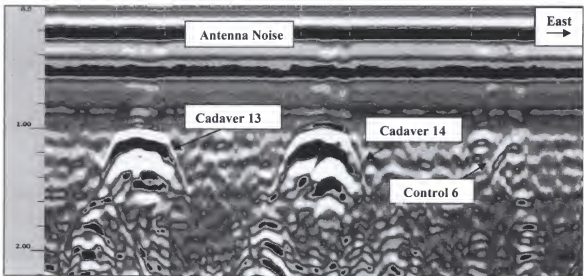


Figure 8-7. An unprocessed GPR profile of two cadavers from the SDLE (13 and 14) and control grave 6 at one month using the 500-MHz antenna. The profile is approximately 2.20 m deep and 17 m long.

Over the first year and a half there were no problems detecting the small cadavers buried at deep depths. Distinctive anomalies were discernable on the unprocessed profiles for the short-term cadavers (17 and 18) from the SDSE scenario that were excavated at 12.25 months. Similarly, there were no problems detecting the long term cadavers (13 and 14) SDLE scenario on the unprocessed profiles after a year. For example, Figure 8-9 is GPR profile at 14 months of cadavers 13 and 14 (SDLE scenario)

and control grave 6. Two distinctive hyperbolic anomalies of similar size begin at 0.80 m and their tails continue to the bottom of the profile at 1.85 m. Furthermore, control grave 6 with only backfill barely exhibits a discernable response, and it is clear from the comparisons between the graves that the grave anomaly is a result of the pig remains and not the disturbed soil. Prominent horizontal banding due to the antenna noise extends from the top of the profile at 0.0 m to a depth of 0.90 m and is therefore not deep enough to mask the grave anomalies. Overall, there were no major changes to the grave anomalies when the file was processed.

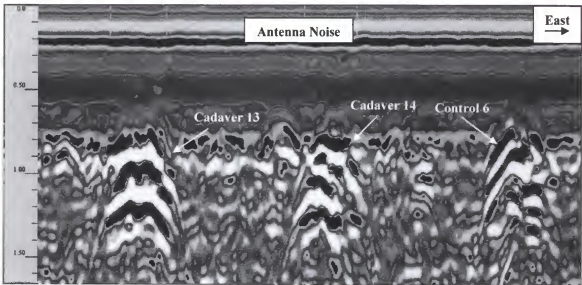


Figure 8-8. An unprocessed GPR profile of two cadavers from the SDLE scenario (13 and 14) and control grave 6 at 9.5 months using the 500-MHz antenna. Note the increased return from the control grave caused by increased moisture in the soil. The profile is approximately 1.65 m deep and 17 m long.

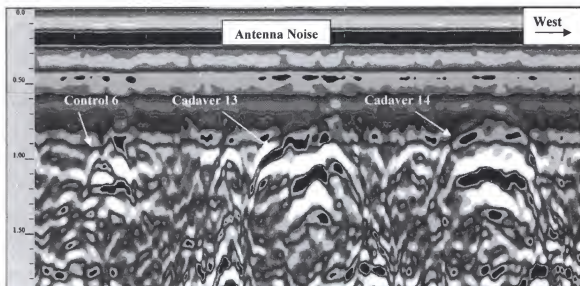


Figure 8-9. An unprocessed GPR profile of two cadavers from the SDLE scenario (13 and 14) and control grave 6 at 14 months using the 500-MHz antenna. The profile is approximately 1.85 m deep and 17 m long.

The returns from the small cadavers buried at deep depths decreased significantly over the last couple of months before the graves were excavated at 21 months. Overall, the grave anomalies were poorly developed, and it was difficult to discern recognizable returns from cadaver 13 and 14 on the unprocessed profile even though the location of the graves was known. For example, Figure 8-10a is a profile at 19 months and 20 days of cadavers 13 and 14. The extensive noise on this profile reduces the contrast of the returns. The prominent banding extends from the top of the profile at 0.0 to 0.70 m, but additional banding due to noise continues to a depth of 1.30 m.

It is important to note that a significant amount of soft tissue was still retained by both cadavers (see chapter 5) when the pig remains were excavated at 21 months. In Figure 8-10a, both cadavers (13 and 14) from the SDLE scenario exhibit distinctive returns and are recognized by their elongated tails. It is difficult to discern the anomalies because the

noise masks the hyperbolic layering that is normally discernable. They are both visible at 0.80 m and the tails extend to the bottom of the profile at 1.70 m. Soil disturbances are not noted above the cadaver anomalies because it is masked by the obtrusive banding. Furthermore, the control grave 6 with only backfill barely exhibits a discernable response, and it is clear from the comparisons between the graves that the distinctive anomalies are the result of the pig remains and not the disturbed soil.

The resolution of the two grave anomalies from cadavers 13 and 14 significantly increased with the removal of the antenna noise (Figure 8-10b). Although the return from cadaver 13 is more prominent, both cadavers are easily discernable as a series of hyperbolic layers and prominent tails. Of particular interest is the increased resolution of the backfill above both cadavers that is prominent between 0.15 m down to the apex of each grave anomaly. In addition, a number of prominent hyperbolic returns are discernable from buried stumps that had been masked by the antenna noise. Furthermore, control grave 6 does not exhibit a discernable response, and it is still clear from the comparisons between the graves that the distinctive grave anomalies are the result of the pig remains and not the disturbed soil.

The return from the remains of cadaver 13 and 14 were still discernable, but further reduced, on the last profile collected before the remains were excavated at 20 months and nine days (Figure 8-11); 20 days after Figure 8-10 was collected. Both anomalies are faintly discernable through the noise. An anomalous response from cadaver 13 is present at 0.80 to 1.50 m, while the return of cadaver 14 is discernable at 0.90 to 1.60 m. Soil disturbances are not noted above the cadavers due to the obtrusive banding. Conversely, control grave 6 does not exhibit discernable return. The hyperbolic

shape of both anomalies is increased when the antenna noise is removed (Figure 8-11b). Of particular interest is the increased resolution of the backfill above both cadavers. However, control grave 6 still does not exhibit a distinctive return on the processed profile. Although there may be a minimal response from the base of the control grave, it can not be distinguished from the general noise throughout the profile. Furthermore, it is still clear from the comparisons between the pig graves with control grave 6 that the anomalies are the result of the pig remains and not the disturbed soil. Overall, removal of the antenna noise may be needed for grave detection in this instance.

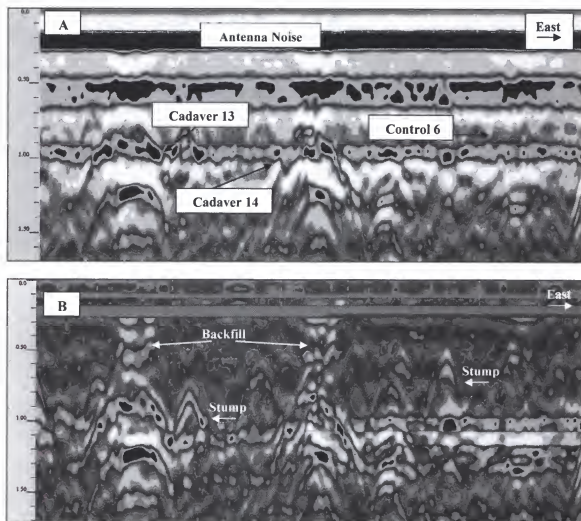


Figure 8-10. Ground-penetrating radar profile of two cadavers from the SDLE scenario (13 and 14) and control grave 6 at 19 months and 20 days using the 500-MHz antenna. A) There is poor resolution of the cadaver anomalies in the unprocessed profile caused by the extensive horizontal banding. B) Note the increased contrast of both cadavers when the antenna noise is removed in the processed profile. The profile is approximately 1.70 m deep and 17 m long.

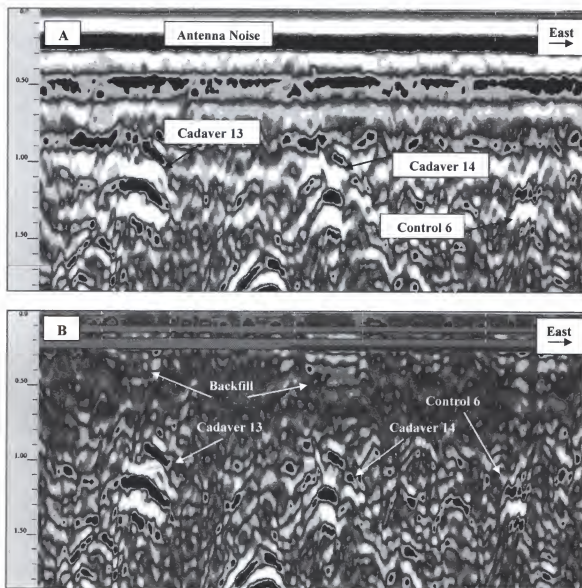


Figure 8-11. An unprocessed GPR profile of two cadavers from the SDLE scenario (13 and 14) and control grave 6 at 20 months and nine days using the 500-MHz antenna. A) There is poor resolution of the cadaver anomalies with the extensive horizontal banding in the unprocessed profile. B) Note the increased contrast of both cadavers when the antenna is noise removed. The profile is approximately 1.85 m deep and 17 m long.

The 900-MHz Antenna

GPR-Soil Profile

Figure 8-12a is a GPR profile that was collected immediately north of row 1 with the 900-MHz antenna (Figure 4-8). The thick horizontal banding across the top of the profile due to antenna noise begins at 0.0 m and extends only to a depth of 0.15 m. The intensity and depth of this banding generally does not increase. There are two major differences between the 900- and 500-MHz GPR profiles that were collected over the Entisol. Processing of the GPR profiles with the 900-MHz is generally not needed for grave detection because the obtrusive banding is shallower with this antenna and does not mask the grave anomalies. The second major difference between antennae is an increase in the resolution, or detail, of background noise caused by stumps and roots with the 900-MHz that is not removed by processing the data (Figure 8-12b). Extensive noise may obscure the intended target by limiting the contrast of the target with that of the soil.

Shallow Cadavers (SSSE and SSLE Scenarios)

Distinctive grave anomalies were produced for the small pig cadavers that were buried at shallow depths. For example, at 19 days, two hyperbolic anomalies from cadavers 19 and 20 (SSSE scenario) begin at approximately 0.40 m and continue inferiorly to 0.75 m (Figure 7-13). Each anomaly consists of a vertical series of hyperbolic curves, and the cadaver is located at the apex of each anomaly. Furthermore, control grave 6 barely exhibits a discernable response, and it is clear from the comparisons between this grave and the pig graves that the grave anomaly was caused by the pig remains and not the disturbed soil. Removing the antenna noise has no effect on the resolution of the grave anomalies because the most prominent banding is at the top

of the profile above the pig cadavers. However, backfill near the ground surface of the pig graves originally masked by the antenna noise is now visible in the processed profile. Overall, there is no need to process the data to remove the antenna noise to detect these cadavers.

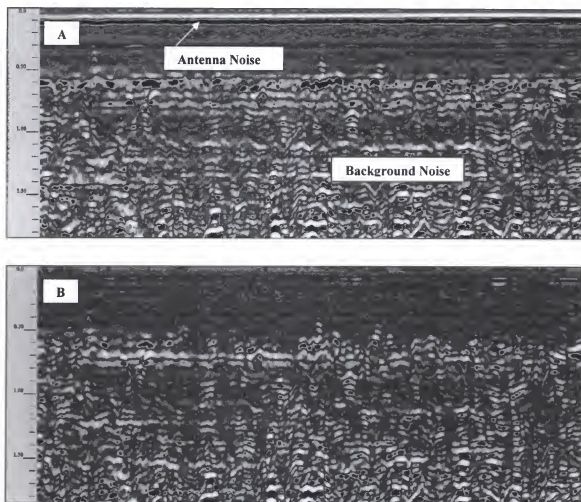


Figure 8-12. Ground-penetrating radar profile of the Entisol using the 900-MHz antenna. A) Note the limited horizontal banding from the antenna noise between 0.0 to 0.15 m, the background noise throughout the profile, and the absence of any distinctive horizons in the unprocessed profile. B) The horizontal banding at the top of the profile is removed in when the profile is processed. The profile is approximately 1.80 m deep and 23 m long.

There are a number of apparent differences in the details of the grave anomalies between the profiles of the 900- and 500-MHz antennae. Comparisons are made between Figure 7-13 and Figure 7-2a to elaborate this point. Although both grave anomalies appear at the same depth, the anomaly from the 500-MHz antenna extends to a deeper depth than the 900-MHz anomaly. In addition, the tails from the 900-MHz anomalies are generally oriented more vertically (there can be exceptions), while the tails from the 500-MHz are oriented further away from the body at a greater angle. As a result, the 500-MHz anomalies appear larger than the 900-MHz anomalies due to the more pronounced tails and the deeper depth to which they extend.

Excavations of cadavers 19 and 20 (SSSE scenario) at 12.5 months indicated variable decomposition patterns ranging from completely decomposed to extensive retention of soft tissue (see Chapter 5). Overall, these small cadavers were easily detected during the monitoring period of 12.25 months. Similarly, the cadavers from the SLSE scenario were also easily detected during the first year of monitoring. For example, Figure 8-14a, is a profile of control grave 7 with only backfill and cadavers 15 and 16 of the SSLE scenario at 12.5 months. There is extensive background noise on the profile as well as less obtrusive horizontal banding due to antenna noise that extends to the bottom of the profile. The thick horizontal banding across the top profile caused by antenna noise is present from 0.0 m and continues inferiorly to a depth of 0.15 m. Less obtrusive horizontal banding is also between 0.35 to 0.90 m on the profile as well as background noise throughout the profile that reduces the contrast of the anomalies. Both cadavers exhibit hyperbolic returns that are easily discernable at approximately 0.50 to 0.75 m. Although cadaver 15 exhibits a larger return, the smaller return of 16 is discernable due

to the hyperbolic shape. In addition, minimal soil disturbances are noted above each cadaver starting at approximately 0.20 m and continuing down to the apex of the grave anomalies.

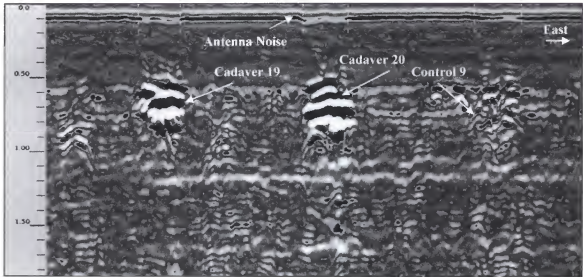


Figure 8-13. An unprocessed GPR profile of two cadavers from the SSSE scenario (19 and 20) and control grave 9 at 19 days using the 900-MHz antenna. The profile is approximately 1.80 m deep and 17 m long.

A soil disturbance is also visible at control grave 6 at approximately 0.30 m and continuing down to 0.75 m. However, this control grave does not exhibit a discernable hyperbolic response, and although there may be a minimal response, it cannot be distinguished from the general noise throughout the profile. At the same time, the absence of a hyperbolic response from control grave 6 easily differentiates it from the cadaver anomalies. Overall, there is no need to process the data to remove the antenna noise for grave detection at one month.

Removing the antenna noise increased the resolution of the cadaver anomalies as well as the backfill (Figure 8-14b). The increase in resolution does not come from the

removal of the prominent banding at the top of the profile, but from the removal of the less obtrusive horizontal banding between 0.35 to 0.90 m. The hyperbolic response from both cadavers has increased, and the contrast of the backfill of control grave 6 has also increased. However, it is still clear from the comparisons between the graves that the hyperbolic anomalies are caused by the pig remains and not the disturbed soil.

The remains of both cadavers still produced discernable returns after 17 months. Figure 8-15 is a profile of cadavers 15 and 16 (SSLE scenario) at 17 months and 11 days to a depth of approximately 1.10 m. Cadaver 15 exhibits a distinctive hyperbolic response at 0.50 m with distinctive tails that continue to approximately 1.00 m. A soil disturbance is also noted directly above the anomaly. Cadaver 16 also exhibits a smaller, but discernable response at 0.60 m with distinctive tails that continue to 0.90 m. Furthermore, control grave 7 exhibits a barely discernable response. Overall, there were no major changes to the grave anomalies or backfill when the antenna noise was removed because the most prominent banding is at the top of the profile above the grave anomalies.

At nearly, 20 months discernable returns were produced by the backfill and remains of cadavers 15 and 16 (SSLE scenario). Figure 8-16a is a profile of cadavers 15 and 16 at 19 months and 20 days to a depth of approximately 1.05 m. The returns from both cadavers are very distinctive because the entire grave shaft is visible directly below the thick banding at 0.2 m to the apex of the anomalies from the pig remains at 0.60 m. The anomalies from the remains continue to the bottom of the profile as hyperbolic tails. The increased response from the backfill and background noise, compare to Figure 8-15, is caused by an increase in the retention of moisture in the soil.

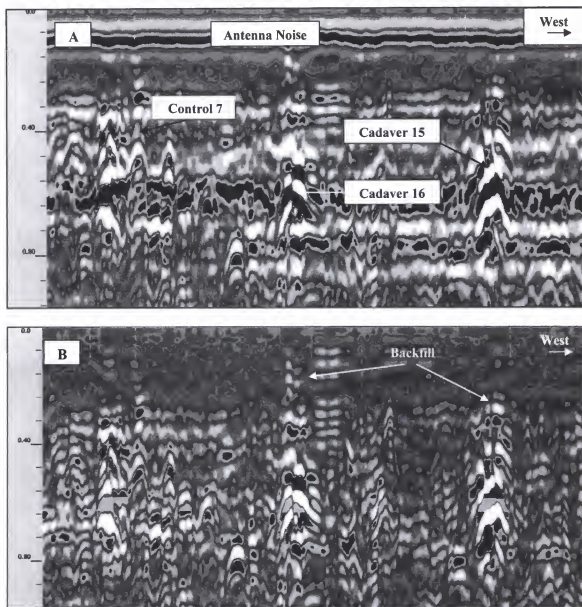


Figure 8-14. Ground-penetrating radar profile of two cadavers from the SSLE scenario (15 and 16) and control grave 7 at 12.5 months using the 900-MHz antenna. A) There is poor resolution of the cadaver anomalies with the extensive horizontal banding in the unprocessed profile. B) Note the increased contrast of the pig remains and backfill when the antenna noise is removed. The profile is approximately 1.00 m deep and 17 m long.

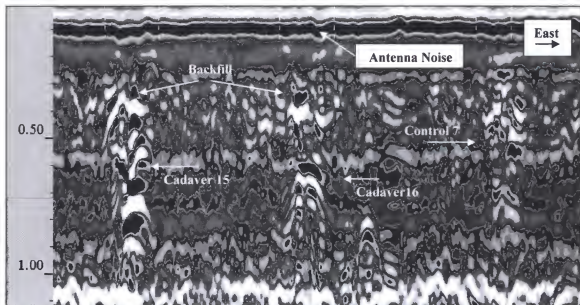


Figure 8-15. An unprocessed GPR profile of two cadavers from the SSLE scenario (15 and 16) and control grave 7 at 17 months and 11 days using the 900-MHz antenna. The profile is approximately 1.10 m deep and 17 m long.

The horizontal banding across the top profile caused by antenna noise is present from 0.0 m and continues inferiorly to a depth of 0.20 m in Figure 8-16a. In addition, less obtrusive banding begins at 0.20 m and continues to the bottom of the profile. Removing the antenna noise on the profile increased the resolution of the grave anomalies as well as the backfill that was masked at the top of the profile (Figure 8-16b). However, there was no problem detecting the graves with the unprocessed profile that included the antenna noise. Of particular interest is a comparison of Figure 8-16b with that of Figure 8-6b, which is the 500-MHz profile collected on the same day over the identical graves. Note the increased return of the backfill in the grave shafts above the graves and of the control grave using the 900-MHz (Figure 8-16b). The high resolution, 900-MHz antenna significantly increases the resolution of the disturbed soil in comparison to the 500-MHz profile (Figure 8-6b) that barely detects the disturbed soil.

Interestingly, while the remains of cadaver 15 were detected during the duration of the monitoring process, the response from cadaver 16 decreased over time until there was barely a discernable response at 21 months. Figure 17 is the last profile of control grave 7 and cadavers 15 and 16 at 20 months and 9 days before they were excavated at 21 months. This profile was collected 27 days after Figure 8-16. It is important to note that both cadavers were completely skeletonized at 21 months (see Chapter 5). The most obvious difference in the profile is the stark contrast between the anomalies from cadaver 15 and 16. The remains of cadaver 15 are visible as a hyperbolic anomaly between 0.45 and 0.70 m, with extensions that continue to the bottom of the profile. Interestingly, there is barely any response from the remains of cadaver 16. A small hyperbolic return is barely distinguishable between 0.50 to 0.80 m. However, it is difficult to differentiate the poor return of cadaver 16 from the background noise throughout the profile. If this grave was not marked, it would most likely be impossible to detect. Finally, there is no recognizable return from control grave 6. Therefore, it can be inferred that the remains of cadaver 15, which is completely skeletonized, is the source of the anomaly and not the backfill. There were no changes worth noting in the processed file.

Although there was no discernable response from the remains of cadaver 16 (SSLE scenario) at 20 months and nine days (Figure 8-17), the remains were detected 20 days earlier in Figure 8-16a when there was an increase in soil moisture. It is possible that the remains of cadaver 16 can still be detected after 20 months with increased soil moisture because the moisture may act to highlight the backfill and pig remains. However, it appears that by 20 months there may be difficulty detecting the small cadavers with the 900-MHz when they are completely skeletonized.

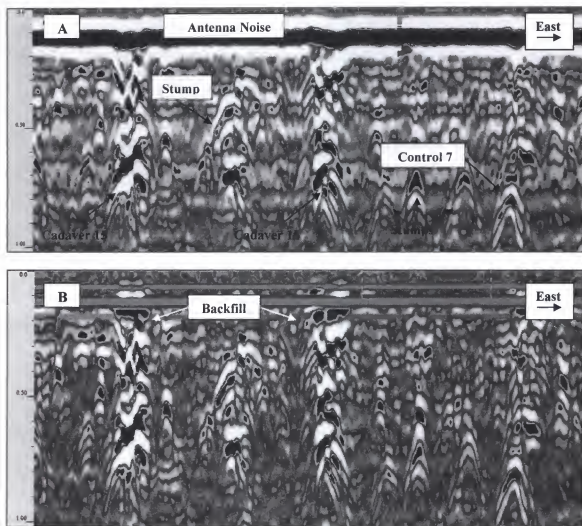


Figure 8-16. Ground-penetrating radar profile of two cadavers from the SSLE scenario (15 and 16) and control grave 7 at 19 months and 20 days using the 900-MHz antenna. A) Note the increased response of the backfill and background noise caused by the increased moisture retained in the soil. B) The contrast of the backfill above the pig remains increased in the processed profile when the banding was removed. The profile is approximately 1.00 m deep and 17 m long.

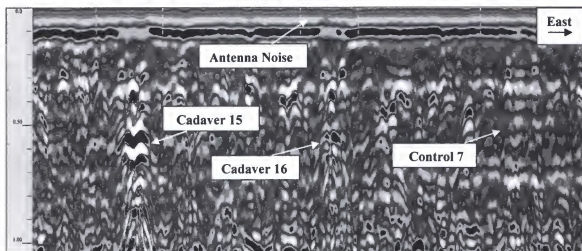


Figure 8-17. An unprocessed GPR profile of two cadavers from the SSLE scenario (15 and 16) and control grave 7 at 20 months and nine days using the 900-MHz antenna. The profile is approximately 1.00 m deep and 17 m long.

Deep Cadavers (SDSE and SDLE Scenarios)

Distinctive grave anomalies were initially produced for the small pig cadavers that were buried at a deep depth in the Entisol using the 900-MHz. For example, in Figure 8-18 two hyperbolic anomalies from cadavers 17 and 18 are clearly distinctive. The apex of cadaver 18 starts at 0.80 m and the anomaly continues inferiorly to 1.40 m. Cadaver 17 begins at approximately 1.00 m and continues inferiorly to 1.40 m. Both anomalies exhibit distinctive tails and backfill is noted above the grave anomalies, starting at 0.40 m and continuing inferiorly to the apex of the anomalies. Furthermore, control grave 8 with only backfill exhibits a flat hyperbolic response starting at 1.10 m that is consistent with the location of the grave floor. Backfill is also noted above the hyperbolic return between 0.40 to 1.10 m. It is clear from the comparisons between these graves that the distinctive grave anomalies were due to pig cadavers and not the disturbed soil. Removing the antenna noise has no effect on the resolution of the grave anomalies

because the most prominent banding is at the top of the profile above the pig cadavers. However, the resolution of the backfill above the three graves increased with processing. Overall, there is no need to process the data to remove the antenna noise to detect these cadavers.

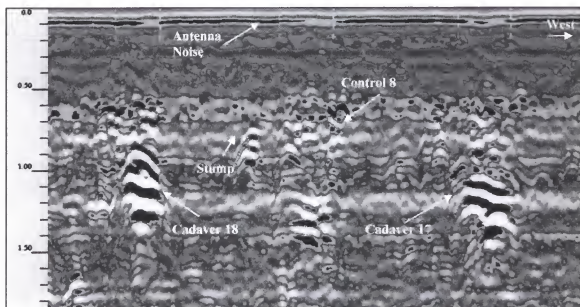


Figure 8-18. An unprocessed GPR profile of two cadavers from the SDSE scenario (17 and 18) and control grave 8 at 19 days using the 900-MHz antenna. The profile is approximately 1.85 m deep and 17 m long.

Although the cadavers have undergone very little decomposition, their hyperbolic returns have decreased by six months. For example, Figure 8-19 is a GPR profile of control grave 6 and cadavers 13 and 14 at six months and 27 days. Both cadavers are recognized by the soil disturbances and hyperbolic responses from the pig bodies. The response from cadaver 13 is more pronounced than that of cadaver 14. Although the backfill from the control grave is detected, there is no prominent hyperbolic response. Removing the antenna noise did not increase the resolution of the grave anomalies.

Overall, there is no need to process the data to remove the antenna noise for grave detection.

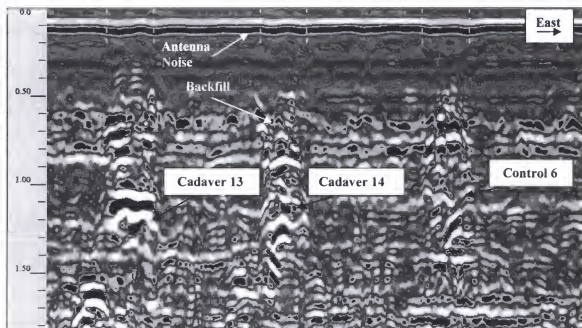


Figure 8-19. An unprocessed GPR profile of two cadavers SDLE scenario (13 and 14) and control grave 6 at six months and 27 days using the 900-MHz antenna. The profile is approximately 1.85 m deep and 17 m long.

Cadavers 17 and 18 (SDSE scenario) were detected during the monitoring period of 13 months, but the intensity of the reflections was somewhat reduced even though both cadavers still retained extensive soft tissue when they were excavated (see Chapter 5). For example, Figure 8-20 is a GPR profile of control grave 8 and cadavers 17 and 18 at 11 months and three days. Both cadavers produced discernable hyperbolic reflections. The return from 17 begins at 0.95 m and continues to 1.40 m with prominent tails that continue to the bottom of the profile. The backfill is detected above the cadaver at a depth of 0.70 m down to the apex of the pig anomaly. Cadaver 18 exhibits a return between 0.75 to 1.30 m. At the same time, two distinctive hyperbolic responses were

produced from the control grave between 0.85 to 1.40 m. Removing the antenna noise did not increase the resolution of the grave anomalies. Although the anomalies from the pig cadavers are overall larger and more consolidated, in an actual forensic situation it would not be possible to visually determine which grave out of the three did not contain a body. However, if the anomalies were ranked in terms of higher probability for detecting a body, the anomaly of cadaver 17 would be ranked first because it is the largest. It would then be difficult to rank the anomaly of cadaver 18 higher than that of control grave 8 because of their similar size.

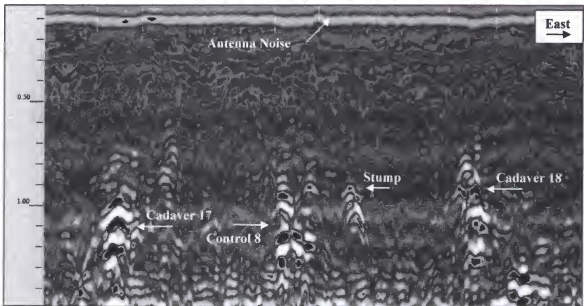


Figure 8-20. An unprocessed GPR profile of two cadavers from the SDSE scenario (17 and 18) and control grave 8 at 11 months and three days using the 900-MHz antenna. The profile is approximately 1.50 m deep and 17 m long.

Figure 8-21 is the last profile of control grave 7 and cadavers 13 and 14 from the SDLE scenario at 20 months and nine days before they were excavated at 21 months. Interestingly, neither the pig graves nor the control grave produced a distinctive

anomalous response using the 900-MHz. It is important to note that cadavers 13 and 14 still retained a considerable degree of soft tissue when they were excavated (see chapter 5). While, a slight hyperbolic response is present between 0.90 to 1.30 m for cadaver 13, there is no response from cadaver 14. Furthermore, there was barely a response from the control grave other than narrow hyperbolic tails continuing to the bottom of the profile.

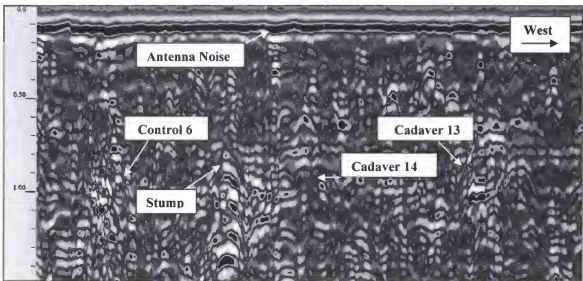


Figure 8-21. An unprocessed GPR profile of two cadavers from the SDLE scenario (13 and 14) and control grave 6 at 20 months and nine days using the 900-MHz antenna. The profile is approximately 1.50 m deep and 17 m long.

The only discernable anomalous response on the profile was due to a stump at 0.80 m that was located between the two pig graves. Overall, if these graves were not marked, it would not be possible to detect the pig graves and the control grave because the scattered background noise further reduces the contrast of these almost nonexistent returns. There were no changes worth noting on the processed file. Interestingly, while the high resolution of the 900-MHz antenna did not produce a discernable response from

either pig grave (Figure 8-21), discernable responses were produced from both graves using the 500-MHz antenna on the same day for both the unprocessed (Figure 8-11a) and processed profiles (Figure 8-11b).

Summary

Overall, the returns from the shallow and deep cadavers decreased after one year. However, the only problems with grave detection occurred for one shallow and one deep cadaver (SSLE and SDLE scenarios) after 20 months. Furthermore, there was increased resolution of the deep cadavers in the Entisol because there is no argillic horizon that masks the signature of the buried pig remains. Postprocessing of the data was generally not needed for grave detection. However, if excessive horizontal banding is noted on the profile, the data should be processed if the forensic target in question is not located because it may be obscured by the antenna noise. Furthermore, the imagery from the 500-MHz antenna was preferred with the small cadavers over the 900-MHz. Table 8-1 summarizes the GPR results for each small cadaver buried in the Entisol using both antennae.

Table 8-1. Summary table of GPR results for each small cadaver buried in the Entisol using both antennae.

Cadaver #	Scenario	500-MHz	900-MHz
13	SDLE	Noticeable decrease in return after 14 months; difficult to detect after 20 months; may need to process the file for the last two months	Excellent detection after one year; not detected after 20 months
14	SDLE	Noticeable decrease in return after 14 months; difficult to detect after 20 months; may need to process the file for the last two months	Weak hyperbolic response by six months; not detected after 20 months
15	SSLE	Detected for duration; moderate to excellent detection for last two months	Detected for duration; moderate to excellent detection for last two months
16	SSLE	Noticeable decreases in return after 18 months; difficult to detect after 20 months	Reduced return by 12.5 months; not detected after 20 months
17	SSSE	Excellent detection for 12 months; may need to process the file for the last month	Moderate detection for duration
18	SDSE	Excellent detection for 12 months; may need to process the file for the last month	Moderate detection for duration
19	SDSE	Excellent detection for duration	Excellent detection for duration
20	SSSE	Excellent detection for duration	Excellent detection for duration

CHAPTER 9 DISCUSSION

The application of GPR is becoming increasingly common for various forensic applications due to the emphasis in forensic archaeology. In the 1980's there was a growing emphasis by forensic anthropologists and archaeologists to use proper archaeological field methods when recovering and excavating human remains from forensic contexts (Berryman and Lahren 1984, Morse et al. 1983, Sigler-Eisenberg 1985, Skinner and Lazenby 1983, Wolf 1986). The early proponents of forensic archaeology recognized the importance of properly collecting human remains and documenting contextual information. Although proper archaeological methods are still not practiced universally by most forensic anthropologists and crime scene personnel today, the continued emphasis in this area throughout the 1990's (Dirkmaat and Adovasio 1997, France et al. 1992, France et al. 1997, Hunter et al. 1994, Hunter et al. 1996, Killam 1990, Scott and Connor 1997) eventually resulted in the recognition of forensic archaeology as a subdiscipline within the field of forensic anthropology.

I recognize three major areas within forensic archaeology: 1) assisting law enforcement in the field with the excavation, mapping, and recovery of human remains; 2) training law enforcement, crime scene technicians, and students at short courses and lectures; 3) and conducting controlled forensic research in taphonomy and archaeological methods. Of the more common areas dealing with controlled forensic research has been using various remote sensing search methods to locate clandestine graves. Since it has

been determined that GPR is the most important tool used to delineate forensic graves (France et al. 1997), there has been increasing emphasis to use this technology for forensic applications. Furthermore, GPR is becoming more popular because the cost of the equipment is decreasing due to an increasing number of commercial manufacturers, and the equipment is becoming easier to operate.

Decomposition

While most of the research objectives in this study focused on the application of GPR and identification of the individual components of a forensic grave that are detected by GPR, this research also provided an opportunity to study decomposition of buried bodies. Although pig cadavers were used as surrogates for humans, variables that affect decomposition of pig cadavers are directly applicable to human cadavers. The rate of decomposition is contingent upon numerous factors acting independently or in concert with one another. Four variables were controlled for in this study to determine their effect on decomposition of buried bodies: depth, length of internment, size of cadaver, and soil type.

It was no surprise that the single greatest variable affecting decomposition was depth because it has been reported in other forensic studies (Mann et al. 1990, Rodriguez 1997, Rodriguez and Bass 1985, Thew 2001). According to Rodriguez (1997), the main factors responsible for reduced decompositional rates below ground include the limitation of carrion insects and animal activity, and as temperature fluctuations decrease with soil depth, so does the rate of decomposition by cooling of the body. Animal activity was not a concern in this study because the deep burials were too deep to be scavenged by carnivores, and screening protected the shallow cadavers.

All of the deep cadavers buried at depths ranging from 1.00 to 1.10 m still retained extensive soft tissue, including those that were interred between 21 to 21.5 months. The extensive soft tissue retention is consistent with observations in the northeast of burials at similar depths. For example, Rodriguez (1997) asserts that it requires approximately two to three years for a buried corpse at depths of at least 4 feet (1.22 m) to reach complete skeletonization. Even in Florida, there is still a significantly reduced decomposition rate of deep burials. Furthermore, there was variation in the degree of skeletonization of all the shallow burials that were excavated between 12 to 13 months. The degree of soft tissue decomposition ranged from complete skeletonization to extensive preservation of soft tissues at the trunk. According to Rodriguez (1997), it takes less than six months to one year in most latitudes in North America for a body to reach complete skeletonization at a shallow depth of 1 foot (30.5 cm) or less. The decomposition of the shallow pig cadavers in this study was decreased because they were buried deeper than 30.5 cm at a depth between 0.50 to 0.60 m. The depth was deep enough to restrict access to insects and reduce thermal fluctuations of the ground.

The minimal insect activity noted was only in a number of the shallow burials because the depth of the deep burials restricted access. Although there were no beetles or maggots noted, extensive ant infestation was observed in a number of the shallow burials. According to Byrd and Castner (2001), ants are known to feed on human skin and body tissues, as well as fly eggs and maggots that are exposed outdoors. In this case, they were not feeding on fly eggs and maggots because there was no obvious evidence of maggots, and the infestation of the ants was observed with skeletonized remains that would not attract maggot infestations due to the lack of soft tissues. The ants were most likely

feeding on the decomposing soft tissue and may have had a role in the skeletonization of a number of the shallow pig cadavers.

It is not a surprise that the length of time a pig cadaver was buried in the ground was a factor in decomposition. Generally, the cadavers that were in the ground for the longest durations exhibited increased skeletonization patterns of the body. The thorax, abdomen, head, and the total body score were significant and at $p < 0.05$ level. However, time was not a factor for the limb regions. The decomposition progression of the limbs was not significant because the limbs generally decomposed significantly quicker than the regions of the trunk, particularly with the small cadavers. The decomposition rate of the limbs was increased in comparison to the trunk because there was less soft tissue and increased surface area at these regions. On average, an increased postmortem interval was always required for skeletonization of the thorax, abdomen and head regions.

Interestingly, body size was not factor in the rate of decomposition in this study. Mann et al. (1990) rates the importance of body size and weight as a “3” out of a 5 point scale, and it is not a major factor of decomposition. Unfortunately, the article only discussed a few examples of bodies deposited on the ground surface and did not discuss the affect of buried bodies and size. The cases that were discussed included only two examples when bodies weighing more than 110 kg (250 pounds) decayed more rapidly than bodies weighing approximately 65 kg (150 pounds), and the comparisons were between an obese and nonobese body. The comparisons were not between bodies of differing sizes due to height or age differences. If the size comparison in Mann et al. (1990) were between different size bodies that were not obese, it is possible that their preliminary results may have been different. The size differences in this study were due

to age and not obesity, and it appears that size is not a major factor of decomposition with the body sizes that were compared.

Since only the large and deep cadavers, and not the small cadavers, were buried in the Ultisol near the clay horizon, it was not possible to directly assess the effect of soil type. The argillic horizon in this study was not a dense horizon; it had a relatively low clay content, and the pH values were essentially identical to those of the dominant sandy horizons in the Ultisol. The decomposition of the large cadavers that were buried near the clay for the short-time period may have been reduced due to the clay because they exhibited the least advanced decomposition patterns. In particular, the sides of the cadavers that were adjacent to the clay exhibited the freshest flesh and reduced decomposition in this study. However, the slightly reduced decomposition of the large cadavers can also be partly due to their size and deep depths and not the soil.

An interesting observation that was noted concerned the decomposition progression of buried bodies. The pattern of skeletonization of buried bodies differs from bodies deposited on the surface. According to Rodriguez and Bass (1985) the disarticulation progression of bodies deposited on the surface proceeds from the head downward, with the separation of the mandible from the head and the head from the body. Decomposition then proceeds from central to peripheral or from the vertebral column to limbs. The head is also one of the first body regions of the buried cadaver to decompose, starting with the snout and cranial vault, followed by disarticulation of the mandible, and finally disarticulation of the head from the trunk. However, while the human body on the ground surface decomposes from central to peripheral, the buried pig cadaver decomposes from peripheral to central. Decomposition begins with the distal

limbs and face, and progresses with skeletonization of the head and limb regions before the trunk is skeletonized. Skeletonization of the trunk generally begins with the cervical and pelvic areas and progresses centrally.

Overall, the progression of decomposition is a general observation in this study regardless of cadaver size or depth. The progression differs from above ground depositions, because access of insects will result in decomposition of the head followed by the trunk, and the limbs last. Without access to insects and carnivores, and reduced decomposition of autolysis and putrefaction from deeper cooler depths, skeletonization is going to be related more to surface area and extent of soft tissue at a body region. With increased surface area and decreased soft tissue at the head and limbs, decomposition is accelerated at these body regions, and decelerated at the thorax and abdominal areas. Although this study analyzed only pig cadavers and not humans, the progression of decomposition for human burials will most likely be similar.

Finally, although the amount of adipocere was not quantified, as a general observation, the degree of adipocere was directly related to the size of the cadaver. More adipocere was noted in the graves from the larger cadavers, because larger bodies have more fat. For the remains that were in advanced stages of skeletonization, adipocere was present at the abdominal areas, the spinal column, the shoulder girdles, and the pelvic girdles. Furthermore, this study also concurs with Evans (1963) and Thew (2000) in noting that adipocere does not appear to correlate to any specific degrees of decomposition. Adipocere was noted in deep graves that retained extensive soft tissue, and it was also noted in graves that were in advanced stages of decomposition.

According to Rodriguez (1997) adipocere formation may result from moist soils or soils with clay. Interestingly with this study, adipocere was noted in the shallow and deep burials. All the shallow burials consist of horizons comprised solely of sand and not clay. In addition, although there was rain, the soils were well drained and never retained saturated conditions during the study period. As a general observation, it would seem that only minimal moisture is required for the conversion of fats to adipocere.

Ground-Penetrating Radar Comparisons

GPR-Soil Profile

Before discussing the length of time that the pig remains were detected in the different soils, the soil imagery using the 900- and 500-MHz antennae is first compared. The only difference between the two soils was the presence of the argillic horizon in the Ultisol, which affected the imagery of the deep graves. However, the shallow graves were in sand horizons for both soils and had similar results. The comparison of the summary data from the soil profile is in Table 9-1. While the argillic horizon is demarcated on the 500-MHz profile, at times the 900-MHz antenna has problems detecting this horizon when profiling the Ultisol. The problem with detection may be related to moisture retention. The moisture retention may have to be at a certain level in the argillic horizon to be detected using the 900-MHz antenna. Obviously not being able to detect the clay poses problems with properly classifying the soil with the GPR. In addition, a useful characteristic that may help discern a forensic target with a weak response is a gap or break in the argillic horizon due to attenuation from the buried remains above the clay horizon. This characteristic may not be present using the 900-MHz if there is poor detection of the horizon.

Table 9-1. Comparison of general GPR soil characteristics for the 900- and 500-MHz antennae.

Characteristics	900-MHz	500-MHz
Detection of argillic horizon	May not detect	Excellent demarcation
Detection of general noise	Increased detection that can limit contrast of forensic targets	Limited detection; does not obscure contrast of forensic targets
Extent of antenna noise due to horizontal banding	Thick banding between 0.0 to 0.15 m.	Thick banding between 0.0 to 0.60 m; less obtrusive banding may continue to 1.20 m
Processing file to remove banding	Does not have to be removed for grave detection	May have to remove if extensive; can mask weak return or shallow grave

The second major disadvantage of the higher resolution 900-MHz antenna is the excessive detail of the general noise that reduces the contrast of anomalies produced by forensic targets. The 900-MHz antenna detects many subsurface features such as roots and stumps that are generally not detected by the 500-MHz antenna. This noise is present as small hyperbolas throughout the profile, and can reduce the contrast of forensic targets because it may not be possible to distinguish the hyperbolic reflection caused by a forensic target from that of natural subsurface features. Conversely, the less detail in the profile produced by the 500-MHz antenna was advantageous in discerning targets because there was increased contrast of the forensic targets with that of the soil.

The only disadvantage of the 500-MHz antenna was the considerable antenna noise that was present in the profile as horizontal banding due to the ringing of the antenna and not due stratigraphic horizons. Generally, the horizontal banding across the 500-MHz profile starting at 0.0 m and sometimes continued to a depth of 1.20 m. Regardless of the extent of the banding on the profile, it was always the thickest and the

most prominent from 0.0 to 0.60 m. In some instance, the thick banding between 0.0 to 0.60 m may obscure weak reflections, thereby reducing the chance of grave detection. Any banding below 0.60 m generally did not obscure grave reflections. In most profiles from this study, the banding only extended from 0.0 to 0.60 m and did not obscure grave detection. However, at times the banding did obscure the shallower response from the disturbed backfill above many of the graves in the 500-MHz profile.

Processing the profile to remove the banding generally resulted in detection of backfill above the grave anomalies and if the resolution of the anomaly increased, it increased only slightly. Unless extensive noise is noted and anomalies have very little contrast, processing of the profile to remove the antenna noise is not needed for grave detection. An assessment concerning the need for processing can initially be determined in the field by noting the resolution of shallower subsurface features and the extent of the banding during calibration of the equipment. However, it is important to note that there may have been a problem detecting the shallow cadavers in this study if they had been buried at a shallower depth. In this study, the response from the shallow graves was generally below the thickest banding. However, for actual forensic cases, processing may be required for grave detection with targets buried at depths of half a meter or less.

Horizontal banding was also present on the profile from the 900-MHz, however, it is minimal and does not obscure grave detection. In most profiles with the 900-MHz, the densest banding across the top of the profile extended to a depth of only 0.15 m. In some instances weak antenna noise may be present between 0.0 to 1.0 m, with the densest banding still only across the top of the profile to a depth of 0.15 m. The weaker banding that is deeper than 0.15 m does not obscure the anomalies and the obtrusive banding at

the top of the profile is too shallow to mask any of the grave features. Overall, processing of the GPR profiles with the 900-MHz is not needed for grave detection.

GPR Anomaly Characteristics

There are a number of obvious differences in characteristics of the cadaver anomalies between the 900- and 500-MHz antennae. The characteristics that will be compared are listed in Table 9-2, and Figures 9-1 and 9-2 will serve to further elaborate the imagery differences between the antennae. Figures 9-1a and 9-1b are unprocessed and processed profiles, respectively, using the 500-MHz antenna, and Figure 9-2 is an unprocessed profile of the 900-MHz that were taken on the same day over the same row of graves. The row of graves consists of two cadavers from the SDLE scenario (11 and 12) and control grave 6 at five months and 11 days. Both pig cadavers would have retained extensive soft tissue, with minimal skeletonization of the limbs, at the time these profiles were collected.

The anomaly characteristics from the pig remains differed significantly between antennae. First, there is an increased and prominent hyperbolic response of both cadavers from the 500-MHz and the anomaly is more consolidated and easily differentiated in the grave shaft from the backfill (Figure 9-1a). In addition, the significantly reduced return from the control grave is a clear indication that the prominent anomalies are the result of the body and not the disturbed soil. In comparison in Figure 9-2, cadaver 11 is represented by a flat anomaly beneath the disturbed backfill, and although there is a hyperbolic response from cadaver 12, it is not possible to separate the returns from the cadaver and the backfill. Furthermore, the return from control grave 6 is very similar to the response from cadaver 12 and the backfill above it. In other words, on this profile it

would be difficult to determine which grave did not contain a cadaver if the location of the control grave was not known. Overall, the 500-MHz anomalies from the pig cadavers are also larger than the imagery from the 900-MHz. The tails extend further inferiorly and splay out more vertically. In addition, the hyperbolic curves of the anomaly project deeper in the profile. For example, although both grave anomalies appear at the same depth, the anomalies from the 500-MHz antenna extend to approximately 2.0 m (Figure 9-1a) and the return from the 900-MHz extends to only 1.50 m (Figure 9-2).

There are also a number of important soil characteristics that were imaged differently between the antennae. For example, the increased resolution of the 900-MHz produces an increased return of the backfill above the pig cadavers and of the control graves with just backfill. It is obvious in Figure 9-2, that there is an increased response with the 900-MHz antenna of the backfill in comparison to the 500-MHz (Figure 9-1a). Even when the horizontal banding is removed from the 500-MHz profile (Figure 9-2a), the return from the backfill is still significantly reduced compared to the 900-MHz. Furthermore, one characteristic of the grave that the 500-MHz generally does not detect is the grave wall. Conversely, the higher resolution of the 900-MHz may be able to detect grave walls in soils comprised of sand. In addition, gaps, breaks, or loss of the signal (whiteout) in the argillic horizon was noted from both antennae from attenuation of the electromagnetic wave by the body that was buried above the horizon. The attenuation below the anomalies was generally greater with the 500-MHz antenna because there was increased demarcation of the argillic horizon with this antenna.

Table 9-2. Comparison of general GPR anomaly characteristics from the buried pig cadavers and graves using the 900- and 500-MHz antennae.

Characteristics	900-MHz	500-MHz
Shape of anomaly	Varies from flat to pronounced hyperbolic	Generally pronounced hyperbolic
Size of anomaly	Small	Large
Tails	Generally small	Large and pronounced
Attenuation below body	Sometimes with argillic horizon	Common with argillic horizon
Detection of backfill	Poor to excellent	Absent to moderate
Differentiation of anomaly with backfill	Varies from absent to excellent	Moderate to excellent
Grave wall	May detect	Does not detect
Moist soil conditions due to rain	Increases resolution of backfill, but might decrease differentiation of cadaver anomaly with backfill	May have increased resolution of cadaver anomaly and backfill

Finally, another characteristic where there is variation in the grave returns is caused by an increase in the soil solution from rain. When the ground is completely saturated, there is going to be little or no differentiation of the pig remains in the GPR profile with that of the soil. Therefore, the GPR should not be used until the ground has had time to sufficiently dry. However, if there are periodic increases of moisture retention by the soil from rain, the increase moisture may actually increase the contrast of the grave due to an increase in electrical conductivity. The increase in moisture of the grave can occur two ways. First, since the porosity of the backfill is increased in comparison to the undisturbed *in situ* soil, there will be greater moisture retention in the backfill because the pore spaces have increased in size. Second, the decomposing remains or skeleton can also retain increased levels of moisture in comparison to the undisturbed soil.

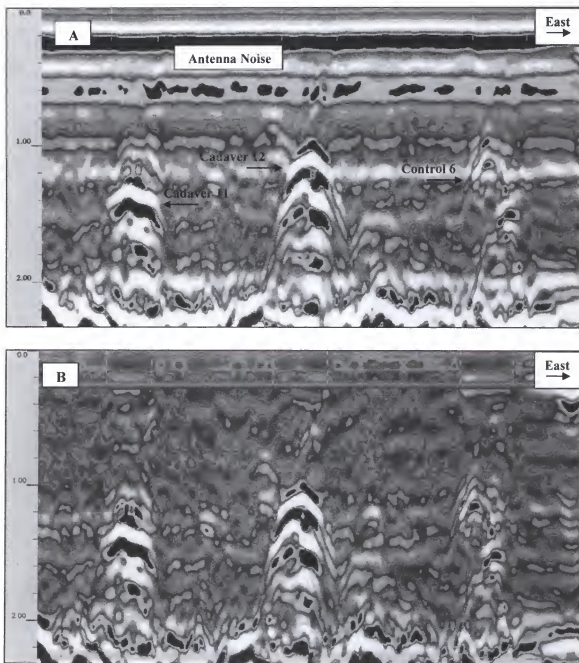


Figure 9-1. Ground-penetrating radar profile of two cadavers from the SDLE scenario (11 and 12) and control grave 6 at five months and 11 days with the 500-MHz antenna. A) The cadaver anomalies are easily discernable in the unprocessed profile with the extensive horizontal banding. B) Note the nearly absent detection of the backfill when the antenna noise is removed. The profile is approximately 2.35 m deep and 17 m long.

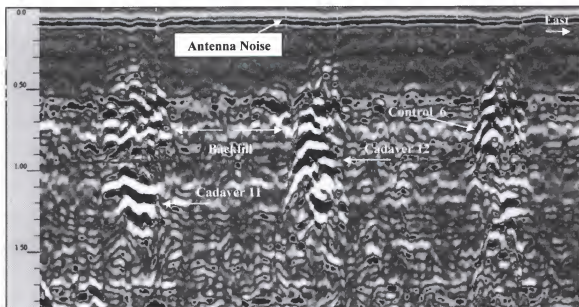


Figure 9-2. An unprocessed GPR profile of two small cadavers from the SDLE scenario (11 and 12) and control grave 6 at five months and 11 days with the 900-MHz antenna. The profile is approximately 1.85 m deep and 17 m long.

During this study, there was excellent drainage of the soils at the BRU.

Generally, the soils were not saturated the day after a heavy rain, but an increase in the moisture content may have been retained. Interestingly, the GPR imagery exhibited different characteristics between antennae when the data was collected while the soil retained increased moisture. Figure 9-3a is a profile of three completely skeletonized large cadavers from the LSLU scenario 20 months and five days using the 500-MHz antenna. Overall, there is excellent detection of these three skeletons. The returns are all large and distinctive, and the auger hole is still noted on the eastern border of cadaver 5. The prominent reflections are partly from an increase in moisture retention from rain that occurred the day before the profile was collected. The increased returns from these cadavers are evident when comparing them to the last profile taken of these graves at 21.5 months, or only 37 days later (Figure 7-3a). Overall, the anomalies in Figure 7-3a

are less prominent and overall smaller. The entire area surrounding the skeleton is highlighted in Figure 9-3a because the increased moisture that is trapped by the bones and soil increases the electrical conductivity of the area. Another characteristic that needs to be mentioned is the lack of a distinctive return from the backfill and control grave 6. The absence of the return from control grave 6 is an indication that the increased returns are caused by the retention of moisture by the skeleton and matrix surrounding the skeleton and not just the disturbed soil. Even when the profile is processed to remove the banding, there is still only a minimal return from the disturbed soil (Figure 9-3b).

When the 500-MHz imagery is compared to the profile from the 900-MHz antenna, there are a number of obvious differences between the imagery of the two antennae after it has rained. Figure 9-4a is the unprocessed 900-MHz profile collected on the same day as the 500-MHz profile (Figure 9-3a and 9-3b). The backfill above the three cadavers is extremely prominent in both the unprocessed (Figure 9-3a) and processed (Figure 9-3b) profiles using the 900-MHz antenna. The backfill was not detected in the unprocessed 500-MHz profile and was poorly detected in the processed profile. The 900-MHz antenna produces an increased return of the backfill because of the increased moisture content in the backfill. In addition, the backfill over the three decomposing cadavers is much more distinctive than the return from control grave 6, which only consists of backfill. It is possible that the stronger return from the backfill in the pig graves is caused by an increase in the moisture content because increased moisture is retained by the pig remains.

Although there was an increase in the return of the backfill using the 900-MHz, there was a decreased return of the pig remains in the unprocessed (Figure 9-4a) and

processed (Figure 9-4b) profiles. For example, cadaver 7 is the only pig grave that exhibits a focused return. The returns from both cadaver 5 and 6 are reduced and poorly demarcated. Under normal conditions the returns from the pig skeletons should be distinctive because they were detected for the duration of the study using the 900-MHz. For example, in Figure 7-12a, there are prominent returns at 19 months of the three cadavers using the 900-MHz.

While resolution of the pig remains was increased using the 500-MHz antenna, the resolution decreased using the 900-MHz. In addition, it is important to note that while target resolution can increase after rain, target resolution can also decrease after rain during high saturated conditions. If the ground is too saturated, there will be problems differentiating targets. However, in certain conditions, an increase in moisture may increase the contrast of a target using the 500-MHz antenna. Although no guidelines are suggested, local conditions and soil type will dictate whether GPR can be used under moist conditions.

Overall, the resolution of the soil and anomaly characteristics make the 500-MHz a far superior antenna to use for forensic applications than the 900-MHz. In many instances, the extension of the anomaly tails using this antenna is a helpful characteristic used to discern a target. The soils in this study are primarily comprised of sand above the buried cadavers, and this is the most likely reason for the poor detection of the backfill using the 500-MHz antenna. In other types of soils with shallower clay horizons, there would likely be an increased response from the backfill with the 500-MHz and possibly detection of the grave walls. Detecting backfill can be a significant clue locating a forensic target. For example, if multiple anomalies of similar size and shape are detected

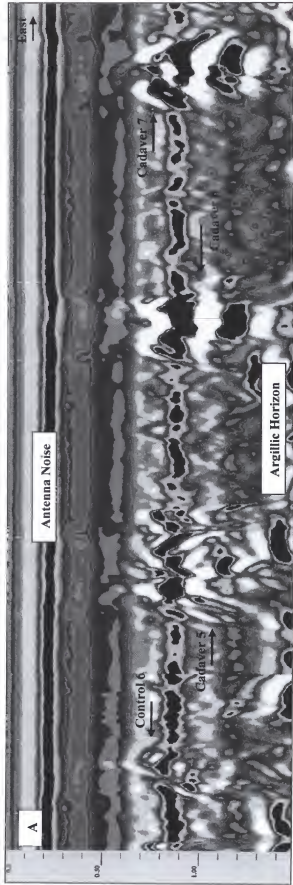


Figure 9-3. Ground-penetrating radar profile of three large cadavers from the LSLU scenario (5, 6, and 7) and control grave 6 at 20 months and 5 days and using the 500-MHz antenna. A) Note the discernable responses caused by the increased moisture content in the soil in the unprocessed profile (compare to Figure 7-3a). B) Note the weak response from the backfill over each anomaly when the horizontal banding is removed in the processed profile (compare to Figure 9-3a). The profile is approximately 1.45 m deep and 27 m long.

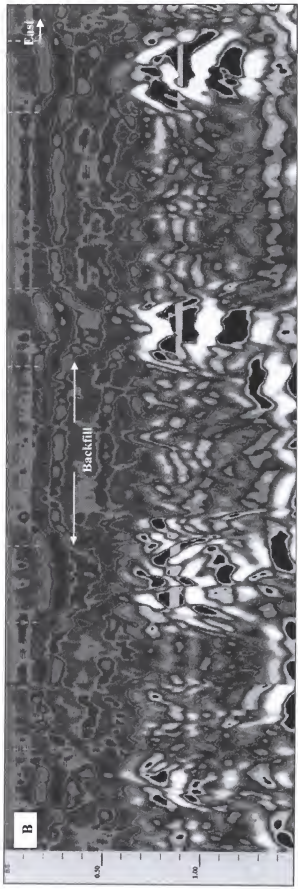


Figure 9-3, Continued

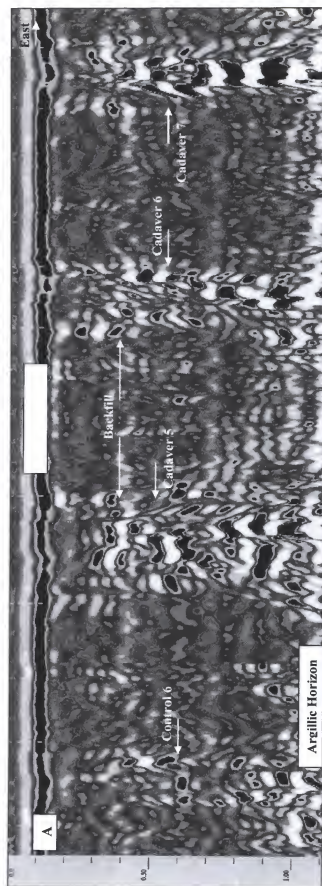


Figure 9-4. GPR profile of three large cadavers from the LSLU scenario (5, 6, and 7) at 20 months and five days and control grave 6 using the 900-MHz antenna. A) Note the lack of demarcation of the anomalies from cadavers 5 and 6 (compare to Figure 7-12a) in the unprocessed profile. B) The resolution of the backfill increased when the banding was removed in the processed profile. The profile is approximately 1.45 m deep and 27 m long.

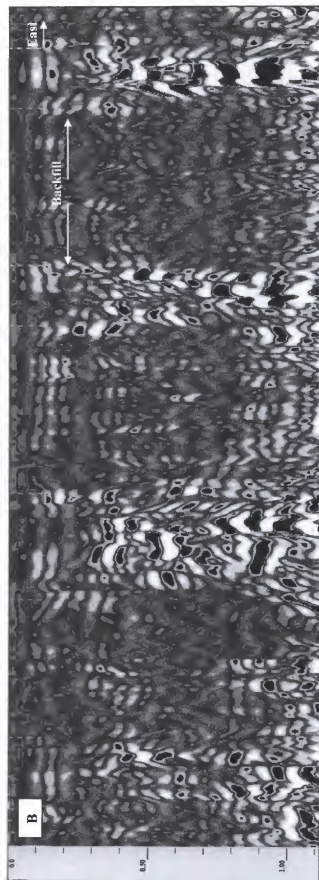


Figure 9-4. Continued

during a search for a forensic target, the detected backfill above one of the anomalies is an indication that something was buried and the anomaly is most likely not due to a natural feature.

Detecting Buried Remains using GPR

One of the main goals of this research was to correlate decomposition state with GPR imagery, and to assess if cadaver size, depth of burial, length of burial, and antenna choice were factors in detecting a forensic grave. Soil type and depth had the greatest effects on producing a distinctive anomaly because these variables are related. Both the large and small cadavers buried at shallow depths were detected for the duration of the study in sand using the 500-MHz antenna.

Overall, there were no major problems detecting the small graves in sand that were buried at a deep depth until 20 months with the 500-MHz antenna. The Entisol provided excellent conditions for detecting of the shallow and deep graves. Conversely, there were problems detecting the larger cadavers buried at deep depth in the Ultisol in as little as six months using the 500-MHz antenna. The resolution of the grave anomalies became less distinctive in as little as six months making it difficult to image large pig cadavers that had undergone very little decomposition. It was not a surprise that the cadavers buried in the clay were difficult to detect. In the literature discussing the detection of cemetery graves, clay has been described as a major factor limiting the detection of graves with GPR even when their location is known (Unterberger 1992, Mellet 1992).

The variables size and time will be discussed together because of their association. Overall size was not a major factor for grave detection of the large, shallow

cadavers in sand for the duration of the monitoring period. They were detected during various stages of decomposition, including when they were completely skeletonized. Over time, the anomalies from the smaller cadavers decreased in size and contrast with the loss of soft tissue. Generally, the imagery from the smaller cadavers exhibited the same characteristics as the larger cadavers, but with smaller returns. However, there were significantly reduced returns of the small cadavers at shallow and deep depths after approximately 20 months.

The cadavers in both deep graves still retained extensive soft tissue, and although their returns were significantly reduced, they were still somewhat discernable after 20 months using the 500-MHz. Conversely, there was variation in the extent of the anomalies produced by the small and shallow cadavers after 20 months using the 500-MHz. For example, although both shallow cadavers were completely skeletonized, one still exhibited a discernable response and the other was not detected.

Numerous advantages of the 500-MHz antenna were already discussed previously in this chapter. This section will provide further support for the use of the 500-MHz over the 900-MHz because there was overall increased detection of a number of the graves using the 500-MHz. For example, the anomalies from the large cadavers that were buried deep in the clay were much more discernable using the 500-MHz over time. Although it was difficult to detect this group of cadavers with both antennae, there was an increased hyperbolic reflection using the 500-MHz antenna that made it possible to discern the returns of the bodies. Furthermore, although there were significantly reduced returns from the small and deep cadavers after 20 months using the 500-MHz, neither of the deep cadavers were detected using the 900-MHz antenna after 20 months.

Detection of Forensic Graves

One of the major objectives of this study was to determine what produces the return when buried remains are detected. A number of studies have suggested that multiple variables of the grave can generate a return. For example, Nobes (2000) asserted that detection of a forensic grave may be due to the displacement of the soil by the body, the clothing, and the soil disturbance from the grave itself. However, he did not conclude that the decomposing body could also generate a distinctive anomaly.

It is obvious from the excavations that the remains of pig cadavers were detected throughout the monitoring period during different stages of decomposition and when the remains were completely skeletonized using the 500-MHz antenna. Excavations confirmed that the anomalies were being produced from only pig skeletons, and blank control graves provided further evidence that the skeleton and not the disturbed soil was producing the anomaly. For example, in almost every instance, there generally was a significantly reduced return from the backfill. Soil analyses confirmed that the chemical properties of the soil did not change the electrical properties of the backfill from mixing of soil horizons.

Forensic graves can be detected due to multiple components. The remains can be detected during various stages of decomposition, including skeletonization. Detection can also result from contrasting properties of the grave with the surrounding soil caused by less dense backfill. Voids created by settling of the backfill and decomposition of the cadaver may be detected. Depending on the soil properties, grave walls or the interface of the disturbed with undisturbed soil may be detected. In some instances, there can be either a gap or unnatural break in a horizon below the remains due to attenuation of the

signal by the body that is above the horizon. Although it was not a major issue in this study, a forensic grave can also be detected if there is a localized loss of a signal, or whiteout, on the imagery due to attenuation by the body.

Finally, in forensic circumstances, detection may be facilitated by nonbiological items that may be added to the grave with the body. In forensic contexts, a buried body will usually be clothed and may also be wrapped in a tarp, rug, etc. The clothing or wrapping can retain moisture, thereby increasing the conductivity of an area. According to Mellett (1996), a body wrapped in a carpet or rug that is buried at a depth of less than a half a meter will provide a highly conductive target. In rarer instances, items may also be placed over the body to assist in concealment before the backfill is placed over the body. Furthermore, weapons used to murder victims have been recovered in forensic graves along with bodies. If it is a metallic object such as a pipe, gun or knife, it can produce an anomaly. As more items are added into the grave with the body, grave detection increases due to a higher probability of generating multiple anomalies.

The following section will explain how the body and backfill can generate a GPR anomaly. When the body is first placed in the burial, a significant reflection can be generated from both the body and the backfill. There are going to be numerous physical changes of the backfill when it is placed back in the grave. Depending on soil type, there may also be detectable chemical changes of the backfill. Changes in soil chemistry will be related more to soils that have horizons with significantly contrasting electrical properties. The disturbed soil will be detected by GPR primarily due to contrasting properties from the surrounding area due to decreased compactness and increased moisture retention. When the backfill is replaced, the soil will be less compact and there

will be larger pore spaces. The less compact soil may result in a reflection caused by and a change in the velocity of the radar wave, and at the interface of the disturbed and undisturbed *in situ* soil. Furthermore, since the pore spaces are larger there can be increased retention of moisture in the soil thereby increasing the electrical conductivity of the backfill.

The radar should also be able to detect the body, particularly when it is fresh and still in the moist state during advanced decomposition because moisture is going to have the greatest influence on electrical properties. In this study, the body was detected because the dielectric constant of body tissues is significantly higher than that of dry sand or clay at the research area within the BRU. For example, the values of the dielectric constant for dry sand and clay range from 2.5 to 6 (Geophysical Survey Systems, Inc. 1999). Conversely, the values of the dielectric constant are considerably higher for human tissues. Hammon et al. (2000) compiled a list of dielectric constants for human and nonhuman body tissues, including bone, from multiple sources including Gabriel et al. (1996a), Gabriel et al. (1996b), and Pethig (1979). Overall, the dielectric constants for biological tissues ranged from 7 to 60 with many values over 40 for a 450-MHz antenna (Hammon et al. 2000). While conducting laboratory research using time domain 2.5 D finite-difference simulations of GPR responses from models of buried human remains, Hammon et al. (2000) concluded that reflections can be produced from the upper layers of the human body because biological tissues have a dielectric constant and high conductivity. Therefore, in this study there was a strong enough contrast between the decomposing cadavers with that of the soils at the BRU to be detected by the radar.

Detection of Bone

Another important issue evaluated with this study concerns whether bone can be detected by GPR. Overall, there is disagreement in the literature concerning this issue. According to Hammon et al. (2000), the dielectric constant for bone that was compiled from the literature for a 450-MHz antenna is 13. It is important to note that this value for the dielectric constant was from fresh, moist bone and not dry bone that has been in the ground for an extended period. Over time, the dielectric constant of fresh bone will equalize to values of the soil due to the loss of the mineral and organic components, reducing the contrast of the bone with the soil. This point was made by Davis et al. (2000) referring to older nonforensic graves, by asserting that it is difficult for GPR to detect bones due to their small size and because they have similar electrical properties to dry soil.

Nevertheless the dielectric constant of fresh, moist bone is slightly higher than the soils at the BRU. However, even if the dielectric constant of the bone is higher than the soil at the BRU, it is more than likely not high enough to produce a distinctive reflection. A distinctive reflection is produced when there is increased contrast between the dielectric constant and electrical properties of buried features with that of the soil matrix. A greater difference in the dielectric constant will result in higher amplitudes of the reflected signal and an increase in the resolution of reflections. However, small differences in the dielectric constant may not result in amplitude differences high enough to produce a distinctive reflection.

If the bones are not detected, why were reflections produced from only skeletons? Mellett (1992) suggests that bone leaches calcium salt into the surrounding soil and the

calcium salts make the bone and immediate area visible to the radar. However, he did not test his theory with soil analyses. The soil analyses that were conducted for this study appear to have confirmed the hypothesis by Mellett (1992). It appears that there may be enough contrast from the skeleton and the surrounding soil that contains soft tissue decomposition products, leached minerals from the skeleton, and other minerals from the soil solution that may have become bound to the minerals in the soil surrounding the skeleton.

It is important to note that although Ca and P are the main inorganic constituents of bone, other ions in bone may also contribute to increasing the cation exchange capacity (CEC) and as a result increase the electrical conductivity of the soil surrounding the body. Sodium, magnesium, potassium, fluoride, chloride, and bicarbonate ions can be substituted into the hydroxyapatite crystal (Paterson 1983). Furthermore, in one study it was noted that the highest concentrations of magnesium that were sampled in the soil solution of above ground bodies were noted after soft tissue decomposition and were attributed to bone seepage (Vass et al. 1992). Paterson (1983) asserts that while the adult body contains approximately 20 to 30 g of Mg, more than half is bound in hydroxyapatite crystals; 1% is in plasma, 45 % in cells, and the rest is bound in bone. The CEC is the sum total of exchangeable cations (Al^{3+} , Ca^{2+} , H^+ , K^+ , Mg^{2+} , and Na^+) that a soil will absorb. The CEC of the soil surrounding bone can increase due to diagenesis because other than Al, all of the other cations that are used to calculate the CEC are minerals maintained at high levels in bone and soft tissues. In addition, the electrical conductivity of the area surrounding the skeleton may also increase due to minerals in the soil that become bound to the leached minerals from the skeleton. For example, Fe was sampled

at very high concentrations in the soil in a number of instances surrounding the skeleton, and was most likely bound with the P as iron phosphates.

In general, when there are high levels of electrical conductivity, CEC, certain dissolved salts, and general moisture content in soils there will be a reduction of signal depth because the penetration of the electromagnetic wave is decreased (Doolittle and Collins 1995, Doolittle and Collins 1998). However, when the above variables only affect a small area within the soil such as a grave, it will provide contrasting properties of the area around the grave because the dielectric constant and the electrical conductivity are increased. Even slight changes in moisture content of the area surrounding the skeleton may also increase the dielectric constant and electrical conductivity. More than likely, the matrix surrounding the skeleton combined with the bones, and not just the individual bones themselves, is detected because it provides a large enough contrast due to an increased dielectric constant with the soil to produce higher amplitudes of the reflected signal and an increase in the resolution of reflections.

Diagenesis of the Pig Skeletons

The following is a model for diagenesis of the pig skeletons in the soils at the BRU with regards to P and Ca levels. Initially, when extensive soft tissue was still retained on the pig remains, high levels of P were sampled, and there was barely an increase of Ca levels. The initial high levels of P were not caused by diagenesis of the skeleton, but were released into the soil through soft tissue decomposition. According to Paterson (1983), about 88 % of the body's P is in bone, but the remainder is in the form of nucleic acids, organic phosphates, and phospholipids. Phosphorous is an important ion

that is present in all animal cells and is important for their structure and function (Paterson 1983).

It is also important to note that the pH increases during soft tissue decomposition to alkaline levels (Rodriguez and Bass 1985, Thew 2001, Vass et al. 1992). This study sampled the highest pH values from decomposition around neutral to slightly alkaline for all of the deep cadavers that still retained extensive soft tissue regardless of length of internment (short and long). If the pH was tested earlier in time, it is likely that higher alkaline values would have been noted. By the time the pH was tested, the values were already decreasing due to water movement through the soil around the body.

While there are high levels of phosphorus in the soft tissues, there is very little calcium in soft tissues. About 99% of the body's calcium is stored in bone (Paterson 1983). Since almost all of the Ca in the body is stored in the skeleton and not the soft tissues, it was not a surprise that the highest levels of Ca were only sampled in the graves when the cadavers were either near skeletonization or completely skeletonized. The soft tissue protected the bones from diagenic forces, but when the bone became skeletonized, the soil characteristics provided conditions for bone apatite dissolution by groundwater. Furthermore, high levels of P were also sampled with the high levels of calcium because of the high P content in bone.

The general soil characteristics at the BRU where the bodies were buried provided favorable conditions for bone hydroxyapatite dissolution. First, before the bodies were buried, the pH levels in the soil were acidic to slightly acidic. Although bone has a higher solubility at pH values that are highly acidic ($\text{pH} < 6.0$), hydroxyapatite solubility in alkaline ($\text{pH} > 7.5$) to slightly acid ($\text{pH} = 6.0$) environments is still possible but reduced

(White and Hannus 1983; Rottander 1976). Although the pH values increased to alkaline levels during soft tissue decomposition, the pH decreases back to normal acidic levels that further promote hydroxyapatite dissolution. Furthermore, Vass et al. (1992) reported that after soft tissue decomposition the soil became even more acidic than the original levels, and suggested that it may be due to an increase in the death of large populations of bacteria and leachates from the bone. The increase in the acidity around the skeleton is most likely due to the release of cations from the bone, and not the death of large populations of bacteria that will probably increase, not decrease pH levels.

Second, the Ca^{2+} and PO_4^{3-} ions in the soil were normally at low levels before the research began. If the immediate area is not saturated with respect to Ca^{2+} and PO_4^{3-} ions, groundwater movement plays an important role in the mineral dissolution of bone, because the less saturated the immediate area of these ions, the increased mineral dissolution (Nielsen-Marsh et al. 2000). It is also important to note that the pig cadavers in this study were juveniles, and the immature bone may also have an increased tendency of mineral dissolution especially in comparison to mature adult bone. For example, studying archaeological bones, Gordon and Buikstra (1981) concluded that there was a strong correlation between bone preservation and age wherein ontogenically younger bones were less preserved than ontogenically older bones.

Although this study has shown that just a skeleton can be detected after 21 months, there have been forensic cases where skeletons were located with GPR at much longer postmortem intervals. For example, Nobes (1999) located a body buried in a field for 12 years using a combination of EM and GPR. However, the forensic case buried for the longest postmortem interval that was located using GPR was buried beneath a

concrete pool deck for 28 years (Davenport 2001a). GPR is obviously the most important search tool for a body that is covered by a concrete or paved slab. Forensic targets such as these may be detected for longer durations than a body in a field because they are protected under a slab. The area surrounding the body may exhibit a contrasting area that lasts for much longer time intervals than unprotected scenarios due to the area being shielded from compaction and water. Overall, the backfill will be less compacted than the surrounding *in situ* soil because it is protected from forces that can compact the area. Voids can also develop in the backfill and between the concrete and the ground surface due to decomposition of the body and settling of the backfill. Furthermore, since there is less water percolating through the area, the chemical properties of the grave caused by decomposition and diagenesis of the body may provide a contrasting area that will last longer than an unprotected scenario.

Detection of Cemetery Graves

How long can a skeleton and the surrounding area provide enough contrast to be detected by the GPR? In order to answer this question, the literature discussing the detection of cemetery graves is reviewed. According to Bevan (1991), the most distinctive feature of a cemetery grave is the disturbed soil in the grave shaft that will have different electrical and magnetic stratification than the surrounding undisturbed earth that could last indefinitely. If the radar can penetrate the backfill, a discernable return can be produced by the metallic properties of a coffin, and if the wooden coffin has not decayed, or if there is a vault of brick or stone with an air cavity, the radar may detect the void (Bevan 1991, Davis et al. 2000, King et al. 1993). While it is obvious that a cemetery grave can be detected if there is a vault or casket still preserved, it may be

difficult to detect if the body was wrapped in a shroud or if the casket has decayed due to extended postmortem intervals.

When the casket is gone and a grave is not detected by a soil disturbance, is bone being detected? There is disagreement concerning if GPR can detect cemetery or archaeological bone. For example, Mellett (1992) asserts that the shape of bones may contribute to their detection, and the leaching of calcium salts into the surrounding soil from the bone could also make cemetery skeletons visible for many years. Conversely, both King et al. (1993) and Davis et al. (2000) assert that it is difficult for GPR to detect bones due to their small size and because they have similar electrical properties as dry soil.

Speaking from experience, I find it very difficult to detect older cemetery graves that are not in a vault or metal casket, even if the grave is marked. Even when the electromagnetic wave can penetrate the backfill and scan the skeleton, it would be difficult to detect just bone because even if the majority of the skeleton is still intact, the extended postmortem interval would reduce any contrast of the skeleton and surrounding soil with that of the undisturbed soils.

Over time, diagenesis and water movement neutralizes the contrasting chemistry of the skeleton, decayed wood, and the surrounding soil with that of the undisturbed soil resulting in similar electrical properties and dielectric constants. This will probably happen long before the wood is completely decayed. At this point, GPR is not going to be able to detect the skeleton because there will not be a strong enough contrast. This is the reason why it is difficult to detect archaeological graves and older cemetery graves. If an older cemetery or archaeological grave is detected with GPR, it is most likely due to

the casket or what remains of it, items that may have been placed in the grave, a buried or collapsed grave marker, a void, or possibly the soil disturbance depending on the type of soil.

Performing a Forensic GPR Survey

The research questions that were addressed in this dissertation focused primarily on the interpretation of GPR imagery. However, throughout the collection of the dissertation data and my varied GPR experiences, I have learned that the quality of the GPR data is immensely contingent on proper survey design and meticulous data collection in the field. The last section of the discussion discusses a number of important setup and collection parameters that should be considered prior to data collection of a forensic GPR survey.

Setup Parameters

Before choosing any setup and survey parameters, it is important to learn as much background information about the suspected clandestine grave in question, the survey area, and the local soil characteristics. Although published soil surveys are useful guides for quickly determining soil types, it is still important to characterize the soil prior to performing a GPR survey for local subtleties, because the soils may have been incorrectly classified during previous surveys. If possible, soils should be characterized with GPR and a physical classification should be performed by soil auguring to corroborate or interpret the GPR profile. Any soil auguring or invasive testing that is required prior to a GPR survey should be performed outside the survey area to prevent damaging any potential evidence.

When conducting a forensic GPR survey, a controlled survey should always be utilized with an orthogonal grid. Even though the electromagnetic wave extends outwards from the sides of the antenna at a 60° angle, the equipment does not detect small objects that are not directly below the antenna when performing shallow surveys. Therefore, spacing of the grid should be equal to the smallest dimension of the target. Grid spacing for an adult should be no more than 1 meter, and the spacing may need to be less for a child depending on their size.

It is almost impossible to identify the subsurface object that produces an isolated anomaly without soil auguring or excavating. It may be possible to eliminate anomalies based on operator experience, site context, and proximity of the anomalies to other features. For example, anomalies that are attributed to roots from nearby trees or underground utilities and waterlines are common during surveys and may be eliminated from excavating with additional GPR surveying. The general size of an anomaly can be determined by performing additional transects that are perpendicular to the initial disturbance. The size of anomalies can be helpful in determining if further investigation is warranted such as probing or a controlled excavation.

After the survey parameters are determined for the equipment based on the soil and local conditions, the depth of viewing should be considered based on information that law enforcement may be able to provide due to witness testimony. However, if no information is available concerning depth, and it is assumed that the grave was hand dug, most forensic bodies will be buried less than 1 meter. For optimum imagery characteristics, the depth should not be set too shallow or excessively deep. As the depth of viewing is set deeper, the shallow features become smaller and less prominent. For

example, Figure 9-1a is an unprocessed profile of cadavers 5 thru 7 at 8 months, LSLE scenario, that exhibit small hyperbolic reflections and breaks in the clay below the bodies. The cadavers are buried at 0.60 m and the anomalies are small because the deep depth of viewing was at 2.70 m. By decreasing the depth, the anomalies will become larger and more distinctive (see Figure 7-3a). Overall, in this case the anomalies are still discernable because there is enough contrast with this soil. However, depending on the soil type, it may not be possible to discern a small object on a deep profile because there may not be enough contrast with the noise on the profile to differentiate the forensic target.

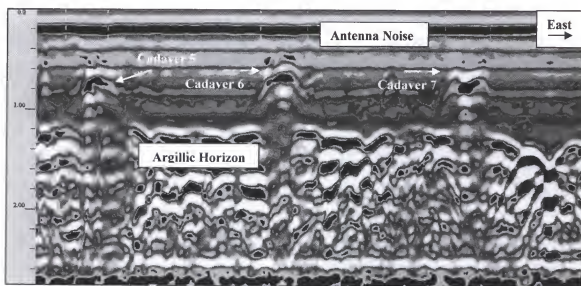


Figure 9-5. An unprocessed GPR profile of three large and shallow cadavers from the LSLU scenario (5, 6, and 7) at eight months with the 500-MHz antenna. Note the small cadaver anomalies caused by the deep depth of viewing. The GPR profile is approximately 2.70 m deep and 17 m long.

At the same time, the depth should not be set too shallow because it may reduce the contrast of the anomalies. One of the characteristics that will increase the contrast of

the anomalies is the continuation of the vertical hyperbolic shape inferiorly in the profile. Choosing your depth is a compromise between a number of variables such as antenna choice, preferred detail of reflections, and soil characteristics. If the depth of viewing is too shallow, it may not be possible to discern the image because the inferior aspect of the hyperbolic shape may be cut off, and there may not be enough contrast to differentiate the anomaly in the profile. Conversely, although depth can decrease the resolution of the anomaly, the depth of viewing should be deep enough so there is enough contrast with the image and the surrounding soil.

Determining the relationship between depth and resolution is demonstrated by showing three profiles from the same row of graves collected the same day utilizing different viewing depths. The graves consist of two large and deep (1.00 m) pig cadavers (13 and 14) from the SDLE scenario and control grave 6 with only backfill at 19 months and 20 days with the 500-MHz antenna.

In Figure 9-6a, the depth is at 1.25 m, approximately 25 cm below the grave floor. Although both cadaver anomalies exhibit weak hyperbolic shapes, they are very difficult to discern. The extensive noise on the profile masks the superior aspect of the anomalies. The only discernable hyperbolic anomaly on the profile is caused by a stump on the eastern border of grave 13. When the antenna noise is removed (Figure 9-6b), the superior aspect of each cadaver anomaly is now visible, although poorly. In addition, a minimal soil disturbance is noted above both cadaver anomalies. Furthermore, there is still no discernable response from control grave 6 when the antenna noise is removed, but a small hyperbolic reflection caused by a root is now visible between cadaver 14 and control grave 6.

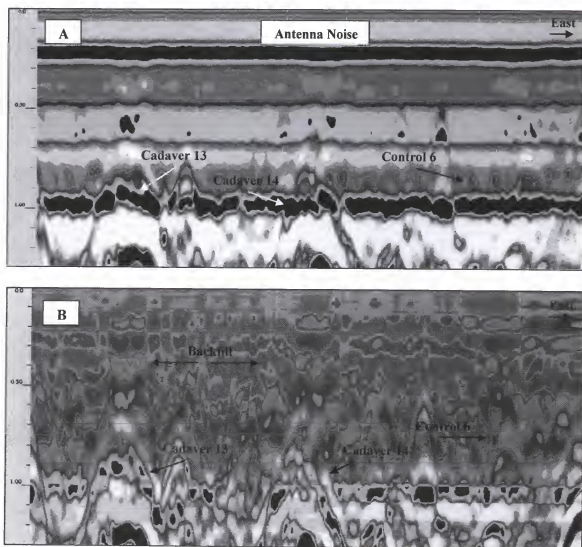


Figure 9-6. Ground-penetrating radar profile of two cadavers from the SDLE scenario (13 and 14) and control grave 6 at 19 months and 20 days with the 500-MHz antenna. A) It is difficult to detect the cadaver anomalies due to the shallow profiling depth and extensive antenna noise in the unprocessed profile. B) Note the increase in the resolution of the cadaver anomalies when the antenna noise is removed in the processed profile. The GPR profile is approximately 1.25 m in deep and 17 m in long.

When the depth of the profile is increased 0.30 to 1.55 m (Figure 9-7a), the contrast of the cadaver anomalies increases significantly. It is now possible to discern their hyperbolic shape in the unprocessed profile even with the extensive antenna noise. Because the depth of viewing is increased, the contrast of the anomalies is increased. The inferior aspect of the hyperbolic anomaly that was cut off on the shallower survey is now visible. Furthermore, when the antenna noise is removed (Figure 9-7b), the resolution of the cadaver anomalies and the backfill above the anomalies increased significantly, and a slight return from control grave 6 is now visible. Finally, on the third profile at a depth of 1.70 m, the resolution of the anomalies increased slightly more in the unprocessed and processed profiles (Figure 8-10a and 8-10b) because the entire hyperbolic anomaly is now visible due to the increased depth.

Overall, this series of profiles demonstrated the importance of choosing an appropriate depth when searching for small forensic targets. Although the depth of viewing will also be contingent on soil properties, antenna choice, and local conditions, I found that when using the 500-MHz antenna, the most favorable results were at depths that were around 1.5 to 2 times deeper than the buried target. Of course, the anomalies can still be detected at shallower or deeper depths. In addition, even when there was extensive antenna noise, as was just demonstrated, there is increased contrast of targets when the entire the anomaly is viewed on the profile.

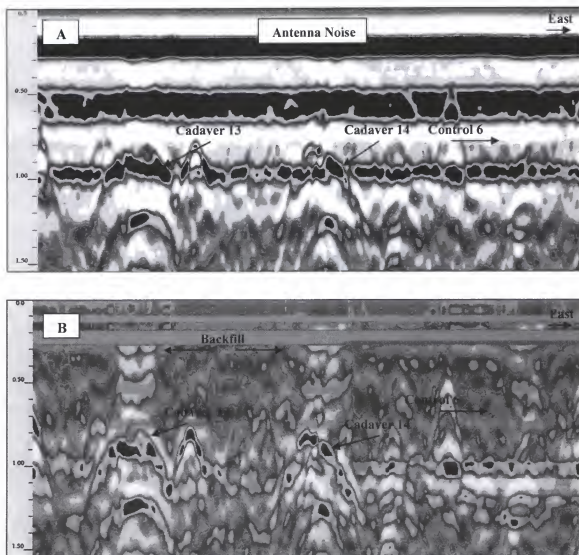


Figure 9-7. Ground-penetrating radar profile of two cadavers from the SDLE scenario (13 and 14) and control grave 6 at 19 months and 20 days with the 500-MHz antenna. A) It is difficult to discern the cadaver anomalies due to the shallow profiling depth and extensive antenna noise in the unprocessed profile. B) Note the increase in the resolution of the cadaver anomalies when the antenna noise is removed in the processed profile. The GPR profile is approximately 1.55 m in deep and 17 m long.

Data Collection

After the grid is constructed and the setup parameters are determined, the two most important variables to consider during data collection are the speed and direction the antenna will be pulled. During field data collection, speed is a very important factor to consider, especially when searching for small subsurface features such as forensic targets. As features or objects decrease in size, obviously their density and surface area also decrease, resulting in reduced contrast of the object with the surrounding soil. As a result, if the antenna is pulled at a pace that is too quick, there may not be enough scans or data collected of the object to produce a discernable anomaly. This is demonstrated in Figure 9-8 which is an unprocessed profile of two small cadavers from the SSLE scenario (15 and 16) and control grave 7 at 19 months and 20 days with the 500-MHz antenna. The GPR transect was pulled west to east over the graves lengthwise. The remains of cadaver 15 barely exhibit a recognizable response, while there is no recognizable response from the remains of cadaver 16 or control grave 7. In addition, there is no response from the backfill above any of the three graves.

Once I realized immediately that the poor imagery from this row of graves was caused by the antenna operator pulling at a pace that was too quick, I asked the operator to reduce the speed on the returning GPR transect in an east to west direction. Figure 8-5a, is the return transect in an east to west direction that was pulled at a slightly reduced pace. The response from the remains of both cadavers 15 and 16, and a weak hyperbolic response from control grave 7 were discernable in the unprocessed profile that exhibits extensive noise. At the same time, backfill is also detected above both cadavers.

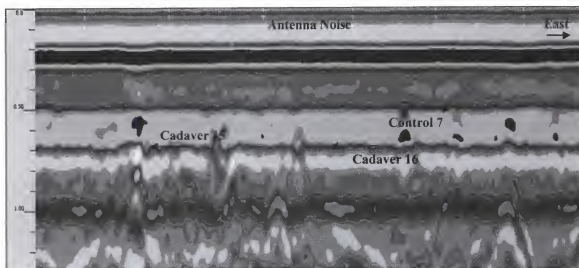


Figure 9-8. An unprocessed GPR profile of two small cadavers of the SSLE scenario (15 and 16) and control grave 7 at 19 months and 20 days with the 500-MHz antenna. Note the poor detection of the cadavers. Compare to Figure 8-5, which was collected the same day but at a slower pace. The GPR profile is approximately 1.30 m deep and 17 m long.

Overall, this was an excellent example demonstrating why speed is a consideration, and why it is important to collect data in both directions along each transect (i.e. west to east and then east to west). The extra time required for this task is minimal because an additional transect setup is not required. It is possible that even when the antenna is pulled at an appropriate speed, a target may be missed due to the antenna jumping up and down. A target can also be missed if the antenna is not pulled exactly along a grid transect. Furthermore, in some instances, an object may exhibit increased contrast or a different anomaly shape in one direction because of its orientation in the ground. The return from the subsurface object may be increased in one direction because the electromagnetic wave scans the object at a different angle.

For example, Figure 9-9 is an example of two large, shallow pig cadavers (5 and 6) from the LSLU scenario (900-MHz) with one of the anomalies exhibiting different

characteristics in both directions. Discernable hyperbolic anomalies were produced for both cadaver anomalies, and adjacent to the eastern boundary of the grave wall from cadaver 5 is a spike, a narrow hyperbolic anomaly that extends vertically, with prominent tails. The narrow anomaly is caused by an old soil auger hole that was placed in the ground to classify the soil. In this direction, the anomaly from the auger hole is easily distinguishable from the much larger cadaver anomalies. Conversely, in the west to east direction (see Figure 7-12a) the anomaly from the auger hole is extremely prominent and is comparable in size and intensity to the anomalies from the pig remains. In this example, it is possible to determine which anomaly was produced from the cadaver because of the detected backfill above the anomaly (see Figure 7-12b). However, if this was an actual forensic scenario with similar anomalies and no detected backfill, it would not be possible to determine which anomaly was produced by a buried body if only the west to east imagery was available. Because the imagery from the east to west profile was available, additional data can be useful to make a determination. In this example, it is obvious that the object producing the spike is not a forensic body, because a spike is generally caused by a highly conductive object with minimal surface area. It is important to reiterate that the 900-MHz antenna was used in this example and not the 500-MHz. However, while it may not be possible to observe such a drastic difference in imagery characteristics from both directions using a 500-MHz antenna, it is still possible to acquire imagery that is more useful in one direction when using this antenna.

The last issue to discuss concerning data collection in the field is whether data needs to be collected in both cardinal directions (i.e. east to west and north to south). When searching for a small forensic target such as a weapon or an infant body, it may be

helpful to search in both directions. This may be less feasible when collecting data over a large search area for a body. However, if a body is not detected during a forensic GPR survey, it is important to feel confident that a buried body was not missed because data were collected in only one cardinal direction.

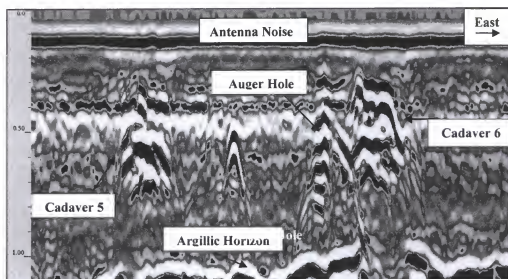


Figure 9-9. Unprocessed GPR profile (900-MHz) of two large cadavers from the LSLU scenario (5 and 6). The GPR profile is approximately 1.20 m deep and 13 m long.

Data were collected in both cardinal directions during this research. The GPR profiles presented so far were all collected lengthwise because the graves were oriented in this direction in rows. In order to present GPR profiles of multiple graves from the same scenario, they had to be shown oriented lengthwise. However, GPR data were also collected by bisecting graves across the middle. When graves were bisected, two graves were scanned from contiguous rows and the GPR profile would include one shallow and one deep grave.

Figure 9-10 is a profile of cadavers 13 (SDLE scenario) and 15 (SSLE scenario) at 18 months and 21 days. It is important to note that at this time period, cadaver 13 still retained extensive soft tissue and cadaver 15 would have been fully skeletonized. Discernable hyperbolic responses were produced from the remains of both cadavers without processing the file to remove the antenna noise. This imagery of this profile is significant because it demonstrates that the buried cadavers can be detected in width as well as length. Therefore, if the spacing is appropriate for the target size, large or small body size, data collection is adequate if it is only collected in one cardinal direction.

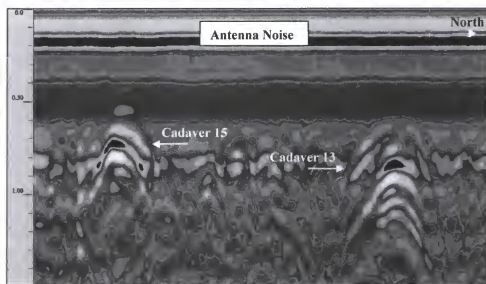


Figure 9-10. An unprocessed GPR profile of cadavers 13 and 15 (SDLE and SSLE scenarios) at 18 months and 21 days with the 500-MHz antenna. The GPR profile was collected by bisecting both graves in width and it is approximately 1.50 m deep and 7 m long.

CHAPTER 10 CONCLUSIONS

The major objectives of this research were focused in two areas that addressed issues in forensic anthropology and forensic archaeology. First, this study investigated the utility of using GPR in Florida to detect controlled forensic burials that contained pig cadavers. A major goal of the GPR research was to correlate the decomposition state of buried pig cadavers with the GPR imagery to understand if bodies could be detected in various stages of decomposition and skeletonization. Second, due to the important emphasis in decomposition, it was also possible to address the role that a number of variables had on decomposition.

It was no surprise that depth and time were the variables that had the greatest effect on decomposition. Conversely, size was not a major factor. The decomposition patterns of the child-sized pig cadavers were similar to the larger adult-sized cadavers. Furthermore, while the human body on the ground surface decomposes from central to peripheral, the pig cadaver buried at deep depths of at least 0.50 m decomposed from peripheral to central. As a generalization, skeletonization of the buried pig cadaver begins with the distal limbs and face. The head and limb regions will become skeletonized before the trunk, and skeletonization of the trunk initiates from the cervical and pelvic areas and progresses centrally. Presumably, this pattern would most likely be similar for human bodies buried at deep depths.

This study has demonstrated that GPR can be a very effective tool for grave detection in Florida. The efficacy of GPR is due to a large portion of the state being dominated by soils comprised of either sand or sand with deep clay horizons. It was possible to detect a decomposing body and a skeleton in soil comprised of sand in either a shallow or deep grave. Salient grave anomalies were produced for the duration of this study because there was a strong enough contrast between the skeleton and the surrounding soil to be detected by GPR due to differences in electrical properties and density. When a skeleton was detected in this study, the GPR was detecting a contrasting area in the soil that included bone and leached minerals from the skeleton. However, in clay it was difficult to image large pig cadavers that were in deep graves in as little as six months even though they had undergone very little decomposition. The argillic horizon masked the grave by limiting the contrast of the pig cadaver, or the dielectric constant of the buried pig remains became similar to that of the clay horizon. Interestingly, pig cadaver size was not a major factor in grave detection. Most of the smaller child-sized pig cadavers were detected for the entire monitoring period.

Overall, the imagery from the 500-MHz antenna was far superior to that of the 900-MHz antenna for grave detection. There was excessive detail produced by the 900-MHz antenna that made it difficult at times to discern forensic targets. Unfortunately, small items can be difficult to detect with either antenna if a grid with narrow transects is not used. The only negative comment concerning the 500-MHz antenna is the horizontal banding that is usually concentrated on the upper third to half of the profile caused by antenna noise. If a shallow grave exhibits a weak return, the anomaly may be obscured by the banding if the grave is below half a meter, and processing of the profile to remove

the banding may be required for grave detection. However, in most instances, processing of the 500-MHz profiles is not needed for grave detecting graves unless excessive noise is noted. Assessments can be made in the field without processing the data back at the laboratory. Overall, the 500-MHz is the best choice for most forensic applications. However, the 900-MHz may be useful to locate small items such as weapons if a higher resolution antenna is preferred due to a particular medium, or this antenna can be used to corroborate the results of the 500-MHz.

Clandestine forensic graves can be detected with GPR due to multiple variables including the remains, disturbed ground, and nonbiologic items in the grave. The remains can be detected during various stages of decomposition and skeletonization. Detecting a grave with GPR can also be due to contrasting properties of the grave with that of the surrounding soil. Variables such as less dense backfill and voids caused by settling of the backfill may be detected because the velocity of the electromagnetic wave will change when scanning the grave. The grave walls or the interface of the disturbed with undisturbed soil may be detected in rarer instances. Grave detection may result from a small focused area on the profile that appears as a loss of the signal (whiteout). Sometimes a gap or break in a horizon below the remains due to attenuation of the signal by the body may be a helpful characteristic if there is a distinctive horizon, such as clay, below the body. Finally, detection may also be facilitated by nonbiological items that may be added to the grave such as clothing the victim is wearing, items added on top of the victim to help with concealment before the backfill is added, items that were used to wrap the victim, and weapons that may have been added to the grave.

Since GPR is becoming more common for forensic applications, many inexperienced operators are conducting forensic surveys and interpreting the results. For example, environmental firms occasionally run surveys because they may be the only local organization with access to GPR equipment. However, the expertise of these operators generally involves applications of large planar features that include stratigraphic horizons, water tables, and sink holes. Conducting a GPR survey for small subsurface objects that are routinely encountered in forensic and archaeological surveys requires additional training not only in interpreting the results, but in setting up the grid and performing the survey. This can be a problem because the most limiting factor of using GPR for forensic applications is experience of the operator. Even if a body is buried within the survey area, it may not be detected if a controlled survey is not conducted with a grid utilizing appropriate spacing between transects. The radar must be pulled at a slow enough pace to collect enough data and to limit the bouncing of the antenna on the ground. If the survey is not conducted properly, the data may be useless. Furthermore, even if the survey is conducted properly, it may still be possible to miss the target if the data is not interpreted correctly.

Obviously, experience can be obtained by constructing controlled graves and monitoring them regularly as was done in this study. Another option is to form a cooperative relationship with local law enforcement to regularly assist with searches for clandestine graves. In addition, it can also be helpful to have a cooperative relationship with law enforcement where they allow the collection of GPR data of known forensic graves. If they are willing to wait before the remains are removed from the grave, the

imagery can be very important to include in a database of known forensic scenarios and decomposition states.

Forensic GPR surveys are not only important to locate clandestine graves, but also to clear suspected areas so searches can be directed elsewhere. Obviously GPR can be a very important tool for various forensic scenarios. However, the forensic scenario where GPR may be the most important search tool is over a suspected area that is covered by a concrete or paved slab. In these instances, if GPR is not used, the only option other than doing nothing is to physically break the slab. This is obviously not a feasible option in most instances, especially when the search area is a private residence or a commercial building. In these instances, GPR can save valuable time and money. A survey can be performed over the slab with limited intrusive testing of select anomalies. Since the location of the anomaly would be known, an auger can be used to drill a hole through the concrete that is large enough to inspect the object producing the anomaly. If the object in question is a false anomaly, the small test hole in the concrete can be easily repaired.

Finally, it is important to note that GPR is a collaborative search tool that should still be used in conjunction with other search methods. In the example of using the GPR over concrete, a cadaver dog can be used to inspect the area after a hole is drilled through the concrete. If the dog hits on the area, this can dictate how further testing is performed. In addition, when cadaver dogs hit on areas in the field where there are no obvious surface indicators of a grave, a GPR survey can be performed to locate the suspected clandestine grave before the entire area is dug up by law enforcement.

GPR can be an effective search tool in other areas of the United States and world where there are soils comprised of either sand or sand with deep clay horizons. Another

area dealing with grave detection where GPR is underutilized and could contribute significantly is in the field of human rights. Although Haglund et al. (2001), lists GPR as one of various methods that may be used for locating mass graves, they do not discuss the impact of GPR in locating any mass graves. In addition, after a large grave is located, delineation is performed to determine the depth of the overburden and the size by cross trenching or digging two perpendicular trenches with a backhoe across the top of the grave until remains are located (Haglund et al, 2001, Schmidt 2002). It would appear that GPR can not only be useful in locating mass graves, but also in delineating the size of the grave, the depth, and the extent of the overburden.

Continued forensic GPR research is essential to clarify the usefulness of GPR in different environments and soils, as well as scenarios. In particular, further research is needed to determine the utility of GPR for locating buried remains that have been interred for extended time frames longer than 21 months. Although preliminary soil analyses indicated that the soil surrounding the skeleton provides enough contrast to be detected in sand, additional soil analyses will further support this theory. For example, it would be important to know how the electrical conductivity and CEC are changing due to soft tissue decomposition products and diagenesis of the skeleton. Significant increases in both will provide additional support for the GPR detecting a contrasting area around the skeleton.

APPENDIX A
SOIL DESCRIPTIONS

Table A-1. Official description of Chipley soil series in Alachua County, Florida.

TAXONOMIC CLASS: Thermic, coated Aquic Quartzipsamments

A1--0 to 6 inches; very dark gray (10YR 3/1) sand; moderate medium granular structure; very friable; few fine roots; strongly acid; clear smooth boundary.

A2--6 to 12 inches; dark grayish brown (10YR 4/2) sand; medium granular structure; very friable; few fine roots; strongly acid; clear smooth boundary.

C1--12 to 25 inches; grayish brown (10YR 5/2) sand; single grained; loose; few fine roots; very strongly acid; gradual irregular boundary.

C2--25 to 49 inches; brownish yellow (10YR 7/2) sand; single grained; loose; few roots; few fine and medium prominent yellowish red (5YR 5/8) mottles and streaks; very strongly acid; gradual irregular boundary.

C3--49 to 81 inches; light gray (10YR 7/1) sand; single grained; loose; strongly acid.

DIAGNOSTIC HORIZONS: Ochric epipedon

Adapted from Thomas BP, Cummings E, Wittstruck WH. 1985. Soil Survey of Alachua County, Florida. United States Department of Agriculture, Soil Conservation Service, p. 123.

Table A-2. Soil description of Chipley series at the BRU

SOIL SERIES: Chipley

CLASSIFICATION: Thermic, coated Aquic Quartzipsamments

GENERAL LOCATION:: Beef Research Unit, northeast Gainesville, FL

SOIL DESCRIBED BY: John Schultz and Michael Tischler

DATE: January 2001

Ap--0 to 19 cm; very dark brown (10YR 2/2) fine sand; loose structure; single grained; many fine and few medium roots; abrupt smooth boundary.

C--19 to 56 cm; dark grayish brown (10YR 4/2) fine sand; few very fine faint reddish brown (5YR 5/4) redox accumulations; single grained; loose; few fine roots; gradual smooth boundary.

Cg1--56 to 89 cm; grayish brown (10YR 5/2) fine sand; common fine distinct reddish brown (5YR 5/4) redox accumulations; few fine faint streaks of light gray (10YR 6/1) redox depletions; single grained; loose; few fine roots; gradual smooth boundary.

Cg2--89 to 159; light grayish brown (10YR 6/2) fine sand; few fine distinct reddish brown (5YR 5/4) redox accumulations; few fine faint streaks of light gray (10YR 6/1) redox depletions; single grained; loose; few fine roots; gradual wavy boundary.

Cg3--159 to 181; white (10YR 8/2) fine sand; with few, fine, reddish brown (5YR 5/4) redox accumulations; single grained; loose; few fine roots.

Table A-3. Soil description of Sparr series at the BRU.

SOIL SERIES: Sparr

CLASSIFICATION: Loamy, siliceous, subactive, hyperthermic Aquic Arenic Paleudults

GENERAL LOCATION: Beef Research Unit, northeast Gainesville, FL

SOIL DESCRIBED BY: John Schultz and Michael Tischler DATE: January 2001

Ap--0 to 17 cm; very dark brown (10YR 2/2) fine sand; moderate granular structure; very friable; many fine and few medium roots; abrupt smooth boundary.

Bw1--17 to 29 cm; dark yellowish brown (10YR 4/4) fine sand; few very fine faint strong brown (7.5 YR 5/6) redox accumulations; very weak fine subangular blocky structure; friable; common fine roots; gradual wavy boundary.

Bw2--29 to 53 cm; light yellowish brown (10YR 6/4) fine sand; common fine faint strong brown (7.5 YR 5/6) redox accumulations; weak fine subangular blocky structure; friable; gradual wavy boundary.

Bw3--53 to 77 cm; light yellowish brown (10YR 6/4) fine sand; many medium distinct strong brown (7.5 YR 5/8) redox accumulations; few fine faint streaks of light gray (10YR 6/1) redox depletions; weak fine subangular blocky structure; friable; gradual smooth boundary.

E--77 to 99 cm; light gray (10YR 7/2) fine sand; moderate granular structure; very friable; clear smooth boundary.

Bt--99 to 108 cm; brownish yellow (10YR 6/6) loamy sand; many medium prominent reddish yellow (7.5YR 6/6) redox accumulations; weak medium subangular blocky structure; friable; clear smooth boundary.

Btg--108+ cm; light gray (10YR 7/2) loamy sand; many coarse prominent reddish yellow (7.5YR 6/8) redox accumulations; few fine faint streaks of light gray (10YR 6/1) redox depletions; moderate medium subangular blocky structure; friable.

Table A-4. Official description of Sparr soil series in Alachua County, Florida.

TAXONOMIC CLASS: Loamy, siliceous, hyperthermic Grossarenic Paleudults

Ap1--0 to 4 inches; dark gray (10YR 4/1) fine sand; moderate medium granular structure; very friable; common grass roots; very strongly acid; clear smooth boundary.

Ap2--4 to 8 inches; dark grayish brown (10YR 4/2) fine sand; weak fine granular structure; very friable; common grass roots; very strongly acid; clear smooth boundary.

E1--8 to 25 inches; pale brown (10YR 6/3) fine sand; weak fine granular structure; very friable; common grass roots; strongly acid; gradual wavy boundary.

E2--25 to 32 inches; very pale brown (10YR 7/3) fine sand; common medium faint light gray (10YR 7/2) and few fine faint light yellowish brown (10YR 6/4) mottles; weak fine granular structure; very friable; few grass roots; few fine distinct white streaks of clean sand grains; very strongly acid; gradual wavy boundary.

E3--32 to 48 inches; light gray (10YR 7/1) fine sand; few medium distinct yellowish brown (10YR 5/6) mottles; weak fine granular structure; very friable; few fine roots; very strongly acid; clear wavy boundary.

EBg--48 to 56 inches; light gray (10YR 7/2) loamy sand; few fine prominent yellowish red (5YR 4/6) and common medium faint very pale brown (10YR 7/3) mottles; weak fine subangular blocky structure; friable; few fine roots; sand grains are well coated and bridged with clay; extremely acid; clear wavy boundary.

Btg--56 to 84 inches; light gray (10YR 7/1) fine sandy loam; common fine distinct pale brown (10YR 6/3), common medium prominent strong brown (7.5YR 5/8) and few medium prominent yellowish red (5YR 5/8) mottles; weak medium subangular blocky structure; friable; few fine roots; extremely acid.

DIAGNOSTIC HORIZONS: Ochric epipedon and argillic horizon

Adapted from Thomas BP, Cummings E, Wittstruck WH. 1985. Soil Survey of Alachua County, Florida. United States Department of Agriculture, Soil Conservation Service, p. 147.

APPENDIX B
SOIL ANALYSES

Table B-1. Soil data for control graves in the Entisol that were collected when graves were originally dug and then when they were excavated.

Depth (cm)	Horizon	Preburial Sample from Control 6				Postburial Sample from Control 8			
		mg/kg		pH		mg/kg			pH
		P	Ca			P	Ca		
0-10	Ap	19.99	20.24	5.80		14.72	22.88	13.10	5.30
10-20	Ap/C	42.60	8.66	5.10		16.34	19.99	9.56	4.70
20-30	C	41.20	6.13	5.40		12.33	12.21	7.14	4.80
30-40	C	25.04	5.42	5.80		11.23	7.42	5.32	5.10
40-50	C	22.92	12.25	5.70		12.12	10.50	6.36	5.20
50-60	C/Cg1	11.82	4.77	6.40		12.69	14.99	6.88	5.00
60-70	Cg1	12.91	4.00	6.60		14.60	14.65	7.54	5.20
70-80	Cg1	11.06	3.42	6.40		10.99	5.57	4.90	5.20
80-90	Cg1/Cg2	9.58	2.20	6.40		9.13	5.05	4.06	5.40
90-100	Cg2	6.15	2.71	5.90		10.59	5.78	4.98	5.0
100-110	Cg2	4.46	4.70	5.90		11.94	9.34	6.39	4.60
100-120	Cg2	4.88	4.70	5.40		5.26	2.86	1.51	4.60

Table B-2. Soil data for graves from the SDLE scenario after the cadavers were excavated.

Depth (cm)	Horizon	Cadaver 13				Cadaver 14			
		P	Ca	Fe	pH	P	Ca	Fe	pH
0-10	Ap	9.29	67.20	11.33	4.50	6.59	39.84	14.59	4.30
10-20	Ap/C	8.45	31.36	20.28	4.80	8.77	40.84	21.00	4.40
20-30	C	10.88	23.32	20.76	4.70	7.58	30.48	17.72	4.40
30-40	C	33.04	12.08	14.92	5.60	5.82	28.04	15.40	3.70
40-50	C	50.32	7.07	5.68	5.30	8.46	6.16	7.29	5.40
50-60	C/Cg1	30.24	3.26	7.24	5.60	8.35	3.84	8.29	4.90
60-70	Cg1	16.96	11.87	6.18	5.70	11.23	4.17	8.57	6.80
70-80	Cg1	29.48	7.08	4.35	6.90	12.61	4.30	7.03	6.70
80-90	Cg1/Cg2	35.00	8.44	4.98	7.30	14.02	4.67	3.25	6.50
90-100	Cg2	92.56	3.56	3.43	7.00	12.57	4.20	2.52	6.70
100-110 (under thorax)	Cg2	134.76	4.13	3.77	6.70	146.28	5.91	4.30	6.90
100-110 (under head)	Cg2	199.40	23.24	18.51	7.00	240.80	17.94	12.17	6.90
100-110 (under pelvis)	Cg2	271.60	8.91	11.31	6.90	187.52	14.43	12.08	7.00

Table B-5. Soil data for graves from the SSSE scenario after the cadavers were excavated.

[illegible]

Table B-6. Soil data for control graves in the Ultisol that were collected when graves were originally dug and then when they were excavated.

Depth (cm)	Horizon	Preburial Sample from Grave 1L				Postburial Sample from Control 3			
		mg/kg		pH		mg/kg			pH
		P	Ca			P	Ca		
0-10	Ap	6.08	23.28	12.24	4.30	4.44	21.16	7.58	4.60
10-20	Ap/Bw1	4.66	13.60	11.28	4.40	4.31	11.00	8.54	4.60
20-30	Bw1/Bw2	3.56	4.18	8.87	4.30	4.60	10.29	8.80	4.50
30-40	Bw2	3.17	4.45	9.15	4.30	4.58	28.92	11.56	4.50
40-50	Bw2	4.28	2.61	10.11	4.40	4.99	17.84	10.89	4.70
50-60	Bw2/Bw3	3.94	1.50	6.43	4.40	4.09	8.74	8.54	4.60
60-70	Bw3	3.34	1.62	4.88	4.10	4.25	11.76	8.68	4.60
70-80	Bw3/E	2.90	1.54	4.07	4.30	6.07	14.73	9.53	4.50
80-90	E	7.01	3.10	11.17	4.30	6.02	4.98	9.90	4.50
90-100	E/Bt	6.32	13.70	25.96	4.30	4.83	4.94	7.43	4.40
100-110	Bt/Btg	8.65	12.45	14.08	4.40	6.36	14.66	2.33	4.50
100-110	Bt/Btg	8.64	8.12	10.20	4.70				

Table B-11. Summarized soil data that was collected under the pig cadavers buried in the Ultisol. The soil values are averages that were calculated using one sample collected under the head and one under the pelvis. If one of the samples was not available, the sample under the thorax was substituted.

Soil analysis	Preburial	Postburial	Cadaver #							
			2	3	5	6	7	8	9	10
P (mg/kg)	8.65	5.60	LDLU	LDLU	LSLU	LSLU	LSLU	LDSU	LDSU	LDSU
Ca (mg/kg)	10.29	9.80	219.24	204.72	418.80	343.40	457.80	245.80	584.40	748.00
Fe (mg/kg)	12.14	4.88	39.26	22.07	374.35	383.60	625.80	13.47	43.02	72.88
pH	4.52	4.45	33.07	49.08	69.18	51.24	62.30	100.58	218.52	181.58
			6.80	6.70	4.68	4.60	4.85	7.10	6.65	6.80

Table B-11. Continued

Soil analysis	Cadaver #	
	11	12
P (mg/kg)	LSSU	LSSU
Ca (mg/kg)	278.16	527.00
Fe (mg/kg)	31.52	383.40
pH	99.26	46.26
	7.00	5.80

Table B-12. Summarized soil data that was collected under the pig cadavers buried in the Entisol. The soil values are averages that were calculated using one sample collected under the head and one under the pelvis. If one of the samples was not available, the sample under the thorax was substituted.

Soil analysis	Preburial	Postburial	Cadaver #							
			13	14	15	16	17	18	19	20
			SDLE	SDLE	SSLE	SSLE	SDSE	SDSE	SSSE	SSSE
P (mg/kg)	4.67	8.60	471.00	214.16	393.00	569.00	154.67	119.88	508.80	201.56
Ca (mg/kg)	4.70	16.10	16.08	16.19	248.00	614.00	15.54	8.81	477.72	18.54
Fe (mg/kg)	1.20	7.90	14.91	12.13	20.72	22.76	13.29	6.61	67.74	33.62
pH	5.60	4.60	6.95	6.95	4.37	4.60	6.48	5.40	5.20	5.10

LITERATURE CITED

- Annan AD, Cosway SW. 1994. GPR frequency selection. Proceedings of the Fifth International Conference on Ground Penetrating Radar, Kitchener, Canada. Waterloo, Canada: Centre for Groundwater Research. p. 747-760.
- Arnold JE, Ambros EL, Larson DO. 1997. Geophysical surveys at stratigraphically complex island California sites: new implications for household archaeology. *Antiquity* 71:157-168.
- Basile V, Carrozzo MT, Negri S, Nuzzo L, Quarta T, Villani AV. 2000. A ground-penetrating radar survey for archaeological investigations in an urban area (Leece, Italy). *Journal of Applied Geophysics* 44:15-32.
- Behrensmeyer AK. 1978. Taphonomic and ecologic information from bone weathering. *Paleobiology* 4:150-162.
- Behrensmeyer AK, Kidwell SM. 1985. Taphonomy's contribution to paleobiology. *Paleobiology* 11:105-119.
- Berryman HE, Lahren CH. 1984. The advantages of simulated crime scenes in teaching forensic anthropology. *Journal of Forensic Science* 20:699-700.
- Bevan BW. 1991. The search for graves. *Geophysics* 56:1310-1319.
- Bloomfield P, Wheatley DJ, Prescott RJ, Miller HC. 1991. Twelve-year comparison of a Bjork-Shiley mechanical heart valve with porcine bioprostheses. *New England Journal of Medicine* 324:573-579.
- Bruschlinsky NN, Danilov AV, Muminov KM, Israilov D, Stetsuk, Usmanov MK. 1997. Magnetometric method of investigating fire sites. *Fire Technology* 33:195-213.
- Byrd JH, Castner JL. 2001. Insects of forensic importance. In: Bryd JH, Castner JL, editors. *Forensic entomology: the utility of arthropods in legal investigations*. Boca Raton, FL: CRC Press LLC. p 43-79.
- Calkin SF, Allen RP, Harriman MP. 1995. Buried in the basement; geophysics role in forensic investigation. Proceedings of the Symposium on the Application of Geophysics to Engineering and Environmental Problems (SAGEEP) 1995:397-403.

- Chaplin TH. 1971. The study of animal bones from archaeological sites. London: Seminar Press.
- Chapman LE, Bloom ET. 2001. Clinical xenotransplantation. *Journal of the American Medical Association* 285:2304-2306.
- Clark MA, Worell MB, Pless JE. 1997. Chemical and ultrastructural aspects of decomposition. In: Haglund WD, Sorg MH, editors. *Forensic taphonomy: the postmortem fate of human remains*. Boca Raton, FL: CRC Press. p.151-164.
- Collins ME. 1990. Aplicaciones del ground penetrating radar. XVII Reunion Nacional Sobre Edafologia, Badajoz, Spain. p. 15-32.
- Collins ME. 1997. Key to soil orders in Florida. Document SL-43, Soil and Water Sciences Department, Institute of Food and Agricultural Services, University of Florida.
- Collins ME, Ovalles FA, Kuehl RJ, Kurtz JL, Miller BK, Kostaanch P. 1996. Characterization and comparison of soils for ground penetrating radar measurements. University of Florida report to MIT/Lincoln Laboratory and the Army Research Laboratory.
- Conyers LB. 1995. The use of ground penetrating radar to map the buried structures and landscape of the Ceren site, El Salvador. *Geoarchaeology* 10:275-299.
- Conyers LB, Goodman D. 1997. *Ground-penetrating radar: an introduction for archaeologists*. Walnut Creek, CA: AltaMira Press.
- Cormack DH. 1987. *Ham's histology*. Philadelphia: J.B. Lippincott.
- Davenport CG. 2001a. Remote sensing applications in forensic investigations. *Historical Archaeology* 35:87-100.
- Davenport CG. 2001b. Where is it? Searching for buried bodies and hidden evidence. Church Hill, MD: SportWork.
- Davenport CG, Griffin TJ, Lindemann JW, Heimmer D. 1990. Geoscientists and law officers work together in Colorado. *Geotimes* 35:13-15.
- Davenport CG, Lindemann JW, Griffin TJ, Borowski JE. 1988. Geotechnical applications 3: crime scene investigation techniques. *Geophysics: The Leading Edge of Exploration* 7:64-66.
- Davis JL, Annan AP. 1989. Ground-penetrating radar for high-resolution mapping of soil and rock stratigraphy. *Geophysics* 37:531-551.

- Davis JL, Hegginbottom JA, Annan AP, Duncan KE. 1998. Plan view presentation of GPR data. Seventh International Conference on Ground Penetrating Radar, Lawrence, Kansas. p. 39-45.
- Day PR. 1965. Particle fractionation and particle-size analysis. *Agronomy* 9:545-567.
- Deacon T, Schumacher J, Dinsmore J, Thomas C, Palmer P, Kott S, Edge E, Penney D, Kassissieh S, Dempsey P, Isacson O. 1997. Histological evidence of fetal pig neural cell survival after transplantation into a patient with Parkinson's disease. *Nature Medicine* 3:350-352.
- De Vore DL. 1990. Ground-penetrating radar as a survey tool in archaeological investigations: an example from Fort Laramie National Historic Site. *The Wyoming Archaeologist* 33:23-38.
- DiMaio VJ, DiMaio SM. 2001. *Forensic pathology*, 2nd ed. Boca Raton, Florida: CRC Press LLC.
- Dirkmaat DC, Adovasio JM. 1997. Applications of archaeological methods to forensic investigations. In: Haglund WD, Sorg MH, editors. *Forensic taphonomy: the postmortem fate of human remains*. Boca Raton: CRC Press. p. 39-64.
- Dodd JR, Stanton RJ, Jr. 1981. *Paleoecology: concepts and applications*. New York: Wiley-Interscience.
- Doolittle JA, Collins ME. 1995. Use of soil information to determine application of ground penetrating radar. *Journal of Applied Geophysics* 33:101-108.
- Doolittle JA, Collins ME. 1998. A comparison of EM induction and GPR methods in areas of karst. *Geoderma* 85:83-102.
- Doolittle JA, Minzenmayer FE, Waltman SW, Benham EC. 2002. Ground penetrating radar soil suitability map of the conterminous United States. In: Koppenjan SK, Lee H, editors. *Ninth International Conference on Ground Penetrating Radar*, Santa Barbara, California. *Proceedings of SPIE* 4758:7-12.
- Efremov JA. 1940. Taphonomy: a new branch of paleontology. *Pan-American Geologist* 74:81-93.
- Engheta N, Papas CH, Elachi C. 1982. Radiation patterns of interfacial dipole antennas. *Radio Science* 17:1557-1556.
- Evans WE. 1963. *The chemistry of death*. Springfield: Charles C. Thomas.
- Fink JS, Schumacher JM, Ellias SL. 2000. Porcine xenografts in Parkinson's disease and Huntington's disease patients: preliminary results. *Cell Transplantation* 9:273-278.

- Fisher PM, Follin SGW, Ulriksen P. 1980. Subsurface interface radar survey at Hala Sultan Tekke, Cyprus. *Studies in Mediterranean Archaeology* 63:48-51.
- France DL, Griffin TJ, Swanburg JG, Lindemann JW, Davenport GC, Trammell V, Travis CT, Kondratieff, Nelson A, Castellano K, Hopkins D. 1992. A multidisciplinary approach to the detection of clandestine graves. *Journal of Forensic Sciences* 37:1445-1458.
- France DL, Griffin TJ, Swanburg JG, Lindemann JW, Davenport GC, Trammell V, Travis CT, Kondratieff, Nelson A, Castellano K, Hopkins D, Adair T. 1997. NecroSearch revisited: further multidisciplinary approaches to the detection of clandestine graves. In: Haglund WD, Sorg MH, editors. *Forensic taphonomy: the postmortem fate of human remains*. Boca Raton: CRC Press. p. 497-509.
- Freeland RS, Yoder RE, Miller ML, Koppenjan SK. 2002. Forensic application of sweep-frequency and impulse GPR. In: Koppenjan SK, Lee H, editors. *Ninth International Conference on Ground Penetrating Radar*, Santa Barbara, California. *Proceedings of SPIE* 4758:533-538.
- Galloway A. 1997. The process of decomposition: a model from the Arizona-Sonoran desert. In: Haglund WD, Sorg MH, editors. *Forensic taphonomy: the postmortem fate of human remains*. Boca Raton, FL: CRC Press, Inc. p. 139-150.
- Galloway A, Birkby WH, Jones AM, Henery TE, Parks BO. 1989. Decay rates of human remains in an arid environment. *Journal of Forensic Sciences* 34:607-616.
- Gabriel C, Gabriel C, Corthout E. 1996a. The dielectric properties of biological tissues: I. Literature survey. *Physics in Medicine and Biology* 41:2231-2246.
- Gabriel S, Lau RW, Gabriel C. 1996b. The dielectric properties of biological tissues: II. Measurements in the frequency range of 10 Hz to 20 GHz. *Physics in Medicine and Biology* 41:2251-2269.
- Geophysical Surveys Systems, Inc. 1999. *Operations manual for subsurface interface radar System-2000*. North Salem, New Hampshire: Geophysical Survey Systems.
- Gill-King H. 1997. Chemical and ultrastructural aspects of decomposition. In: Haglund WD, Sorg MH, editors. *Forensic taphonomy: the postmortem fate of human remains*. Boca Raton, FL: CRC Press, Inc. p. 93-108.
- Goodman D, Nishimura Y. 1993. A ground-radar view of Japanese burial mounds. *Antiquity*. 67:349-354.
- Gordon CC, Buikstra JE. 1981. Soil pH, bone preservation, and sampling bias at mortuary sites. *American Antiquity* 46:566-571.

- Haglund WD, Connor M, Scott DD. 2001. The archaeology of contemporary mass graves. *Historical Archaeology* 35:57-69.
- Haglund WD, Sorg MH. 1997. Method and theory in forensic taphonomic research. In: Haglund WD, Sorg MH, editors. *Forensic taphonomy: the postmortem fate of human remains*. Boca Raton, FL: CRC Press. p. 13-26.
- Hammon WS, McMechan GA, Zeng X. 2000. Forensic GPR: finite-difference simulations of responses from buried human remains. *Journal of Applied Geophysics* 45:171-186.
- Hare PE. 1980. Organic geochemistry of bone and its relation to the survival of bone in natural environments. In: Behrensmeyer AK, Hill AP, editors. *Fossils in the making*. Chicago: Chicago University Press. p. 156-181.
- Henderson J. 1987. Factors determining the state of preservation of human remains. In: Boddington A, Garland AN, Janaway RC, editors. *Death, decay, and reconstruction*. Manchester, England: Manchester University Press. p. 43-54.
- Hunter JR. 1996. Locating buried remains. In: Hunter JR, Roberts CA, Martin AL, editors. *Studies in crime: an introduction to forensic archaeology*. London: BT Batsford LTD. p. 86-100.
- Hunter JR, Heron C, Janaway RC, Martin AL, Pollard AM, Roberts CA. 1994. Forensic archaeology in Britain. *Antiquity* 68:758-769.
- Hunter JR, Roberts CA, Martin AL. 1996. *Studies in crime: an introduction to forensic archaeology*. London: BT Batsford LTD.
- Imai T, Sakayama T, Kanemori T. 1987. Use of ground-probing radar and resistivity surveys for archaeological investigations. *Geophysics* 52:137-50.
- Killam EW. 1990. *The detection of human remains*. Springfield, IL: Charles C. Thomas.
- King JA, Bevan BW, Hurry RJ. 1993. The reliability of geophysical surveys at historic-period cemeteries: an example from the Plains Cemetery, Mechanicsville, Maryland. *Historical Archaeology* 27:4-16.
- Koch CP. 1989. *Taphonomy: a bibliographic guide to the literature*. Orono: University of Maine Center for the Study of the first Americans.
- Komar DA. 1998. Decay rates in a cold climate region: a review of cases involving advanced decomposition from the medical examiner's office in Edmonton, Alberta. *Journal of Forensic Sciences* 43:57-61.

- Koppenjan SK, Allen CM, Gardner D, Wong HR. 1998. Lightweight ground penetrating radar. Seventh International Conference on Ground Penetrating Radar, Lawrence, Kansas. p. 771-773.
- Koppenjan SK, Allen CM, Gardner D, Wong HR, Lee H, Lockwood SJ. 2000. Multi-frequency synthetic-aperture imaging with a lightweight ground penetrating radar system. *Journal of Applied Geophysics* 43:251-258.
- Koppenjan SK, Schultz JJ, Falsetti AB, ME Collins, Sashi Ono, Lee H. 2003. The application of GPR in Florida for detecting forensic burials. *Proceedings of the Symposium on the Application of Geophysics to Engineering and Environmental Problems (SAGEEP) 2003:635-649.*
- Kraus JD. 1950. *Antennas*. New York: McGraw-Hill.
- LeGeros RZ. 1981. Apatites in biological systems. *Progress in Crystal Growth and Characterization of Materials* 4:1-45.
- Lindsay WL. 1979. *Chemical equilibria in soils*. New York: Wiley.
- Lowenstein HA, Weiner S. 1989. *On mineralization*. Oxford: Oxford University Press.
- Lyman RL. 1994. *Vertebrate taphonomy*. Cambridge: Cambridge University Press.
- Mann RW, Bass WM, Meadows L. 1990. Time since death and decomposition of the human body: variables and observations in case and experimental field studies. *Journal of Forensic Sciences* 35:103-111.
- Martill DM. 1990. Bones as stones: the contribution of vertebrate remains to the lithologic record. In: Donovan SK, editor. *The process of fossilization*. New York: Columbia University Press. p. 270-292.
- Megyesi MS. 2001. The effects of temperature on the decomposition rate of human remains. Masters Thesis in Human Biology, University of Indianapolis, Indiana.
- Mehlich A. 1953. Determination of P, Ca, Mg, K, Na, and NH₄ by North Carolina soil testing laboratories (mimeo). North Carolina State University, Raleigh.
- Mellet JS. 1992. Location of human remains with ground-penetrating radar. In: Hänninen P, Autio S, editors. *Ninth International Conference on Ground Penetrating Radar. Special Paper - Geological Survey of Finland* 16:359-365.
- Mellet JS. 1996. GPR in forensic and archaeological work: *Proceedings of the Symposium on the Application of Geophysics to Engineering and Environmental Problems (SAGEEP) 1996:487-491.*

- Micozzi MS. 1991. Postmortem changes in human and animal remains. Springfield, IL: Charles C. Thomas.
- Miller ML, Freeland RS, Koppenjan SK. 2002. Searching for concealed human remains using GPR imaging of decomposition. In: Koppenjan SK, Lee H, editors. Ninth International Conference on Ground Penetrating Radar, Santa Barbara, California. Proceedings of SPIE 4758:539-544.
- Miller PS. 1996. Disturbances in the soil: finding buried bodies and other evidence using ground penetrating radar. *Journal of Forensic Science* 41:648-52.
- Morse D, Duncan J, Stoutamire J. 1983. Handbook of forensic archaeology and anthropology. Tallahassee, FL: Rose Printing.
- Murray RC, Tedrow JCF. 1992. Forensic geology. Englewood Cliffs, NJ: Prentice-Hall.
- Nawrocki SP. 1995. Taphonomic processes in historic cemeteries. In: Grauer AL, editor. Bodies of evidence. New York: John Wiley & Sons, Inc. p. 49-66.
- Nielsen-Marsh C, Gernaey AG, Turner-Walker G, Hedges R, Pike Alistair, Collins M. 2000. The chemical degradation of bone. In: Cox M, Mays S, editors. Human osteology in archaeology and forensic science. London: Greenwich Medical Media Ltd. p. 439-454.
- Nobes DC. 1999. Geophysical surveys of burial sites: a case study of Oaro urupa. *Geophysics* 64:357-67.
- Nobes DC. 2000. The search for "Yvonne": a case example of the delineation of a grave using near-surface geophysical methods. *Journal of Forensic Science* 45:715-21.
- Noon DA, Longstaff, Yelf RJ. 1994. Advances in the development of step frequency ground penetrating radar. Proceedings of the Fifth International Conference on Ground Penetrating Radar, Kitchener, Canada. Waterloo, Canada: Centre for Groundwater Research. p.117-131.
- Olhoeft GR. 1981. Electrical properties of rocks. In: Touloukian YS, Judd WR, Roy RF, editors. Physical properties of rocks and minerals. New York: McGraw-Hill. p. 257-230.
- Olhoeft GR. 1998. Electrical, magnetic, and geometric properties that determine ground penetrating radar performance. Seventh International Conference on Ground Penetrating Radar, Lawrence, Kansas. p. 177-182.
- Paterson CR. 1983. Essentials of human biochemistry. London: Pitman Publishing Limited.

- Payne JA. 1965. A summer carrion study of the booby pig *Sus scrofa Linnaeus*. Ecology 46:592-602.
- Payne JA, King EW. 1970. Coleoptera associated with pig carrion. Nature 219:1180-1187.
- Payne JA, King EW. 1972. Insect succession and decomposition of pig carcasses in water. Journal of the Georgia Entomological Society 7:153-62.
- Payne JA, King EW, Beinhardt G. 1968a. Arthropod succession and decomposition of buried pigs. Entomologist's Monthly Magazine 105:224-32.
- Payne JA, Mead FW, King EW. 1968b. Hermiptra associated with pig carrion. Annals of the Entomological Society of America 61:565-567.
- Pething R. 1979. Dielectric and electronic properties of biological materials. New York: John Wiley and Sons, Ltd.
- Reed HB. 1958. A study of dog carcass communities in Tennessee, with special references to insects. American Midland Naturalist 59:213-245.
- Reynolds JM. 1997. An introduction to applied and environmental geophysics. New York: John Wiley and Sons, Inc.
- Rhine S, Dawson JE. 1998. Estimation of time since death in the southwestern United States. In: Reichs K, editor. Forensic osteology: advances in the identification of human remains, 2nd ed. Springfield: Charles C. Thomas. p 145-159.
- Roark MS, Strohmeyer J, Anderson N, Shoemaker M, Oppert S. 1998. Applications of the ground-penetrating technique in the detection and delineation of homicide victims and crime scene paraphernalia. Proceedings of the Symposium on the Application of Geophysics to Engineering and Environmental Problems (SAGEEP) 1998:1063-1071.
- Rodriguez WC. 1997. Decomposition of buried and submerged bodies. In: Haglund WD, Sorg MH, editors. Forensic taphonomy: the postmortem fate of human remains. Boca Raton: CRC Press. p. 459-467.
- Rodriguez WC, Bass WM. 1983. Insect activity and its relationship to decay rates of human cadavers in east Tennessee. 28:423-432.
- Rodriguez WC, Bass WM. 1985. Decomposition of buried bodies and methods that aid in their location. Journal of Forensic Sciences 30:836-852.
- Rottander RCA. 1976. Variation in the chemical composition of bone in archeological soils as an indicator of diagenetic change. Journal of Archaeological Science 3:83-88.


- Sassaman KE, Blessing ME, Connaughton SP, Endonino JC, Flores A, O'Day P, O'Day SJ, Schultz J, Weser AB. 2003. St. Johns archeological field school 2000-2001: Blue Springs and Hontoon Island State Parks. Laboratory of Southeastern Archaeology, Department of Anthropology, University of Florida, Technical Report 4.
- Schmitt S. 2002. Mass graves, and collection of forensic evidence: genocide, war crimes, and crimes against humanity. In: Haglund WD, Sorg MH, editors. *Advances in forensic taphonomy: method, theory, and archaeological perspectives*. Boca Raton, FL: CRC Press LLC. p. 227-292.
- Schoen FJ, Levy RJ. 1999. Tissue heart valves: current challenges and future research perspectives. *Journal of Biomedical Research* 47:439-465.
- Schultz JJ, Falsetti AB, Collins ME, Koppenjan SK, Warren MW. 2002. The detection of forensic burials in Florida using GPR. In: Koppenjan SK, Lee H, editors. *Ninth International Conference on Ground Penetrating Radar*, Santa Barbara, California. *Proceedings of SPIE* 4758:443-448.
- Scott DD, Connor M. 1997. Context delecti: archaeological context in forensic work. In: Haglund WD, Sorg MH, editors. *Forensic taphonomy: the postmortem fate of human remains*. Boca Raton: CRC Press. p. 27-38.
- Sheriff RE. 1991. *Encyclopedic dictionary of exploration geophysics*, third edition. Tulsa, Oklahoma: Society of Exploration Geophysics.
- Shih DG, Doolittle JA. 1984. Using radar to investigate organic soil thickness in the Florida everglades. *Soil Science Society of America Journal* 48:651-656.
- Sigler-Eisenberg B. 1985. Forensic research: expanding the concept of applied archaeology. *American Antiquity* 50:650-655.
- Skinner M, Lazenby RA. 1983. *Found! Human Remains: a field manual for the recovery of the recent human skeleton*. Burnaby, British Columbia: Archaeology Press, Simon Fraser University.
- Soil Survey Staff. 1996. *Soil survey laboratory methods manual*. Soil survey investigation report n. 42 (revised). Washington, DC : U.S. Dept. of Agriculture, Natural Resources Conservation Service, U.S. Government Printing Office.
- Soil Survey Staff. 1999. *Soil taxonomy: a basic system of soil classification for making and interpreting soil surveys*, 2nd edition. Washington, DC : U.S. Dept. of Agriculture, Natural Resources Conservation Service, U.S. Government Printing Office.
- Sorg MH, David E, Rebman AJ. 1997. Cadaver dogs, taphonomy, and postmortem interval in the northeast. In: Reichs K, editor. *Forensic osteology: advances in the identification of human remains*, 2nd ed. Springfield: Charles C. Thomas. p 120-144.

- Sternberg BK, McGill JW. 1995. Archaeology studies in southern Arizona using ground penetrating radar. *J Applied Geophysics* 33:209-25.
- Strongman KB. 1992. Forensic applications of ground penetrating radar. In: Pilon JA, editor. *Ground penetrating radar. Paper - Geological Survey of Canada*, 90-04:203-211.
- Thew HA. 2000. Effects of lime on the decomposition of buried remains. Master's Thesis in Human Biology, University of Indianapolis, Indiana.
- Thomas BP, Cummings E, Wittstruck WH. 1985. Soil Survey of Alachua County, Florida. United States Department of Agriculture, Soil Conservation Service.
- Unterberger RR. 1992. Ground penetrating radar finds disturbed earth over burials. In: Hänninen P, Autio S, editors. *Ninth International Conference on Ground Penetrating Radar. Special Paper - Geological Society of Finland* 16:351-357.
- Vass AA, Barshick SA, Sega G, Caton J, Skeen JT, Love JC, Synstelién JA. 2002. Decomposition chemistry of human remains: a new methodology for determination the postmortem interval. *Journal of Forensic Sciences* 47:542-53.
- Vass AA, Bass WM, Wolt JD, Foss JE, Ammons JT. 1992. Time since death determinations of human cadavers using soil solution. *Journal of Forensic Science* 37:1236-1253.
- Vaughn CJ. 1986. Ground-penetrating radar surveys used in archaeological investigations. *Geophysics* 51:595-604.
- Von Endt DW, Ortner DJ. 1984. Experimental effects of bone size and temperature on bone diagenesis. *Journal of Archaeological Science* 11:247-253.
- Von Hippel AR. 1954. *Dielectrics and waves*. Cambridge, Massachusetts: MIT Press.
- White EM, Hannus LA. 1983. Chemical weathering of bone in archaeological soils. *American Antiquity* 48:316-322.
- Wolf DJ. 1986. Forensic anthropology scene investigations. In: Reichs K, editor. *Forensic osteology: advances in the identification of human remains*. Springfield: Charles C. Thomas. p 3-23.

BIOGRAPHICAL SKETCH

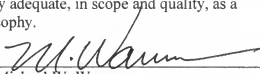
John J. Schultz received his Bachelor of Arts with Honors in anthropology from State University of New York at Stony Brook in 1994. He received his Master of Science in human biology with an emphasis in forensic anthropology in 1998 from the University of Indianapolis. In August 1998, John enrolled at the University of Florida to obtain his Ph.D. in anthropology with a specialization in forensic anthropology. Finally, in August 2003, he will be an assistant professor of anthropology in the Department of Sociology and Anthropology at the University of Central Florida.

I certify that I have read this study and that in my opinion it conforms to acceptable standards of scholarly presentation and is fully adequate, in scope and quality, as a dissertation for the degree of Doctor of Philosophy.



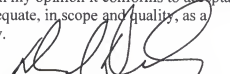
Anthony B. Falsetti, Chairman
Associate Professor of Anthropology

I certify that I have read this study and that in my opinion it conforms to acceptable standards of scholarly presentation and is fully adequate, in scope and quality, as a dissertation for the degree of Doctor of Philosophy.



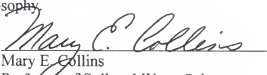
Michael W. Warren
Assistant Professor of Anthropology

I certify that I have read this study and that in my opinion it conforms to acceptable standards of scholarly presentation and is fully adequate, in scope and quality, as a dissertation for the degree of Doctor of Philosophy.




David Daegling
Associate Professor of Anthropology

I certify that I have read this study and that in my opinion it conforms to acceptable standards of scholarly presentation and is fully adequate, in scope and quality, as a dissertation for the degree of Doctor of Philosophy.



Mary E. Collins
Professor of Soil and Water Science

I certify that I have read this study and that in my opinion it conforms to acceptable standards of scholarly presentation and is fully adequate, in scope and quality, as a dissertation for the degree of Doctor of Philosophy.



Steve Nawrocki
Associate Professor of Biology
University of Indianapolis, Indiana

This dissertation was submitted to the Graduate Faculty of the Department of Anthropology in the College of Liberal Arts and Sciences and to the Graduate School and was accepted as partial fulfillment of the requirements for the degree of Doctor of Philosophy.

August 2003

Dean, Graduate School